Sequence 27: Laboratory and Field Testing on FRP Composite Decks for the City of St. James, Phelps County, MO.

Combined Final Report for Contracts RI00-021 and RI00-031

LABORATORY AND FIELD TESTING OF FRP COMPOSITE BRIDGE DECKS AND FRP-REINFORCED CONCRETE BRIDGE FOR CITY OF ST. JAMES, PHELPS COUNTY, MO

Draft Final Report

Prepared for

Missouri Department of Transportation

by

Dr. Halvard Nystrom
Department of Engineering Management

Dr. Steve Watkins
Department of Computer and Electrical Engineering

Dr. Antonio Nanni
Danielle K. Stone
Department of Civil Engineering

University of Missouri-Rolla

August 2002

Sequence 27: Laboratory and Field Testing on FRP Composite Decks for the City of St. James, Phelps County, MO.

Technical Report Documentation Page

1. Report No. RI00-021 and RI00-031	**2. Government Accession No.**	**3. Recipient's Catalog No.**
4. Title and Subtitle PC I-girder Cracking - Phase II: Causes and Design Detail		**5. Report Date** August 2002
		6. Performing Organization Code UMR
7. Author/s H. Nystrom, S. Watkins, D. Stone, and A. Nanni		**8. Performing Organization Report No.** RI00-021 and RI00-031
9. Performing Organization Name and Address Center for Infrastructure Engineering Studies, UMR 223 ERL Rolla, MO 65409		**10. Work Unit No. (TRAIS)**
		11. Contract or Grant No.
12. Sponsoring Organization Name and Address MODOT 105 West Capital Av., Jefferson City, MO 65102 UTC 223 Engineering Research Lab., Rolla, MO 65409		**13. Type of report and period covered** Technical Report; 5/00 – 8/02
		14. Sponsoring Agency Code MoDOT

15. Supplementary Notes
This investigation was conducted in cooperation with the U.S. Department of Transportation.

16. Abstract

The overall objective of this research project was to conduct an extensive study of the behavior and use of glass fiber-reinforced polymer (GFRP) and carbon FRP (CFRP) materials for bridge construction. In particular, GFRP honeycomb sandwich panels were used as bridge panels and steel-supported bridge deck panels and CFRP and GFRP bars were used as internal reinforcement for precast concrete bridge panels. More specifically, this research program provides laboratory characterization of FRP bars and FRP-reinforced concrete (FRP-RC) panels, laboratory characterization of FRP honeycomb sandwich panels and their constituent materials, in-situ characterization of FRP-RC panels and FRP honeycomb sandwich panels, investigation of the durability performance of FRP bars and FRP honeycomb sandwich panels, and evaluation of construction techniques for FRP-RC panels and FRP honeycomb sandwich panels.

The research program consisted of a series of investigations in the field and in the laboratory. Four short-span bridges were installed so as to outline the construction-related issues associated with the use of these materials. The bridges are located in a residential area of St. James, Missouri; each bridge utilizes FRP materials in a different structural system to investigate the feasibility of using FRP in each of these applications. In-situ load tests of the constructed bridges were conducted to illustrate the behavior of the overall structures, in terms of panel behavior and installation details. Load testing following construction and at later ages was undertaken allowing the examination of the bridges' long-term performance under ambient outdoor environmental conditions. Finally, the third investigative series dealt with the laboratory characterization of these materials, considering both the overall panel behavior and the individual materials.

Investigations focused on determining factors for design using FRP materials in bridge construction. In particular, the necessary material properties, design parameters (e.g., live load impact factors and wheel load distribution factors), and design protocols (e.g., serviceability predictions) were the focus of this research with the ultimate goal being the assistance of industry in developing material and design standards for FRP materials. In this way, the materials may become a viable alternative to traditional materials for the improvement of our Nation's deteriorating infrastructure.

17. Key Words bridge structure, in-situ testing, deflection, reinforced concrete, carbon, glass, design guidelines, fiber-reinforced polymer	**18. Distribution Statement** No restrictions. This document is available to the public through NTIC, Springfield, VA 22161		
19. Security Classification (of this report) Unclassified	**20. Security Classification (of this page)** Unclassified	**21. No. of Pages** 199 w/o Appendices	**22. Price**

ABSTRACT

The overall objective of this research project was to conduct an extensive study of the behavior and use of glass fiber-reinforced polymer (GFRP) and carbon FRP (CFRP) materials for bridge construction. In particular, GFRP honeycomb sandwich panels were used as bridge panels and steel-supported bridge deck panels and CFRP and GFRP bars were used as internal reinforcement for precast concrete bridge panels. More specifically, this research program provides laboratory characterization of FRP bars and FRP-reinforced concrete (FRP-RC) panels, laboratory characterization of FRP honeycomb sandwich panels and their constituent materials, in-situ characterization of FRP-RC panels and FRP honeycomb sandwich panels, investigation of the durability performance of FRP bars and FRP honeycomb sandwich panels, and evaluation of construction techniques for FRP-RC panels and FRP honeycomb sandwich panels.

The research program consisted of a series of investigations in the field and in the laboratory. Four short-span bridges were installed so as to outline the construction-related issues associated with the use of these materials. The bridges are located in a residential area of St. James, Missouri; each bridge utilizes FRP materials in a different structural system to investigate the feasibility of using FRP in each of these applications. In-situ load tests of the constructed bridges were conducted to illustrate the behavior of the overall structures, in terms of panel behavior and installation details. Load testing following construction and at later ages was undertaken allowing the examination of the bridges' long-term performance under ambient outdoor environmental conditions. Finally, the third investigative series dealt with the laboratory characterization of these materials, considering both the overall panel behavior and the individual materials.

Investigations focused on determining factors for design using FRP materials in bridge construction. In particular, the necessary material properties, design parameters (e.g., live load impact factors and wheel load distribution factors), and design protocols (e.g., serviceability predictions) were the focus of this research with the ultimate goal being the assistance of industry in developing material and design standards for FRP materials. In this way, the materials may become a viable alternative to traditional materials for the improvement of our Nation's deteriorating infrastructure.

ACKNOWLEDGEMENTS

The researchers would like to express their appreciation to the City of St. James, Missouri, the Missouri Department of Transportation (MoDOT), the Department of Economic Development (DED) through the Missouri Enterprise Business Assistance Center (MEBAC), the University Transportation Center (UTC) and the National Science Foundation (NSF) for funding this research project.

Furthermore, they would like to thank the City of St. James for the opportunity to conduct this project. The support of the Mayor, Jim Morrison, the City Engineer, Steve Franz, and the City crews has been outstanding throughout the project.

The authors would like to acknowledge the contribution of fibers for the bridge reinforcement from Owens Corning Fibers and Toray Industries, Inc. and the in-kind donations of Marshall Industries Composites, Inc.; their support is much appreciated. Furthermore, the contractors, Kansas Structural Composites, Inc. and Oden Enterprises, and engineers-of-record, Elgin Surveying and Engineering, Incorporated and WSW Hydro Consulting Engineers and Hydrologists, LLC, should be commended for their willingness to conduct innovative projects such as this one.

Special thanks also go to Denzil Hills, Randy Mayo, and Ronnie Rinehart of MoDOT for providing the truck utilized during in-situ bridge load testing.

TABLE OF CONTENTS

Page

LIST OF FIGURES

LIST OF TABLES

NOTATIONS

a	distance from the support to the point of load application, in. (Equation 5.1)
A_{fv}	area of shear reinforcement for the FRP, in^2.
A_v	area of shear reinforcement for the steel, in^2.
b	width of the panel, in.
C	length of exposure to the alkaline solution, days. (Equation 6.8)
C_E	environmental reduction factor.
d	depth to the centroid of the reinforcing bars, in.
d_b	diameter of the bar, in.
E	modulus of elasticity of the material, psi.
E_f	longitudinal modulus of elasticity of the longitudinal FRP reinforcement, psi.
E_s	longitudinal modulus of elasticity of the steel reinforcement, psi.
f'c	concrete compressive strength, psi
f_{fv}	design stress level for the FRP shear reinforcement, ksi.
f_y	yield stress of the steel shear reinforcement, ksi.
I	moment of inertia of the section, in^4.
I_{cr}	cracked moment of inertia of the section, in^4. (Equation 6.1)
I_e	effective moment of inertia of the section, in^4. (Equation 6.1)
I_g	gross moment of inertia of the section, in^4. (Equation 6.1)
IF	live load impact factor.
L	span length, ft.
M_a	moment applied to the section, kip-ft. (Equation 6.1)
M_{cr}	cracking moment of the section, kip-ft.
M_{max}	maximum live load moment per 1-ft (0.30-m) width, kip-ft. (Equation 3.1)
M_n	ultimate moment capacity, kip-ft.
Mt	percentage of fluid content at time, t.
M_u	design moment demand, kip-ft.
N	predicted natural age of the conditioned specimens, days. (Equation 6.8)
P	magnitude of one of the applied loads, kips. (Equation 5.1)

P	failure load, lb. (Equation 6.9)
P_{20}	load on one rear wheel of the HS20-44 loading truck, kip. (Equation 3.1)
P_n	load carried by panel *n.* (Equation 7.1)
S	apparent horizontal shear strength, lb. (Equation 6.9)
S	effective span length, ft. (Equation 3.1)
s	spacing of the shear reinforcement, in.
T	elevated conditioning temperature, °F. (Equation 6.8)
T_g	glass transition temperature, °F.
V_c	concrete contribution to the shear capacity, kip.
V_f	FRP reinforcement contribution to the shear capacity, kip.
W	weight of the moist specimen after some time, t, of conditioning, g.
W_d	weight of the dry specimen at the initiation of the test, g.
x	constant relating load to deflection for the given material and loading configuration.
Δ_n	measured deflection of panel *n.*
β_d	modification factor based on the ratio of the modulus of the FRP reinforcement to that of steel reinforcement. (Equation 6.1)
ϕ	strength reduction factor.
ϕM_n	design moment capacity, kip-ft.
ρ_f	reinforcement ratio of the FRP-reinforced section.
ρ_s	reinforcement ratio of a steel-reinforced section of equal capacity.

1. INTRODUCTION

1.1. BACKGROUND AND PROBLEM STATEMENT

Of the approximately 590,000 bridge structures in the National Bridge Inventory of the United States Federal Highway Administration (FHWA) (1998), approximately 50,000 are classified as structurally deficient, 89,000 are functionally obsolete and 54,000 are both structurally deficient and functionally obsolete. These numbers indicate that over 40 percent of the Nation's bridges are in need of repair or replacement. Budget constraints prohibit many states from repairing or replacing even a fraction of these bridges; consequently, many states are forced to close or post load restrictions on their bridges as temporary solutions until additional funds become available for repair or replacement.

This aging and deteriorating infrastructure has prompted government leaders and engineers to consider new construction technologies to enhance life span and strength of bridge structures. Advanced composites made of fibers embedded in a polymeric resin, also known as fiber-reinforced polymer (FRP) materials, have recently emerged as a viable and practical construction material. The acceptance of FRP materials into mainstream construction, however, has been hindered by various barriers including increased material costs compared to traditional materials, unquantified maintenance costs, the lack of verification of the long-term durability of FRP materials subjected to various environmental conditions, and the lack of design guidelines, codes, and specifications (Zoghi et al., 2002). An excellent review of FRP material properties in general, which will not be included herein, is outlined by Busel and Lockwood. (2000)

Two particular types of FRP materials have been utilized predominantly in recent years and are the focus of this research study. They are FRP materials in the form of reinforcing bars for concrete and FRP panels for use with or without steel girders as supporting members. In the mid-1950's the first demonstrations of FRP bars for use as reinforcement for concrete were conducted and in the 1980's interest in the area was reignited based the need for more durable materials became apparent in severe environments. The first FRP-reinforced concrete (FRP-RC) bridge in the United States, the Buffalo Creek Bridge in McKinleyville, West Virginia, was constructed in 1996 by the West Virginia Department of Transportation. The first vehicular bridge constructed entirely of FRP panels, the No-Name Creek Bridge in Russell, KANSAS, was installed by the Kansas Department of Transportation. (Lockwood and Busel, 2001)

Several national agencies are involved in the advancement of the construction industry utilizing FRP composites. A review of the work of each particular agency is given by Lockwood and Busel (2001) and Scott and Wheeler (2001). They are the American Society of Civil Engineers (ASCE); the American Concrete Institute (ACI) ; ASTM International; the Civil Engineering Research Foundation (CERF) Highway Innovative Technology Evaluation Center (HITEC); the Intelligent Sensing for Innovative Structures (ISIS), a Canadian Center of Excellence; The International Conference of Building Officials (ICBO); the FHWA Innovative Bridge Research and Construction (IBRC) Program; the Department of Defense (DoD) Defense Advanced Research Projects Agency (DARPA); and the Market Development Alliance (MDA) of the FRP Composites Industry. Further support for these efforts is provided by several State Departments of Transportation and City and County engineering offices.

The current status of standards in the United States is as follows. The recent publication of the ACI 440 document "Guide for the Design and Construction of Concrete Reinforced with FRP Bars" (2001) is a major step toward the establishment of accepted design protocols in the United States. The standardization of FRP panels for vehicular bridge applications have not progressed this far; a recent publication (Bank et al., 2002) outlines the suggested parameters and guidelines of a model specification for the use of FRP, in general, in structures. No design guidelines for FRP panels are currently available for public use. A product selection guide is currently available from MDA (2000); the guide outlines the current status of FRP specifications in the United States, as well as in Canada, Europe, and Japan. It also outlines a list of current FRP product manufacturers and their products, detailing both the material properties and bridge projects completed utilizing the FRP products. Moreover, based on their findings, MDA is in the development stage of a performance standard and contractual standards for the use of FRP panels in bridge construction. The issue of industry standards for FRP materials in the United States will be discussed in further detail in Section 9.

The feasibility and effectiveness of using FRP composite bridge materials need to be demonstrated. Currently there are fewer than 50 vehicular bridges that have been constructed using FRP composites as the primary structural material in the United States; a number of these will be outlined in the Section 1.3. In 2001, the Ohio State Legislature partially funded an initiative to replace 100 bridge decks in the State of Ohio using this FRP composite technology; this is evidence that the technology has been developing rapidly in recent years. Nonetheless, both laboratory and in-situ validation of the

technology of FRP composite materials for bridge construction are still needed to verify, among other things, their constructability and long-term in-situ durability.

If this technology can be proven as a viable construction material, there is a great potential for enhancing the transportation infrastructure in the United States. FRP materials have an attractive potential in both the rehabilitation of existing structures and in new construction. For new construction, FRP bars for reinforcement of concrete or FRP bridge panels could be utilized. For rehabilitation of existing structures, FRP bridge deck panels hold the most promise, while a smaller area of application would be for FRP-RC deck panels to be supported by steel girders. Some key elements that FRP materials could address would be (a) combating the corrosion of steel reinforcement in severe environments, (b) addressing the issue of slow construction processes for bridge replacement with traditional materials, and (c) decreasing dead load when FRP panels are utilized as replacement bridge deck panels, potentially addressing load posting and seismic concerns.

1.2. OBJECTIVES/TECHNICAL APPROACH

The overall objective of this research project was to conduct an extensive study of the behavior and use of glass fiber-reinforced polymer (GFRP) and carbon FRP (CFRP) materials for bridge construction. In particular, GFRP honeycomb sandwich panels were used as bridge panels and steel-supported bridge deck panels and CFRP and GFRP bars were used as internal reinforcement for precast concrete bridge panels.

The research program consists of a series of investigations in the field and in the laboratory. Four short-span bridges are installed so as to outline the construction-related

issues associated with the use of these materials. The bridges are located in a residential area of St. James, Missouri, located in Phelps County. Each bridge utilizes FRP materials in a different structural system to investigate the feasibility of using FRP in each of these applications. In-situ load tests of the constructed bridges were conducted to illustrate the behavior of the overall structures, both in terms of panel behavior and installation details (e.g., panel-to-panel connections). Load testing following construction and at later ages was undertaken allowing the examination of the bridges' long-term performance under ambient outdoor environmental conditions. Finally, the third investigative series deals with the laboratory characterization of these materials as reinforcement in concrete and as bridge panels. In each case, the overall panel behavior is investigated in addition to characterizing the individual materials.

As previously mentioned, the use of FRP materials in bridge construction has been increasing steadily over the last several years with the construction of bridges using FRP sandwich bridge panels, FRP sandwich bridge deck panels supported by steel girders, and FRP bars as reinforcement for concrete. This research program utilizes all three of these technologies with the overall scope including the procurement of the design, manufacturing, and installation of four bridges. Of the three bridges that utilize FRP panels, one is comprised only of FRP panels, while the other two are FRP bridge deck panels supported by steel girders. One of the girder-supported bridge decks consists of longitudinal panels, the other of transverse panels. The bridge comprised solely of FRP panels illustrates the use of this technology for new construction. The FRP composite bridge decks illustrate the possibility of using this technology for bridge deck replacement. The FRP-RC bridge consists of longitudinal panels reinforced with FRP

bars and illustrates the potential for new bridge construction. Both types of construction consist of bridge panels that are pre-manufactured, transported to the site, erected, and assembled on-site. Table 1.1 outlines the location of each bridge according to the structure type.

Table 1.1 Bridge Location by Structure Type

Bridge Location	Bridge Structure
St. Johns Street	Transverse FRP deck panels supported by steel girders
Jay Street	Longitudinal FRP deck panels supported by steel girders
St. Francis Street	FRP panels
Walters Street	FRP-RC

GFRP materials are used to construct the FRP honeycomb sandwich panels for the St. Johns Street, Jay Street, and St. Francis Street Bridges. The phrase FRP honeycomb sandwich refers to the construction of the panels themselves, which are comprised of a core of corrugated FRP material "sandwiched" between two faces of solid FRP material. Kansas Structural Composites, Inc. located in Russell, Kansas, manufactured and installed the bridge panels. The method of fabrication of the panels is manual hand lay-up, which is described in Appendix A. The reinforced concrete (RC) panels for the Walters Street Bridge are reinforced with commercially available CFRP and GFRP reinforcing bars. The FRP bars were provided by Marshall Industries Composites, Inc. located in Lima, Ohio, and the FRP-RC panels were manufactured and

installed by Oden Enterprises, Inc. located in Wahoo, Nebraska. Figure 1.1 illustrates the FRP materials utilized for this project.

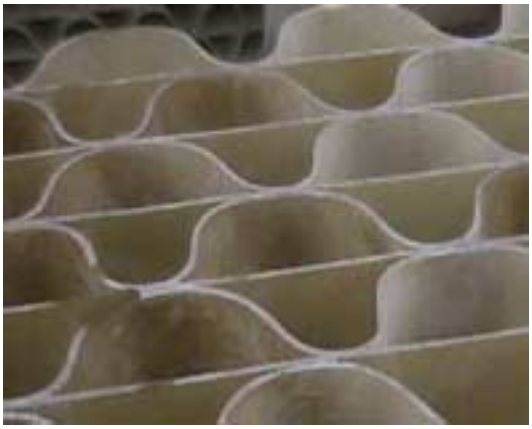

(a) Corrugated GFRP core

(b) Bundled CFRP Bars

Figure 1.1 FRP Materials Utilized

The expected benefits of this research program are:

- Laboratory characterization of FRP bars and FRP-RC panels
- Laboratory characterization of FRP honeycomb sandwich panels and their constituent materials
- In-situ characterization of FRP-RC panels and FRP honeycomb sandwich panels
- Investigation of the durability performance of FRP bars and FRP honeycomb sandwich panels
- Evaluation of construction techniques for FRP-RC panels and FRP honeycomb sandwich panels

- Provide assistance in the development of specifications for bridge construction with FRP materials by adding to the body of knowledge

This research program focuses on determining the appropriate factors for design using FRP materials in bridge construction. In particular, the necessary material properties, design parameters (e.g., live load impact factors and wheel load distribution factors), and design protocols (e.g., serviceability predictions) are the focus of this research with the ultimate goal being to assist the industry in developing material and design standards for FRP materials. In this way, FRP materials may become a viable alternative to traditional materials for the improvement of our Nation's deteriorating infrastructure.

1.3. PREVIOUS RESEARCH

Previous research in three particular areas will be delineated herein. The areas are related to the particular FRP materials examined in this study and consist of FRP bridge panels, FRP-RC, and durability of FRP materials.

1.3.1. FRP Bridge Panels. At present, there are only a few FRP panel manufacturers in the United States. They are Hardcore Composites located in New Castle, Delaware; Kansas Structural Composites, Inc. located in Russell, Kansas; Infrastructure Composites International located in San Diego, California; Martin Marietta Composites located in Raleigh, North Carolina; Webcore Technologies located in Kettering, Ohio; CON/SPAN Bridge Systems located in Dayton, Ohio; Creative Pultrusions, Inc. located Alum Bank, Pennsylvania; 3Tex, Inc. located in Cary, North

Carolina; Composite Products, Inc. located in St. Louis, Missouri; and Strongwell located in Bristol, Virginia. Each offers FRP panels of a slightly different configuration; the two main structural configurations are (a) sandwich panels, which consist of a mostly hollow core material between two solid faces of FRP material, and (b) adhesively bonded pultruded shapes. A brief comparison of the systems provided by several of these FRP panel manufacturers is provided by Zhou (2001).

Information regarding several others of the bridges utilizing FRP panels installed in the United States can be found in the following references organized by bridge. When provided in the literature, the relevant design parameters are outlined herein. It should be noted that this is not a comprehensive list, providing only an outline of selected projects to provide details regarding the first major projects and to give a sense of the geographical distribution of projects within the United States. A brief summary of these projects is outlined in Table 1.2.

No-Name Creek Bridge – The No-Name Creek Bridge is located in Russell, Kansas and was the first vehicular bridge constructed entirely of FRP panels in the United States. The total span length of the single span structure is 23 ft (7.01 m). The FRP panels were provided by Kansas Structural Composites, Inc. The bridge was design using finite element modeling (FEM) satisfying American Association of State Highway and Transportation Officials (AASHTO) (1996) recommendations for a standard HS20-44 truck loading and a minimum span-to-deflection ratio of 500. Details about the project have been outlined by Gill and Plunkett (2000).

Laurel Lick, Wickwire Run, and Market Street Bridges – The Laurel Lick, Wickwire Run, and Market Street Bridges are located in Lewis County, West Virginia;

Table 1.2 Summary of Bridges with FRP Panels

Date	Bridge	Location	Manufacturer
October 1996	No-Name Creek Bridge	Russell, Kansas	Kansas Structural Composites, Inc.
May 1997	Laurel Lick	Lewis County, West Virginia	Creative Pultrusions
June 1997	INEEL Bridge	Idaho Falls, Idaho	Martin Marietta Composites
July 1997	Tech21 Bridge	Butler County, Hamilton, Ohio	Martin Marietta Composites
September 1997	Wickwire Run Bridge	Taylor County, West Virginia	Creative Pultrusions
1997	Market Street Bridge	Ohio County, West Virginia	Creative Pultrusions
September 1998	Bennett's Creek	West Union, New York	Hardcore Composites
October 1998	Laurel Run	Somersat County, Pennsylvania	Hardcore Composites
November 1998	Muddy Run	Newark, Delaware	Hardcore Composites
Summer 1999	I-192	New Castle County, Delaware	Hardcore Composites
September 1999	Bentley Creek	Elmira, New York	Hardcore Composites
September 1999	Salem Avenue	Dayton, Ohio	Composite Deck Solutions, Creative Pultrusions Inc., Hardcore Composites, Inc. and Infrastructure Composites International

Taylor County, West Virginia; and Ohio County, West Virginia, respectively. The overall bridge lengths of these single span structures are 20 ft (6.10 m), 31 ft (9.45 m) and 179 ft (54.56 m), respectively. The Laurel Lick Bridge utilizes FRP girders spaced at 2.5 ft (0.8 m) on-center to support FRP deck panels, while the Wickwire Run and Market Street Bridges consist of FRP deck panels supported by steel girders spaced at 6 ft (1.8 m) and 8.5 ft (2.6 m), respectively. Deck panels for the project were provided by Creative Pultrusions Inc. The bridges were designed satisfying AASHTO (1996) recommendations for a standard HS25-44 truck loading. Details about these projects have been outlined by Shekar et al. (2002).

INEEL Bridge – The INEEL Bridge is located in Idaho Falls, Idaho. The overall bridge length of this single span structure is 30 ft (9.1 m); the bridge consists of FRP deck panels. FRP materials for the project were provided by Martin Marietta Composites. The bridge was designed satisfying AASHTO (1996) recommendations for a standard HS20-44 truck loading.

Tech21 Bridge – The Tech21 Bridge is located on Smith Road in Butler County, Ohio. The total span length of this single span structure is 33 ft (10.1 m); the bridge consists of FRP box beams and deck panels. FRP materials for the project were provided by Martin Marietta Composites. The bridge was designed using FEM satisfying AASHTO (1996) recommendations for a standard HS20-44 truck loading and a minimum span-to-deflection ratio of 800. Details about the project have been outlined by Zoghi et al. (2002).

Bennett's Creek – The Bennett's Creek Bridge is located in Steuben County, New York. The overall bridge length is 23 ft (7.0 m); the bridge consists of FRP bridge

panels. FRP panels for the project were provided by Hardcore Composites. The bridge was designed satisfying AASHTO (1996) recommendations for a standard HS25-44 truck loading and a minimum span-to-deflection ratio of 800; the strain in the FRP materials was limited to 20 percent of ultimate. Details about the project have been outlined by Alampalli et al. (2000) and Alampalli et al. (2001).

Laurel Run Bridge – The Laurel Run Bridge is located in Somerset County, Pennsylvania. The overall bridge length of this single span structure is 25 ft (7.62 m); the bridge consists of FRP deck panels supported by steel girders spaced at 2.9 ft (0.9 m) on-center. Deck panels for the project were provided by Creative Pultrusions Inc. The bridges were designed satisfying AASHTO (1996) recommendations for a standard HS25-44 truck loading. Details about the project have been outlined by Shekar et al. (2002).

Muddy Run Bridge – The Muddy Run Bridge is located on I-351 over Muddy Run in Glasgow, Delaware. The overall bridge length of this single span structure is 32 ft (9.7 m); the bridge consists of FRP bridge panels. FRP panels for the project were provided by Hardcore Composites. The bridge was design according to AASHTO Load and Resistance Factor Design (LRFD) (1994) recommendations for service, fatigue, and strength limit states for a standard HS25-44 truck loading. Details about the project have been outlined by Chajes et al. (2000).

Bridge I-192 – Bridge I-192 is located in New Castle, Delaware. The total span length of this single span structure is 35 ft (10.7 m); the bridge consists of FRP bridge panels supported by steel girders spaced 2.8 ft (0.9 m) on-center. FRP panels for the project were provided by Hardcore Composites. The bridge was design according to

AASHTO (1996) recommendations for minimum span-to-deflection ratio of 800. Details about the project have been outlined by Chajes et al. (2001).

Bentley Creek Bridge – The Bentley Creek Bridge is located in Chemung County, New York. The simple-span through truss bridge is 140 ft (42.7 m) in length; the bridge consists of FRP deck panels supported by the steel truss floor beams of the superstructure which are spaced at 14 ft (4.3 m) on-center. FRP panels for the project were provided by Hardcore Composites. The bridge was designed satisfying AASHTO (1996) recommendations for a standard HS25-44 truck loading, while limiting the compressive, tensile and shear stresses in the FRP materials to 56 percent of the respective ultimate strength values. Details about the project have been outlined by Wagh (2001). It should be noted that this project was presented an award by National Steel Bridge Alliance (NSBA) in 2000 for its use of FRP panels in bridge reconstruction; the FRP panels replaced the deteriorated concrete decks panels and the steel superstructure of the bridge was utilized.

Salem Avenue Bridge – The Salem Avenue Bridge is located in Dayton, Ohio. The overall bridge length is 679 ft (207.0 m), with span lengths of 130 ft (39.6 m), 137 ft (41.8 m), 145 (44.2 m), 137 ft (41.8 m), and 130 ft (39.6 m). The bridge consists of FRP deck panels supported by steel girders spaced 8.75 ft (2.7 m) on-center. Deck panels for the project were provided by Composite Deck Solutions, Creative Pultrusions Inc., Hardcore Composites, Inc. and Infrastructure Composites International, the intent being to evaluate several FRP panel technologies in one project. Details about the project have been outlined by Henderson (2000) and Reising et al. (2001).

Published laboratory test results from testing conducted on the FRP panels manufactured by Kansas Structural Composites, Inc. are limited. Research presented by Gill and Plunkett (2000) and Nagy and Kunz (1998) details laboratory testing, panel failure modes, and material property determination. Davalos et al. (2001) and Nagy et al. (1996) present FEM of the FRP sandwich panels and theoretical material property determination. This work is referenced within Section 5 for comparison with the results obtained in this study.

Considerable work in the area of sandwich panel theory application to civil engineering was developed by Allen (1969) and Vinson (1986). Due to the construction of the sandwich panels, it is assumed that the tensile and compressive forces are primarily carried by the top and bottom faces, while the shear forces are primarily carried by the core material. The same concepts are illustrated when the behavior of I-shaped members are considered; most often sandwich panels are analyzed by disregarding the hollow spaces in the core and approximating the section as an I-shaped member resulting in a conservative approach. Sandwich panel theory considers both the contributions of bending-induced and shear-induced deflections of the member to its overall behavior. Further details regarding sandwich panel theory will be discussed in Section 5, taking into account the specific properties of the FRP panels examined in this study.

1.3.2. FRP-Reinforced Concrete. There are only a handful of FRP reinforcing bar manufacturers in North America. They include Marshall Industries Composites located in Lima, Ohio; Hughes Brothers Composites located in Seward, Nebraska; Composite Rebar Technology located in Salem, Oregon; Nubar, Inc. located in Tulsa, Oklahoma; and Pultrall located in Quebec, Canada. Each offers FRP panels of a slightly

different configuration however the main idea is the same; the two main structural features are (a) longitudinal fibers embedded in a polymeric resin and (b) a means of providing for bond between the bars and the concrete. The aforementioned ACI 440 design guidelines (2001) contain a plethora of information regarding FRP reinforcing bars for concrete. The basic idea is the same as conventional reinforced concrete, whereby instead of using steel reinforcing bars, FRP reinforcing bars are utilized. The design protocols are outlined in Section 3.4.

The majority of FRP-RC projects conducted have been undertaken in Japan, Europe and Canada, with more than 100 projects conducted in Japan alone to date (ACI, 2001). In light of the fact that FRP-RC technology is more developed than that of FRP bridge panels and the fact that fewer demonstration projects have been conducted in the United States, a shorter review of other bridge projects will be given herein. A brief summary of these projects is outlined in Table 1.3. The results of the research conducted prior to publication of the ACI 440 guidelines (2001) would be contained therein and will not be reiterated here.

Worth noting is the first FRP-RC bridge constructed in the United States, the Buffalo Creek Bridge, which is a 177-ft (54-m) three-span continuous bridge; FRP bars provided by Marshall Industries Composites, Inc. are the primary flexural reinforcement. Designed and constructed prior to the release of the ACI (2001) design guidelines, the bridge was design according to procedures developed by the Constructed Facilities Center at West Virginia University.

The previously mentioned Salem Avenue Bridge in Dayton, Ohio, in addition to utilizing FRP panels for the superstructure, utilized FRP-RC for the concrete deck on one

portion of the structure. GFRP bars provided by Marshall Industries Composites Inc. were used for the compression reinforcement.

Alkhrdaji (2001) details the construction of an FRP-reinforced box culvert bridge. The structure is located in Rolla, Missouri, and used only GFRP reinforcement; the reinforcing bars were provided by Hughes Brothers Composites. Laboratory testing to assess the ultimate performance of the box culverts and in-situ load testing to assess the service performance of the structure are outlined. The bridge was designed according to AASHTO (1996) recommendations for a standard HS15-44 truck loading using the ACI 440 design guidelines (2001).

A comprehensive outline of the design considerations for FRP-RC is given by Bradberry (2001). The Sierrita de la Cruz Creek Bridge, located in Potter County, Texas, is 553 ft (168.6 m) long and utilizes GFRP bars, manufactured by Hughes Brothers Composites, as the top mat for two of the four bridge spans. The concrete deck is supported by prestressed concrete Texas Type “C” beams. Hughes Brothers provided the GFRP bars for this project. The bridge was design according to AASHTO (1996) recommendations for a standard HS20-44 truck loading using the ACI 440 design guidelines (2001).

Nanni (2001) outlines recent applications where FRP reinforcement, specifically several of the projects mentioned herein are detailed, including the box culvert just mentioned, the project detailed by Bradberry (2001) and the FRP-RC bridge covered by this project.

Table 1.3 Summary of Bridges with FRP-RC

Date	Bridge	Location	Manufacturer
October 1996	Buffalo Creek Bridge	McKinleyville, West Virginia	Marshall Industries Composites, Inc.
September 1999	Salem Avenue	Dayton, Ohio	Marshall Industries Composites, Inc.
October 1999	Walker Street Bridge	Rolla, Missouri	Hughes Brothers Composites
March 2000	Sierrita de la Cruz Creek	Potter County, Texas	Hughes Brothers Composites

1.3.3. Durability of FRP Materials. Although GFRP materials have been steadily gaining acceptance for use in the construction industry, there remains a need to document their long-term durability performance and predict their service life. The majority of FRP durability research is conducted on GFRP materials, with the belief that CFRP materials are less susceptible to degradation. The durability of CFRP bars will not be examined in this study; therefore, previous research on the subject will not be discussed.

A comprehensive report on the current state of FRP durability research is outlined by CERF (2001). The report defines durability as the ability of a material or structure "to resist cracking, oxidation, chemical degradation, delamination, wear, and/or the effects of foreign object damage for a specified period of time, under the appropriate load conditions, under specified environmental conditions." Detailed within the report are previous research and prioritized future research needs in the major research areas of (a) the effects of moisture and aqueous solutions, (b) the effects of alkaline environments, (c)

thermal effects, (d) the effects of creep and relaxation, (e) the effects of fatigue, (f) the effects of ultraviolet (UV) radiation, and (g) the effects of fire. Salient points provided by CERF (2001) and ACI (2001) are summarized as follows:

- Some glass fibers have been shown to degrade when subjected to moisture and/or alkaline solutions.
- Some resin systems are more effective than others in protecting the glass fibers from moisture and/or alkaline attack.
- Since the vulnerability of undercured FRP materials to the absorption of water increases, it is recommended that FRP materials be fully cured prior to their use in the field.
- Recommendations, due to water absorption properties, that FRP material are cured at a temperature such that the resulting glass transition temperature, T_g, will be considerably higher than the service temperature of the material.
- The use of epoxy resins and vinyl ester resins are preferred, versus less durable polyester resins, due to their ability to protect the fibers within the FRP materials.
- Exposure to elevated temperatures, in some cases, will provide additional strength to the FRP materials as the exposure to a temperature above the processing temperature will facilitate further curing of the resin.
- Curing of FRP materials at ambient conditions can result in undercured products that are more susceptible to creep and micro-crack initiation.
- The combined effects of moisture/immersion in solution and thermal conditioning need a considerable amount of further research.

- The composition of alkaline solutions should be formulated such that the chemical composition and the pH of the solution are representative of concrete pore water.
- When testing at elevated temperatures is conducted in combination with solution immersion, a maximum temperature of 140ºF (60ºC) is recommended.

It should be noted that only general comments regarding the durability of GFRP materials are made in this Section. This is due primarily to the fact that the results of the durability testing conducted to date are very difficult to interpret for widespread application to all GFRP materials. There exist a vast number of GFRP materials with various combinations of fiber and resin types that have been tested after exposure to a number of different conditioning regimens. As reported by CERF (2001), a standard set of testing protocols will need to be developed, including both conditioning regimens and test methods, in order to facilitate comparison and application of the durability testing results obtained.

The durability investigations conducted in this study were modeled after work previously conducted by Micelli and Nanni (2001) and Myers et al. (2001) and take into consideration the recommendations put forth by CERF (2001). The methods of testing the specimens were taken from their recommendations and the method of conditioning was maintained to facilitate comparison of results. This work also considered the recommendations of the manufacturer of the FRP reinforcing bars, who had conducted durability studies of the GFRP bars subjected to an alkaline solution, and the studies of Springer (1984), Vijay and GangaRao (1999). Other researchers in the area include

Karbhari, Benmokrane, Dutta, Lesko, and Bakis who contributed significantly to the aforementioned CERF publication (2001).

1.4. OUTLINE OF THE REPORT

First, in Section 2, the contractual events leading up the initiation of the project, specifically the selection of the project contractors, are detailed so that all parties involved are clearly identified. Sections 3 and 4 are outlined by bridge and contain the details of the design of the four project bridges and the installation of the four project bridges, respectively. Please note that this information is presented prior to information regarding the laboratory testing because the configuration of the specimens was identical to that of the constructed bridges.

Sections 5 and 6 describe the laboratory testing conducted on the FRP panels and the FRP-RC panels, respectively, and include a discussion of the results as they pertain to each of these structure types. Laboratory testing is followed by in-situ bridge load testing, which is outlined in Section 7. Relevant parameters, including deflection, obtained during testing are compared to the parameters utilized during design. Section 8 contains the conclusions of the research as they relate to the laboratory and field testing. Recommendations both in terms of FRP standard development and for future research are delineated in Sections 9 and 10, respectively.

1.5. OTHER PROJECT PUBLICATIONS

Publications detailing several aspects of this research investigation have been written throughout the project. Not included in this listing are a number of short article in newsletters, etc. that have described small portions of the project (e.g., the installation of the bridges or an overall description of the project).

- "Durability of GRFP Rods, Laminates, and Sandwich Panels subjected to Various Environmental Conditions." D. Stone, D. Koenigsfeld, J. Myers and A. Nanni. Second International Conference on Durability of Fiber Reinforced Polymer (FRP) Composites for Construction, May 29-31, 2002, Quebec, Canada. (In print)
- "Deflection Assessment of an FRP-Reinforced Concrete Bridge." D. Stone, A. Prota and A. Nanni. ACI Spring Convention, April 21-26, 2002, Detroit, MI. (ACI Special Publication to be in print late 2002)
- "Performance Evaluation of an FRP-Reinforced Concrete Bridge." D. Stone, A. Prota and A. Nanni. 81st Annual Transportation Research Board Meeting, January 13-17, 2002, Washington, D.C. (CD-Rom version)
- "Investigation of FRP Materials for Bridge Construction." D. Stone, S. Watkins, H. Nystrom and A. Nanni. Fifth National Workshop on Bridge Research in Progress, C.K. Shield and A.E. Schultz, Eds. University of Minnesota, Twin Cities, October 8-10, 2001, Minneapolis, Minnesota, pp. 145-150. (In print)
- "Field and Laboratory Performance of FRP Bridge Panels." D. Stone, A. Nanni and J. Myers. Proc., Composites in Construction International Conference, J. Figueiras, L. Juvandes, and R. Faria, Eds. October 10-12, 2001, Porto, Portugal, pp. 701-706. (In print)

- Shipley, Tom. *FRP Reinforced Concrete: An Infrastructure Solution.* University of Missouri-Rolla Video Communications Center, 2001. (Video format, included in Appendix C)
- Shipley, Tom. *FRP Sandwich Panels: An Infrastructure Solution.* University of Missouri-Rolla Video Communications Center, 2001. (Video format, included in Appendix C)

2. PROJECT PARTICIPANTS

Generally speaking, the University of Missouri – Rolla (UMR) does not become involved in full-scale construction projects in the role of general contractor. Due to the unprecedented opportunity presented by this project, the fact that the City of St. James initiated UMR involvement and the use of the innovative materials, it was concluded that the direct involvement of the University was justified. A summary of the contractual issues related to this project is included as follows. It should be noted that all contractual agreements entered into by UMR were, as is standard procedure, managed and administered by the Construction Management Office of Physical Facilities.

This project initiated when the City of St. James, Missouri, received a Community Development Block Grant (CDBG) from the Missouri Department of Economic Development to re-channel a creek that had been prone to flooding. To oversee the engineering aspects of the project, the City of St. James, hired two engineers-of-record: Elgin Surveying and Engineering, Incorporated and WSW Hydro Consulting Engineers and Hydrologists, LLC. The project, entitled the "St. James CDBG Stormwater Project," was let for bid on January 20, 2000, with bids accepted until February 7, 2000. Included in the bid items for the project were the moving of several utilities, the demolition of the existing bridges, the casting of the abutments for four bridges, the installation of one box culvert bridge, and the seeding and mulching of the project area. Upon review of the submitted bids, the City of St. James contracted with A&D Construction of California, Missouri.

Wanting to incorporate a research component into this project, the City of St. James and UMR entered into a research agreement. According to the research agreement the University is classified as an independent contractor of the City of St. James and would be required to procure the manufacturing and installation of the four project bridges. Specifically, the University would need to provide three FRP composite bridges and one FRP-RC bridge. Moreover, the research agreement detailed liability issues, financial assistance, publication issues, and the obligations of both parties.

Given that the University has no bridge manufacturing or installation capabilities, an FRP bridge manufacturer and concrete precaster would need to be identified. The following figure, Figure 2.1, illustrates the initial project participants. The next sections will outline the selection of the FRP bridge contractor and the FRP-RC bridge contractor, respectively.

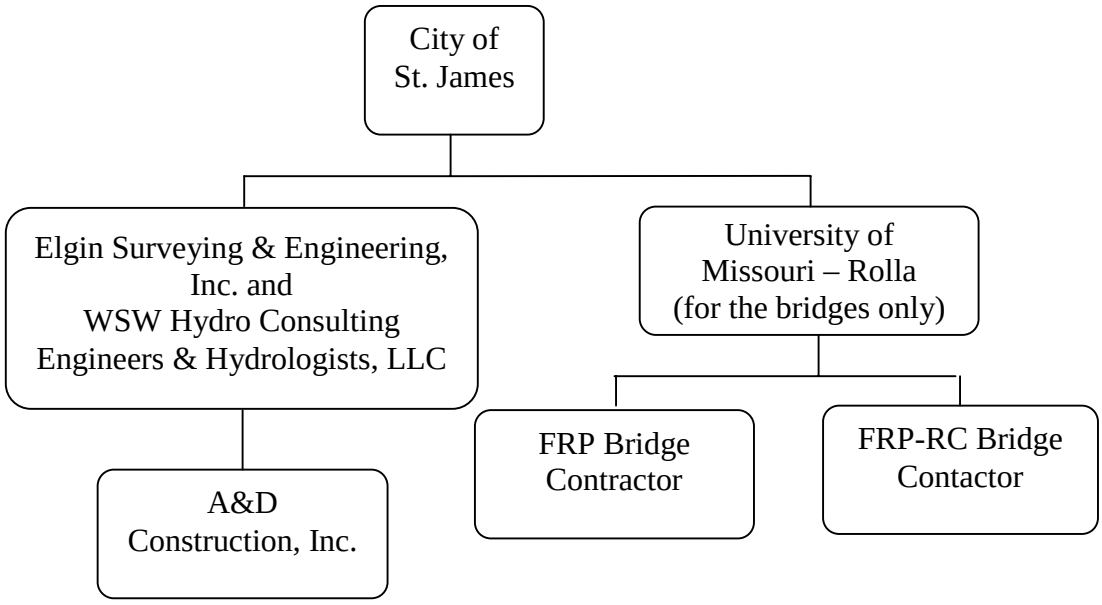

Figure 2.1 Project Participants

2.1. FRP BRIDGE CONTRACTOR

In all cases where the total cost of a purchase exceeds $5000, per University regulations, a process by which bids are submitted and reviewed is utilized. In this case, a request for proposals (RFP) was employed due to the technical specifications required within the project.

The process of selecting an FRP bridge contractor was accomplished with an RFP, which was sent on March 1, 2000, to several companies with FRP bridge panel manufacturing capabilities. A list of the companies to whom the RFP was sent can be found in Appendix B.

The RFP was written so as to guard the University from any and all liability. It included information about the contract, payments, schedule, program requirements, and proposal evaluation and selection. Refer to Appendix B for Sections 1.F and 1.G of the RFP, which outline the program requirements and the standards for proposal evaluation and selection, respectively.

The program requirements for the bridges were broken up into the following sections: bridge design, bridge manufacturing, bridge installation, transportation, research specimens, and inspection and maintenance manual. Key requirements include the need for the bridge design to be sealed by a registered professional engineer (P.E.), the design load and deflection requirements, the submission of an inspection and maintenance manual, and the necessary dates for installation. Once the program requirements were defined a means of evaluating the submitted proposals for selection of the “apparent low proposer” was necessary. Each of the program requirements, with the exception of transportation, was assigned a point value and an addition evaluation criterion of

engineering and specifications was added. The evaluation criteria would establish a justifiable ranking scale; using the total point value divided by the cost of the proposal the "apparent low proposer" could be selected.

The deadline for proposal submission was March 15, 2000 and of the 13 companies to whom the RFP was provided only two submitted a proposal; Hardcore Composites of New Castle, DE, and Kansas Structural Composites, Inc. of Russell, Kansas. An evaluation team was established and consisted of Richard Elgin, Owner of Elgin Surveying and Engineering, Inc.; John Johnson, Assistant Director of Physical Facilities at UMR; Randy Mayo, Area Engineer for the Missouri Department of Transportation; Dave Meggers, Research Development Engineer for the Kansas Department of Transportation; Antonio Nanni, Jones Professor of Civil Engineering at UMR; Halvard Nystrom, Assistant Professor of Engineering Management at UMR; Marvin Patton, Director of Physical Facilities; and Danielle Stone, Ph.D. Candidate in Civil Engineering at UMR. Following individual review of the proposals, the evaluation team met to discuss their findings.

The evaluation meeting was conducted by reviewing the program requirements, as outlined in Section 1.F of the RFP and determining how each proposal addressed each requirement. It should be noted that the proposals were initially evaluated without knowledge of the price quote. As the evaluation of each section (i.e., bridge design, bridge manufacturing, etc.) was completed the team assigned points for that section and then proceeded to the next section. The following table, Table 2.1, outlines the point breakdown for each section and the total number of points awarded to each proposal. It

may be noted that the number in parentheses is the total number of points possible for the criteria.

Table 2.1 Proposal Evaluation

Evaluation Criteria	Hardcore Composites	Kansas Structural Composites, Inc.
1.a. Bridge Design – General Requirements (65)	50	60
1.b. Bridge Design – Innovation (40)	20	40
1.c. Bridge Design – Aesthetic Issues (10)	6	6
1.d. Bridge Design – Maintenance Issues (10)	7	5
2. Bridge Manufacturing (75)	50	65
3. Bridge Installation (100)	30	80
4. Research Specimens (100)	80	100
5. Inspection and Maintenance Manual (50)	50	35
6. Engineering and Specifications (50)	25	25
Total Quality Points	**318**	**416**

After the evaluation was completed, the selection began. The portion of the proposal containing the price quote for each proposal was opened. The proposal with the lowest cost/point ratio would be selected as the apparent low proposer. Based on the criterion outlined in the RFP, the apparent low proposer was Kansas Structural Composites, Inc. They had the highest number of quality points, the lowest cost, and therefore the lowest cost/point ratio. Clarification and negotiation of a contract with Kansas Structural Composites, Inc. (hereafter referred to as KSCI) was initiated.

2.2. FRP-RC BRIDGE CONTRACTOR

A sole-source agreement was established with Oden Enterprises for the manufacturing and installation of the FRP-RC panel bridge. Oden Enterprises was identified as a potential contractor when they requested a copy of the RFP for the bridges utilizing FRP panels. Their willingness to cast concrete panels utilizing the FRP reinforcement and their ability to provide a proven bridge system warranted their selection under a sole-source agreement. The FRP reinforcing bars were provided by Marshall Industries Composites, Inc. under a separate sole-source agreement.

2.3. OTHER PARTICIPANTS

It is worth mentioning at this point the involvement of three additional firms with design of the bridges. The first two firms, Kirkham Michael Consulting Engineers and BG Consultants, Inc., were under contract with KSCI to design the steel girders (i.e., for the two bridges that utilize FRP deck panels) and the FRP panels, respectively. The third design firm, Speece Lewis Engineers, is under contract with Oden Enterprises, Inc. for the overall design of the precast concrete bridge panels. The design firms mentioned provided the professional engineers seal for the construction plans for the drawings. The final organization of project participants is illustrated in Figure 2.2 below.

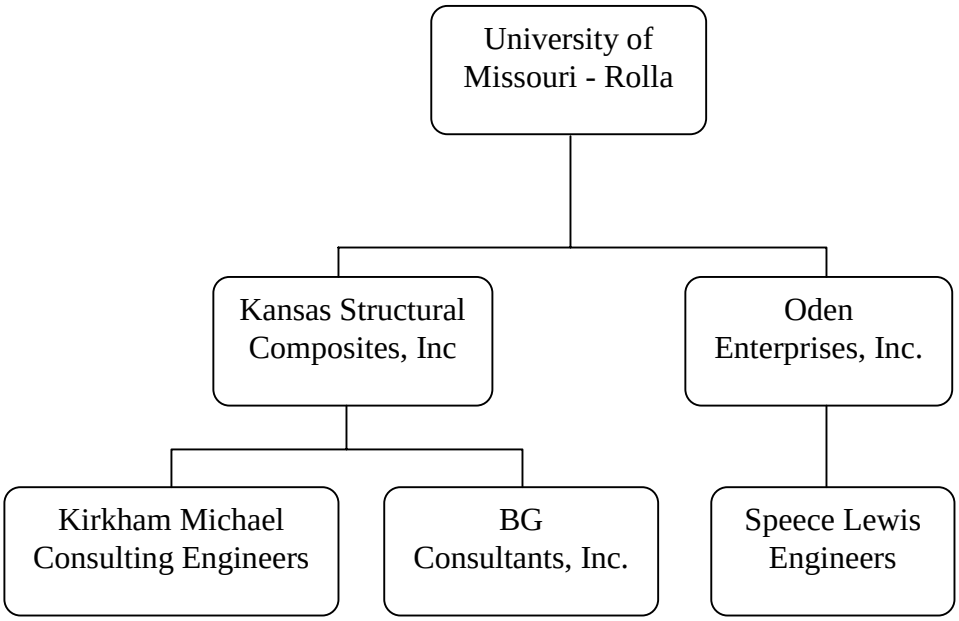

Figure 2.2 Final Project Participant Organization

3. DESIGN OF THE BRIDGES

The design of all four of the St. James Bridges was based on AASHTO deflection criteria and standard loads. Standard HS20-44 and HS15-44 truck loading configurations were utilized based on AASHTO Section 3.7.4. (1996); the HS15-44 truck loading was utilized only for the Walters Street Bridge, with details given in Section 3.4. Figure 3.1 illustrates axle loading for the HS20-44 truck; the spacing between the respective axles is 14 ft (4.27 m). For the HS15-44, which utilizes the same axle spacing, the axle loads from the front of the truck to the rear are 6,000 lb (26.7 kN), 24,000 lb (106.8 kN) and 24,000 lb (106.8 kN), respectively. Although this could be considered excessive for a residential area, following current design practices was considered to be the most appropriate procedure.

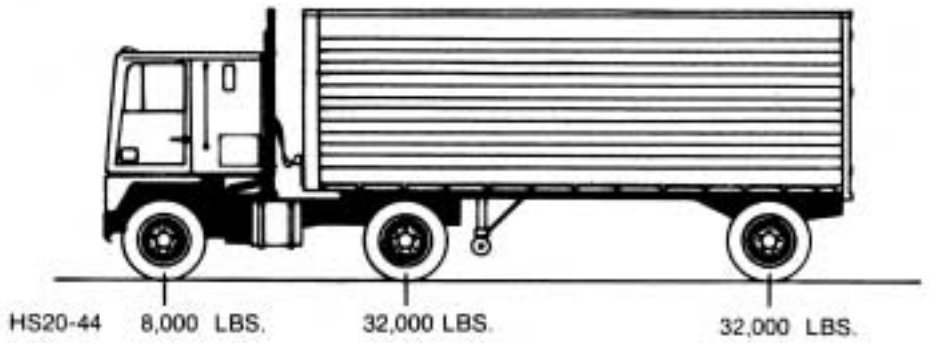

Note: 1000 lb = 4.448 kN

Figure 3.1 HS20-44 Truck Loading

The deflection criterion for the design of the bridges was set at a maximum value of span length divided by 800, based on AASHTO Section 8.9.3.1 (1996). It is important to note that due to the relative low modulus of the FRP materials utilized, serviceability is

often the controlling factor for design. Design calculations for each of the four bridges are outlined in the following sections. Appendix C contains the as-built drawings for each of the bridges as a reference.

With respect to the design of the FRP panels, various installation calculations were also performed on the FRP panel structures including backfill pressure, uplift pressures, etc. for transient and permanent loads, considering the connection of the panels to the girders, the panels to one another, and the guardrail system. While these issues are vital to the proper performance of the bridge as a whole, as the focus of this research is the FRP technology, the particulars of these issues will not be discussed herein other than to say that they need to be considered in design. These calculations along with the structural capacity calculations presented by KSCI and BG Consultants are presented in Appendix D. The calculations for the FRP-RC bridge are detailed in Section 3.4. As a side note, it should be stated that a cross-slope was incorporated into the design of each of the bridges to facilitate drainage.

3.1. ST. JOHNS STREET BRIDGE

The St. Johns Street Bridge was designed by KSCI with the assistance of BG Consultants, Inc. for the FRP panel design and the assistance of Kirkham Michael Consulting Engineers for the design of the steel girders. The design of the steel girders will not be covered in this report as the focus is on the use of FRP technologies; several significant parameters of the girder design will however be mentioned for reference purposes. An outline of the deflection and stress checks on the final panel design as conducted by KSCI and BG Consultants, Inc. is provided herein.

The girders were designed according to AASHTO recommendations (1996) to meet the span length divided by 800 deflection requirement. A wheel load distribution factor of 1.096 was utilized as was a live load impact factor of 0.3. Furthermore, the girders were designed assuming no composite action with the panels. The final steel girder design consisted of seven built-up steel members of size W14 × 90. The center-to-center spacing of the girders was 3.92 ft (1.19 m), the flange width was 12 in (0.30 m) and the overall section depth was 14 in (0.36 m). The steel girders were connected by steel diaphragms at four longitudinal positions with spacing of 6.25 ft (1.91 m) between the diaphragms.

The FRP panels manufactured by KSCI are composed of glass fiber and isophthalic polyester resin. As mentioned previously, they are comprised of a layer of corrugated core materials between two solid face layers of FRP, which is comprised of several layers of oriented glass fibers. It should be noted that the panels are constructed by proportion of fiber and resin weight; the fiber weight fraction of the FRP materials is approximately 40 percent. The configuration of the core is illustrated in Figure 1.1, with the overall panel structure exhibited in Figure 3.2; it should be noted that both the thickness of the core and faces can be varied depending on design of the bridge.

The final dimensions of the panels for the St. Johns Street Bridge are a top face thickness of 0.375 in (9.5 mm), a core thickness of 4 in (101.6 mm) and a bottom face thickness of 0.375 in (9.5 mm). Each of the six panels measures approximately 8.86 ft (2.70 m) in length and 12.75 ft (3.89 m) in width. The thickness of the individual layers in the core is 0.09 in (2.3 mm), resulting in a total thickness of 1.08 in (27.4 mm) for the 12 layers of core material in a representative 1-ft (0.30 m) section. Considering that the

corrugations of the core of the FRP panels run perpendicular to the direction of traffic, spanning from girder to girder, the moment of inertia based on these measurements is 48.932 in4 (2036.7 cm4) per 1-ft (0.3-m) wide section. It should be noted that for all of the FRP sandwich panels, the calculation of the moment of inertia is conducted assuming the section to be representative of an I-beam, whereby the hollow spaces in the core are ignored and only the FRP materials are considered. Figure 3.3 illustrates the overall structure of the St. Johns Street Bridge, exhibiting the seven steel girders and six FRP panels.

Figure 3.2 FRP Sandwich Panel Structure

Figure 3.3 St. Johns Street Bridge Structure

The distribution of load in the FRP deck panels was calculated assuming the same design factors utilized in the AASHTO design specifications (1996) for concrete slabs. The panels are assumed to be simply supported on the girders due to the connection method utilized between the panels and the girders, which will be outlined in Section 4.1. The worst-case loading condition for the HS20-44 loading truck would be the case where one wheel of the rear axle of the truck is located at mid-span between girders, generating the maximum positive moment. For the case where the main reinforcement is perpendicular to the traffic, the live load moment per 1-ft (0.30-m) width is determined by Equation 3.1 as follows:

$$M_{\max} = 0.8\left(\frac{S+2}{32}\right)P_{20} \qquad \textbf{(3.1)}$$

where Mmax is the maximum live load moment per 1-ft (0.30-m) width, S is the effective span length, and P20 is the load on one rear wheel of the HS20-44 loading truck and is equal to 16 kips (71.2 kN). Moreover, the factor of 0.8 is applied as a continuity factor and is used in this case considering an interior panel section. Using the calculated moment value, equal to 2.817 kip-ft (3.82 kN-m) for this bridge configuration, an equivalent load at the center of the span is determined. Recall that this value will be the equivalent load per 1-ft (0.30-m) width.

Assuming that there is no shear transfer between panels (i.e., that the entire wheel load is carried by one panel), the equivalent load per 1-ft (0.30-m) width, a value of 3.297 kips (14.67kN), is multiplied by the width of the panel, 8.86 ft (2.70 m), to determine the maximum load that could be carried by the panel. The allowable load on the panel, equal to 29.29 kips (130.29 kN) is greater than the HS20-44 wheel load plus impact, a value of

20.8 kips (92.52kN). It should be noted that the AASHTO live load impact factor, in this case equal to 0.30, is calculated via Equation 3.2 as follows:

$$IF = \frac{50}{L + 125} \quad \textbf{(3.2)}$$

where IF is the live load impact factor and L is the span length, in feet. This value is limited to a maximum of 0.30.

The maximum live load and dead load deflections are calculated based on simple beam theory utilizing a modulus of elasticity value of 1.94x103 ksi (13.38 GPa). It should be noted that this value was determined experimentally by KSCI and can be viewed in Appendix D; the determination of the modulus of elasticity is contained in the calculations for the St. Francis Street Bridge. In this case, utilizing the equivalent point load defined above and a dead load of 15.22 psf (0.72 kN/m2), the maximum deflection is 0.504 in (1.28 mm), which is comprised of deflections of 0.0499 in (1.27 mm) and 0.0005 in (0.01 mm) for the live and dead loads, respectively. The maximum predicted deflection corresponds to a span-to-deflection ratio of 821, meeting the design limit of 800.

Of additional interest in the design is the maximum stress in the panel. According to previous testing conducted by KSCI the maximum stress at failure of the specimen is 9825 psi (67.74 MPa). A factor of safety of 3.0 was applied to this value due to the experimental nature of the project and the materials used; the allowable stress in the FRP material was limited to 3275 psi (22.58 MPa). According to mechanical principles the bending stress in the extreme fiber of the panel was calculated utilizing the design parameters outlined previously; a maximum stress of 1640.7 psi (11.31 MPa) was

calculated for the St. Johns Street panels. This value is well below the allowable stress limit of 3275 psi (22.58 MPa).

3.2. JAY STREET BRIDGE

The Jay Street Bridge was designed by KSCI with the assistance of BG Consultants, Inc. for the FRP panel design and the assistance of Kirkham Michael Consulting Engineers for the design of the steel girders. Again, the design of the steel girders will not be covered in this report as the focus is on the use of FRP technologies. A brief discussion of the salient points of the girder design was outlined in Section 3.1 for the St. Johns Street Bridge; the quantity, size, and lateral spacing of the steel girders for the Jay Street Bridge were identical to those used for the St. Johns Street Bridge. An outline of the deflection and stress checks on the final panel design as conducted by KSCI and BG Consultants, Inc. is provided herein.

The final dimensions of the panels for the Jay Street Bridge are a top face thickness of 0.375 in (9.5 mm), a core thickness of 5.5 in (139.7 mm) and a bottom face thickness of 0.375 in (9.5 mm). The two interior panels measure approximately 7.83 ft (2.39 m) in width, while the two exterior panels measure approximately 4.92 ft (1.50 m) in width; all four of the panels measure approximately 26.92 ft (8.20 m) in length. The thickness of the individual layers in the core is 0.09 in (2.3 mm), resulting in a total thickness of 1.08 in (27.4 mm) for the 12 layers of core material in a representative 1-ft (0.30 m) section. As was the case for the St. Johns Street Bridge, the corrugations of the core of the FRP panels run perpendicular to the direction of traffic, spanning from girder to girder, resulting in a moment of inertia of 92.74 in^4 (3860.13 cm^4) per 1-ft (0.3-m)

wide section. The overall structure of the Jay Street Bridge, including the steel girders and FRP panels, is illustrated in Figure 3.4.

Figure 3.4 Jay Street Bridge Structure

The design procedure for the Jay Street Bridge is nearly identical to that followed for the St. Johns Street Bridge. Again, the panels are assumed to be simply supported on the girders due to the connection method utilized between the panels and the girders, which will be outlined for the Jay Street Bridge in Section 4.1. The worst-case loading condition for the HS20-44 loading truck would be the case where one wheel of the rear axle of the truck is located at mid-span between girders, generating the positive maximum moment. The distribution of load in the FRP deck panels was calculated assuming the same design factors utilized in the AASHTO design specifications (1996) for concrete slabs. For an exterior panel where the main reinforcement is perpendicular to the traffic, the live load moment per 1-ft (0.30-m) width is determined by Equation 3.3 as follows:

$$M_{max} = \left(\frac{S+2}{32} \right) P_{20} \qquad \textbf{(3.3)}$$

where M_{max} is the maximum live load moment per 1-ft (0.30-m) width, S is the effective span length, and P_{20} is the load on one rear wheel of the HS20-44 loading truck and is

equal to 16 kips (71.2 kN). Using the calculated moment value, equal to 3.52 kip-ft (4.77 kN-m) for this bridge configuration, an equivalent load at the center of the span was determined per 1-ft (0.30-m) width. Assuming that there is no shear transfer between panels (i.e., that the entire wheel load is carried by one panel), the equivalent load per 1-ft (0.30-m) width was calculated as 4.12 kips (18.33 kN). Again, the live load impact factor outlined in Equation 3.2 is utilized, which is equal to 0.30 in this instance.

The maximum deflection is calculated based on simple beam theory; utilizing the equivalent point load defined above and a dead load of 16.7 psf (0.77 kN/m2), the maximum deflection is 0.03318 in (0.84 mm), which is comprised of deflections of 0.0329 in (0.836 mm) and 0.00028 in (0.007 mm) for the live and dead loads, respectively. The maximum predicted deflection corresponds to a span-to-deflection ratio of 1247, meeting the design limit of 800. Furthermore, a maximum stress of 1423.7 psi (9.82 MPa) was calculated for the Jay Street panels. This value is well below the allowable stress limit of 3275 psi (22.58 MPa) outlined in Section 3.1.

3.3. ST. FRANCIS STREET BRIDGE

The St. Francis Street Bridge was designed by KSCI with the assistance of BG Consultants, Inc. for the FRP panel design. An outline of the deflection and stress checks on the final panel design as conducted by KSCI and BG Consultants, Inc. is provided herein.

The final dimensions of the panels for the St. Francis Street Bridge are a top face thickness of 0.881 in (22.4 mm), a core thickness of 22 in (558.8 mm) and a bottom face thickness of 0.651 in (16.5 mm). Each of the four panels measures approximately 26.25

ft (8.0 m) in length and 6.83 ft (2.08 m) in width. The thickness of the individual layers in the core is 0.09 in (2.3 mm), resulting in a total thickness of 1.08 in (27.4 mm) for the 12 layers of core material in a representative 1-ft (0.30 m) section. In this case, the corrugations of the core of the FRP panels run parallel to the direction of traffic, spanning from abutment to abutment. The moment of inertia based on these measurements is 3320.0 in^4 (138188.8 cm^4) per 1-ft (0.3-m) wide section. Figure 3.5 illustrates the structure of the St. Francis Street Bridge.

Figure 3.5 St. Francis Street Bridge Structure

Unlike the St. Johns Street and Jay Street Bridges, the St. Francis Street Bridge consists solely of FRP panels. The panels are assumed to be simply supported due to the connection method utilized between the panels and the abutments, which will be outlined in Section 4.2. The worst-case loading condition for the HS20-44 loading truck would be the case where the rear axle of the truck is located at mid-span, generating the maximum positive moment. In the interest of obtaining a conservative design, it is assumed the there is no shear transfer between panels, that is, that the entire line wheel load is carried by one panel. The maximum deflection is calculated based on simple beam theory

utilizing the equivalent point load defined above and a dead load of 36.26 psf (1.72 kN/m^2); the maximum deflection is 0.296 in (7.5 mm), which is comprised of deflections of 0.252 in (6.4 mm) and 0.044 in (1.1 mm) for the live and dead loads, respectively. The maximum predicted deflection corresponds to a span-to-deflection ratio of 983, meeting the design limit of 800. Moreover, a maximum stress of 886.1 psi (6.11 MPa) was calculated for the St. Francis Street panels. This value is well below the allowable stress limit of 3275 psi (22.58 MPa) outlined in Section 3.1.

Further innovation was incorporated into the design of the St. Francis Street Bridge with the attachment of the bridge guardrails to the FRP panels, which is something that has, to the best of the authors' knowledge, not been undertaken by other research projects. The panel manufacturer, KSCI, has worked in conjunction with the University of Nebraska to develop and test a guardrail connection to FRP panels modeled after that used on timber decks. The assembly consists of two steel plates, one placed on top of the panel and one placed on the bottom of the panel, through which bolts are placed to secure the guardrail to the panel. The details of the system are illustrated in Section 4.3; however the work conducted at the University of Nebraska-Lincoln in the area of timber decks (Faller et al., 2001) and FRP panels, which is believed to be unpublished to date, warranted mention.

It should also be noted that the live load impact factor, as calculated per Equation 3.2, was equal to 0.30. Furthermore, as previously mentioned, the design assumed that the entire load on one wheel line was carried by one panel; this would correspond to a wheel load distribution factor of 1.0. The AASHTO (1996) recommendations for a multi-beam concrete deck were utilized to calculate a wheel load distribution factor for

the St. Francis Street Bridge; a value of 1.298 was obtained. Since there are no recommendations for FRP panel bridges currently available this value was only utilized as a means of comparison.

3.4. WALTERS STREET BRIDGE

Utilizing the American Concrete Institute (ACI) document entitled "Guide for the Design and Construction of Concrete Reinforced with FRP Bars," (2001) the bridge was designed to meet the load and deflection requirements of AASHTO. The bridge was designed to carry a standard HS15-44 truck loading within the span length divided by 800 deflection requirement. Strength reduction factors, ϕ, of 0.7 and 0.85 were used for the flexure and shear design, respectively. It should be noted that AASHTO (1996) design guidelines were utilized; the live load impact factor was calculated as 0.30 and the wheel load distribution factor was calculated as 0.49.

Design of the Walters Street Bridge was conducted using the standard HS15-44 truck loading to be conservative. Based on the assumed design values for live load impact factor and wheel load distribution factor, strength and serviceability requirements could not be met for the standard HS20-44 truck loading. However, the assumed design values are prescribed for concrete reinforced with steel bars; validation of the assumption that these design protocols are applicable to FRP-RC was under investigation.

The FRP-RC panel reinforcement consists of commercially available CFRP and GFRP reinforcing bars with the following properties. The bars were manufactured by Marshall Industries Composites, Inc.; Figure 3.6 illustrates the appearance of the bars. The latest formulation for the GFRP bars consists of 35 percent urethane modified vinyl

ester resin, 60 percent E-glass fibers, and 3 percent ceramic fibers to reinforce the deformations. Approximately the same proportions are utilized for the CFRP; however in this case epoxy resin and carbon fibers are utilized. Until recently, the GFRP bars consisted of a mixture of polyester and vinyl ester resins.

For the CFRP bars, a guaranteed design tensile strength of 270 ksi (1862 MPa) and a tensile elastic modulus of 15.2 Msi (104.8 GPa) were given by the manufacturer. For the GFRP bars these values were 105 ksi (724 MPa) and 6 Msi (41.4 GPa), respectively. A design compressive strength of 4000 psi (27.6 MPa) was used for the concrete in the FRP-RC bridge panels. Verification of the FRP and concrete material properties was conducted and is outlined in Section 6.

Figure 3.6 FRP Bars Produced by Marshall Industries Composites, Inc.

For the flexural design, the procedure is similar to that used in the case of steel reinforcement once the appropriate modes of failure are recognized. The two possible failure modes are (a) rupture of the FRP reinforcement prior to crushing of the concrete and (b) crushing of the concrete prior to rupture of the FRP reinforcement. According to

ACI 440 (2001) both modes of failure are acceptable; due to the linear-elastic behavior of FRP materials up to failure, the concrete crushing failure is marginally preferred because a small degree of plasticity is exhibited prior to failure. Compared to the flexural design strength reduction factor used in steel-RC design (i.e., 0.9), the factors used for FRP-RC range from 0.7, for concrete-controlled failure, to 0.5, for FRP-controlled failure, to account for the decreased ductility of the section. In this specific situation, the section was designed to ensure concrete crushing prior to rupture of the FRP bars.

For the shear design, the separate contributions to the shear capacity of the concrete, V_c, and the reinforcement, V_f, are still considered. However, the ratio $\rho_f E_f / \rho_s E_s$ is used as a multiplier of the concrete shear strength contribution to account for the reduced stiffness of the FRP bars compared to steel reinforcing bars; the reduced stiffness will lead to larger shear cracks thereby decreasing the contribution of the concrete to the shear capacity. It should be noted that ρ_f is the reinforcement ratio of the FRP-RC section, E_f is the longitudinal modulus of elasticity of the FRP reinforcement, ρ_s is the reinforcement ratio of a steel-RC section of equal capacity, and E_s is the modulus of elasticity of the steel reinforcement. It should be underlined that the term "equal capacity" refers to the design flexural moment capacity, ϕM_n. The reinforcement ratio for the FRP-RC panels is 0.0116 and the corresponding steel reinforcement ratio for the same design moment capacity is 0.0121, yielding a value of 0.50 for the ratio of $\rho_f E_f / \rho_s E_s$.

Based on the material properties and design parameters, the longitudinal reinforcement consists of 12 bundles of three 3/8-in (9.5-mm) CFRP bars, while for the shear stirrups 3/8-in (9.5-mm) GFRP bars are utilized. Although their contribution to the flexural capacity of the member is not considered, 1/2-in (12.7-mm) GFRP bars are

utilized in the top side of the cage. Top transverse reinforcement consisting of 1/2-in (12.7-mm) GFRP bars at 4 ft (1.2 m) is also provided in the panels. Due to the fact that thermoset resins are used in the manufacturing of the FRP bars, the FRP manufacturer conducted all necessary bending of the reinforcing bars prior to their shipment to the concrete precaster. Figure 3.7 illustrates the layout of the FRP reinforcement in each panel. Each of the nine bridge panels measure 2.83 ft (0.9 m) in width, 24 ft in (7.3 m) length, and 1 ft (0.3 m) in depth. The overall structure of the bridge is illustrated in Figure 3.8.

Figure 3.7 FRP Reinforcement Layout

Figure 3.8 Walters Street Bridge Structure

As previously mentioned, verification of the FRP and concrete material properties was conducted and is outlined in Section 6. Due to the fact that the actual values are so close to the design values, the flexural and shear capacities of the FRP-RC panels are discussed in detail in Section 6. The fundamentals are outlined presently. It should be noted these values incorporate the aforementioned AASHTO (1996) design factors.

The ultimate moment capacity, M_n, of one panel is 283.9 kip-ft (405.6 kN-m), while the design moment capacity, ϕM_n, of one bridge panel is 198.7 kip-ft (283.9 kN-m). The moment demand, M_u, which is based on a standard HS15-44 truck loading, was determined to be 137.9 kip-ft (197 kN-m). The design shear capacity of 30.8 kips (137 kN) for the panels is composed of the contributions of the concrete, V_c, equal in this case to 21.3 kips (94.7 kN), and the reinforcement, V_f, equal in this case to 9.5 kips (42.3 kN). The maximum shear demand on the panels occurs just over the support and has a value of 26.0 kips (115.7 kN). For both moment and shear, the capacity of the panel exceeds the demand on the panel. Serviceability issues, in terms of deflection and crack width of the panels, were also considered in the design; due to the experimental nature of this project and the possibility of close long-term monitoring, the thresholds were pushed with the design marginally exceeding these limitations.

In this case, a note about precasting of the FRP-RC panels is warranted. The existing forms of the concrete precaster were utilized without modification. The FRP bars are considerable lighter than steel bars, which allow them to be moved by fewer workers. Due to the decreased stiffness, the bars deflect more and may require more support chairs during the assembly of the reinforcing cage. Plastic chairs were used to support the reinforcement cages within the forms during casting and plastic ties were used to secure

the reinforcing bars in the desired reinforcement configuration. Note the plastic ties in Figure 3.7.

3.5. DISCUSSION OF BRIDGE DESIGN TECHNIQUES

The designs of all four bridges were based on AASHTO (1996) standard HS20-44 and HS15-44 truck loading configurations and a maximum deflection of the span length divided by 800. It is important to note that due to the relative low modulus of the FRP materials utilized, serviceability is often the controlling factor for design. Of additional interest in the design is the maximum stress in the panel. According to the manufacturer, the maximum fiber stress at failure is 9825 psi (67.74 MPa); with a factor of safety of 3.0, the allowable stress in the FRP material was limited to 3275 psi (22.58 MPa).

Due to the fact that design guidelines for FRP panels do not currently exist, the distribution of load in the FRP panels was calculated assuming the same design factors utilized in the AASHTO design specifications (1996) for concrete slabs. For the St. Johns Street and Jay Street Bridges, the panels are assumed to be simply supported on the girders and the protocols for the case where the main reinforcement is perpendicular to the traffic were utilized. For the St. Francis Street, the panels are assumed to be simply supported on the abutments and the protocols for a multi-beam concrete deck were utilized to calculate a wheel load distribution factor. The FRP-RC bridge at Walters Street was designed utilizing the ACI document entitled “Guide for the Design and Construction of Concrete Reinforced with FRP Bars,” (2001). Again, the AASHTO (1996) protocols for a multi-beam concrete deck were utilized to calculate a wheel load distribution factor.

4. BRIDGE INSTALLATION

The installation of the three bridges utilizing FRP panels (St. Johns Street, Jay Street, and St. Francis Street) was conducted by KSCI and the installation of the FRP-RC panel bridge (Walters Street) was conducted by Oden Enterprises, Inc. The installation of all four bridges was overseen and documented as part of this research project. This Section details the installation of the four bridges. Further information including several pictures in chronological order for the installation of each of the bridges in the order in which they are presented in this Section is contained in Appendix E. Furthermore, Appendix C contains the as-built plans for the bridges; the as-built plans contain specific information about the materials utilized during the installation process.

4.1. INSTALLATION OF THE ST. JOHNS AND JAY STREET BRIDGES

Since the configuration of the St. Johns Street and Jay Street Bridges is so similar their installation will be covered in a combined section. It should be noted that in addition to the standard highway truck (HS20-44) loading the bridges were also designed for the dead load of the deck, which is approximately 15 lb/ft^2 (0.72 kN/m^2) and 16 lb/ft^2 (0.77 kN/m^2), respectively for the St. Johns Street and Jay Street Bridges.

The St. Johns Street Bridge, an FRP deck supported by steel girders, is comprised of six lateral half-width panels, having a thickness of 5.125 in (130.2 mm) including a 0.375-in (9.5-mm) wearing surface of polymer concrete, and 7 built-up steel girders of size W14 $\times$ 90. The overall span length and width of the bridge are 26.5 ft (8.08 m) and 25.5 ft (7.77 m), respectively.

The Jay Street Bridge is comprised of four longitudinal panels, having a thickness of 6.625 in (168.3 mm) including a 0.375-in (9.5-mm) wearing surface of polymer concrete, and 7 built-up steel girders of size W14 × 90. The overall span length and width of the bridge are 27 ft (8.23 m) and 25.5 ft (7.77 m), respectively.

Installation of both bridges proceeded based on the following outline of tasks:

- Install steel girders – drill holes into the abutment for the anchor bolts (Figure D.1); place bearing pads and plates (Figure D.2); anchor the plates to the abutment with the anchor bolts; place girders and weld them to the plates (Figure D.4); install steel diaphragms (Figure D.5).
- Install FRP decks – place panels onto the steel girders (Figure D.6 and Figure D.7); attach panels together and secure to the girders (Figure D.8 through Figure D.11); secure girders/panels to the abutments (Figure D.12 and Figure D.13); fill the panel joints (Figure D.14).
- Install guardrails – connect guardrail posts to the girders (Figure D.16); attach guardrail to posts (Figure D.17).

Tasks unique to the use of steel-supported FRP panels that warrant further attention are the connection of the panels to one another and to the girders and the connection of the panels/girders to the abutments. The connection of the panels together and to the girders was achieved through the use of a GFRP tube inserted between adjacent panels. The panels are mechanically clamped to the girders at the intersection of the panels and girders in eight locations and nine locations for the St. Johns Street and Jay Street Bridge, respectively. A detail of the panel joint and girder clamp connection for the St. Johns Street Bridge is illustrated in Figure 4.1. A similar configuration was

used for the Jay Street Bridge, with slight modification due to the alignment of the girders and panels; see Figure 4.2.

Figure 4.1 Cross Section of Panel Joint and Clamp Assembly – St. Johns Street

Figure 4.2 Cross Section of Panel Joint– Jay Street

The clamping assembly used on the St. Johns Street Bridge consists of two bolts extended down through the tube, one of either side of the girder flange, two steel plates one on the top and one on the bottom of the FRP tube, and small steel angles, which

clamp under the girder flange to secure the panels to the girders. The clamping assembly for the Jay Street Bridge consists of a steel plate that has two bolts affixed to the top of the plate and four bolts affixed to the bottom of the plate. The plate rests on top of the girder, while the two bolts on the top of the plate extend up through the tube and the four bolts on the bottom of the plate extend down around the girder flange, two on either side. Small angles placed onto the four bolts are the means of securing the panels to the girders.

Once the panels are clamped down to the girders, the connection of the panels/girders to the abutments is made. This connection consists of a steel T-beam installed over the edge of the panel, which is welded to the girder and also to the corrugated sheet piling, which is installed roughly 1.5 ft (0.45 m) below the top of the abutment perpendicular to the direction of traffic along the abutment. Figure 4.3 illustrates this detail, which serves to restrain the ends of the panels against vertical movements.

Figure 4.3 Cross Section of Abutment Detail

Following the installation of the clamps and the connection of the panels/girders to the abutments, the joint between the panels is sealed using FRP strips and the same polymer concrete used for the wearing surface for the Jay Street Bridge and only polymer concrete for the St. Johns Street Bridge.

The installation of the St. Johns Street and Jay Street Bridges took place concurrently with the setting of the first panels taking place on September 25, 2000. Installation was completed on October 4, 2000 and both bridges were opened to traffic on October 6, 2000.

4.2. INSTALLATION OF THE ST. FRANCIS STREET BRIDGE

The St. Francis Street Bridge consists solely of FRP panels and utilizes no concrete or steel. The four FRP panels are each 23.625 in (600.1 mm) thick, including a 0.375-in (9.5-mm) wearing surface of polymer concrete. The overall span length of the bridge is 26.25 ft (8.00 m) with a bridge width of 27.33 ft (8.33 m). The bridge was designed according to AASHTO deflection requirements for a standard highway truck (HS20-44) loading and also for the dead load of the deck, which is approximately 36 lb/ft^2 (1.72 kN/m^2).

Installation proceeded based on the following outline of tasks:

- Install FRP decks – place panels onto the abutments (Figure D.18); attach panels together; secure the panels to the abutments; fill the panel joints.
- Install the bridge guardrails – drill holes through the deck (Figure D.20); attach the guardrail posts to the panels; attach guardrail to posts.

Tasks unique to the use of FRP panels in this application that warrant further attention are the connection of the panels to one another, the connection of the panels to the abutments, and the connection of the guardrail posts to the panels.

The connection of the panels together and to the abutments was achieved through the use of GFRP tubes connected together and inserted between adjacent panels. A bolt inserted through the tubes in the joint was secured at the top of the tubes by a steel plate and at the bottom of the panel to a steel angle bolted to the abutment. Additionally, the panels are supported by the abutment itself. A detail of the panel joint and abutment connection are illustrated in Figure 4.4 and Figure 4.5, respectively.

Figure 4.4 Cross Section of the Panel Joint – St. Francis

Figure 4.5 Abutment Connection Detail

Once the panels are connected together and to the abutment, the joint between the panels is sealed using polymer concrete to fill the joint and to cover the four layers of FRP, which are laid-up over the joint. As mentioned in Section 3.3, the connection of the guardrails to the FRP deck is done using the same connection used to attach guardrails to timber decks. The guardrail post is attached to two steel plates (Figure D.19), which are secured, one on the top and one on the bottom, to the deck using steel bolts.

Installation of the St. Francis Street Bridge began on November 13, 2000 and was completed on November 17, 2000. The bridge was officially opened to traffic on November 29, 2000.

4.3. INSTALLATION OF THE WALTERS STREET BRIDGE

The Walters Street Bridge consists of nine precast concrete panels, each with a depth of 1 ft (0.30 m) and a width of 2.83 ft (0.86 m). The panels were designed for a standard HS15-44 truck loading in accordance with the now available ACI Committee

440 guidelines for reinforcing concrete with FRP bars and AASHTO deflection requirements. Overall, the bridge measures 24 ft (7.32 m) in span and 25.5 ft (7.77 m) in width and has a skew of approximately 12 degrees. Marshall Industries Composites, Inc. was the manufacturer of the FRP bars utilized in this project and Oden Enterprises, Inc. was responsible for the precasting of the bridge panels and the installation of the bridge.

Installation proceeded based on the following outline of tasks:

- Install precast concrete panels – place panels onto the abutments (Figure D.22); connect panels; secure the panels to the abutments (Figure D.23); fill the panel joints (Figure D.24).
- Install the bridge guardrails – attach the guardrail posts to the panels; attach guardrail to posts (Figure D.25).

Tasks unique to the use of precast concrete panels that warrant further attention are the connection of the panels to one another, the connection of the panels to the abutments, and the connection of the guardrail posts to the panels.

The connection of the panels together was accomplished through the use of steel angles, which were embedded in the panel edges and then welded together once the panels were in place on the abutments. See Figure 4.6 for a detail of the angles just before welding. It should be noted that this is the only steel detail left in the panels; this issue will be addressed in Section 10, which outlines recommendations for future research.

For the connection of the panels to the abutments, a void was formed approximately 6 in (0.15 m) from each end of each panel, through which a hole was drilled into the abutment to receive an anchor bolt. The anchor bolts were secured into

the abutments with a two-part epoxy and a nut was tightened down to secure the panels. Once the panels were connected together and to the abutment, non-shrink grout was used to fill the joints and to cover the anchor bolts. The connection of the guardrails to the panels was accomplished using the same type of steel angles embedded at the panel joints. Once the guardrail posts were welded to the panels, the guardrails were bolted to the posts completing the installation of the bridge.

Figure 4.6 Panel Connection Detail

Installation of the Walters Street Bridge began on June 18, 2001. Installation was completed and the bridge was officially opened to traffic on June 28, 2001.

4.4. DISCUSSION OF BRIDGE INSTALLATION TECHNIQUES

For all four of the bridges there is great appeal in the short timeline for installation. Due to the precast/prefabricated panels installation of each bridge took

approximately one week; this is in sharp contrast to the three to four weeks that traditional cast-in-place construction would have taken.

The difference in panel alignment for FRP panel bridges necessitated different connections to the girders, however both could allow for installation of half of the bridge at a time. In an urban environment, this could be beneficial due to the possibility of closing only one lane at a time.

FRP deck panels are light enough to move without heavy equipment. With a weight of approximately 15 to 16 psf (0.72 to 0.77 kN/m^2) they could be moved with equipment readily available to city and county municipalities. The fact that special equipment is not necessary for installation could be attractive in many instances.

The technique of attaching the guardrail posts to the FRP panels in the case of the St. Francis Street Bridge, although difficult during installation due to the drilling of the holes through the depth of the FRP panels, seems to be performing well. A small test of the guardrail system conducted by KSCI, whereby a static horizontal load was applied to one of the guardrail posts, indicated deflection/rotation of the guardrail post without damage to the FRP panel.

As mentioned in Section 1.3, the application of FRP layers in the field (i.e., cured under ambient conditions) could pose durability issues in the future. Several FRP layers were applied over the panel joints of the Jay Street and St. Francis Street Bridges; these two bridges will be monitored closely in order to detect whether such issues will arise. Close monitoring of the St. Johns Street Bridge, also for the durability of the joints, and the Walters Street Bridge, for serviceability issues will be conducted.

Utilizing FRP in the form of reinforcing bars allows for the use of many steel-RC concrete practices. The fabrication and installation details were nearly identical to the methods utilized by the concrete precaster for steel-reinforced panels.

Installation of the bridges highlighted the fact that having an efficient system is equally as important as having the adequate components. As well, for a new technology its learning curve must be overcome before applications of that new technology can be conducted proficiently. Specifically, the importance of design tolerances and detailed installation procedures was exemplified by the contact between the FRP panels and the girders which was not continuous immediately following installation due to variations in the surface of the FRP panels. Small gaps were observed between the panels and girders in several locations; this could have been remedied by placing a layer of pressurized grout between the panels and the girders during installation (Shekar et al., 2002).

In contrast to the system utilized for the FRP panles, the system utilized for the FRP-RC bridge at Walters Street is a very good system which has been previously refined and developed for the precast panels due to its use also with “conventional” technology. The system for the connection of the FRP panels needs to be examined further to develop a comprehensive system. However, as mentioned, these types of minor difficulties should be expected during the first applications of new technology and overall, all of the systems and installation techniques worked satisfactorily.

5. FRP PANEL LABORATORY EXPERIMENTATION

The first series of experiments was conducted on cured single ply FRP laminates to determine their tensile strength and tensile modulus of elasticity and the virgin properties of the laminates were compared to the properties of environmentally conditioned specimens. Following this individual material characterization, laboratory experimentation was conducted on the FRP composite deck panels. For the second series of tests, two full-scale specimens, representative of the St. Francis Street Bridge in size and shape, were tested to determine the flexural and shear characteristics of the panels. For the third series of tests, three small-scale specimens were subjected to controlled environmental conditioning. Following conditioning, the flexural behavior of the specimens was compared to that of the control specimen.

5.1. FRP LAMINATE CHARACTERIZATION

In order to determine the tensile properties of the constituent materials of the FRP composite deck panels, a set of coupon-sized specimens of the single ply FRP laminates as tested. The FRP laminates were manufactured in the same manner as the FRP panels, utilizing 40 percent fiber by weight. An Instron 4485 testing machine was utilized during the testing of the six 1.5 in (38.1 mm) by 15 in (381.0 mm) specimens. The thickness of the laminates was 0.06 in (1.5 mm). The results are outlined in Table 5.1 below.

In general, the failure of the FRP laminates was exhibited by cracking of the resin matrix followed by rupture of the fibers themselves; this is the desired failure mode. Based on a slipping failure between the FRP laminate and the grips of the testing

machine, the results from specimens C1 and C4 are not included in the average results. The average of the four remaining specimen results indicates that the ultimate failure load was 3739 lb (16.63 kN), the ultimate tensile strength of the specimens was 42.98 ksi (296.3 MPa) and the tensile modulus of elasticity was 2256.5 ksi (15.62 GPa). The standard deviation for the tensile strength and tensile modulus were 3.06 ksi (21.09 MPa) and 217.1 ksi (1.50 GPa), respectively.

Table 5.1 Tensile Test Results - GFRP Laminates - Control

Specimen	Failure Load (lb)	Tensile Strength (ksi)	Tensile Modulus (ksi)
C1	2254	25.9	2473.7
C2	3546	40.8	2071.1
C3	3501	40.2	2567.5
C4	2234	25.7	2650.4
C5	3842	44.2	2158.7
C6	4068	46.8	2228.7
Average*	3739	42.98	2265.5

* Average values do not include specimens C1 and C4.

Note: 1 psi = 6.89 kPa, 1000 lb = 4.448 kN

5.2. FRP PANEL FLEXURAL BEHAVIOR

Characterization of the behavior of the FRP sandwich panels was accomplished through the testing of two full-scale specimens. It should be noted that the FRP panels used for testing were constructed in the same manner as those constructed for the bridges; all of the same types and quantities of fiber and resin were utilized. One exception is the polymer concrete wearing surface which was not applied to the laboratory panels as the contribution of the wearing surface to the panel behavior was assumed to be negligible due to the relative thin layer utilized on the bridge structures. The testing of the

specimens will determine the overall flexural behavior of the panels, with the ultimate goal of determining the material properties of the FRP panels. A comparison between the ultimate load, stress, span-to-deflection ratio, and failure mode is presented.

Testing of two sections, approximately 23 in (584.2 mm) wide and 23 in (584.2 mm) deep, representative of the St. Francis Street Bridge, was conducted under four-point bending. The specimen depth is equal to the depth of the bridge panels at 23.625 inch (600.1 mm). The 14–ft (4.27-m) specimens were tested over a clear span of 13 ft (3.96 m) with equal loads applied approximately 5 ft (1.52 m) from each support, leaving a constant-moment region 3 ft (0.91 m) in length. It should be noted that the span-to-depth ratio for this test setup was 2.6. Figure 5.1 illustrates the test schematic for both specimens, SF-2-1 and SF-2-2.

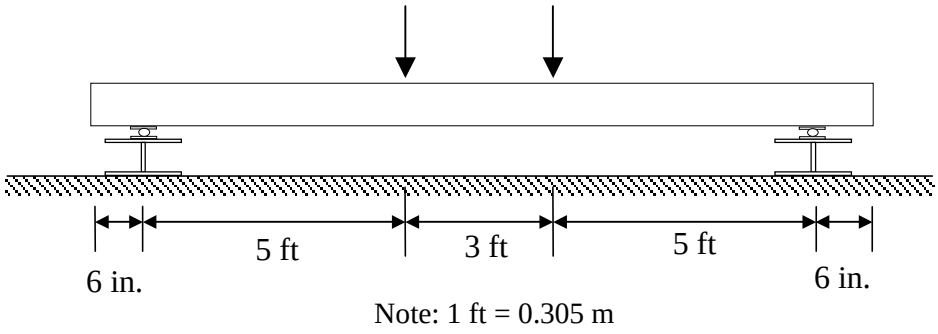

Figure 5.1 Flexural Test Schematic - SF-2-1 and SF-2-2

The load was applied with a Baldwin compression testing machine, which has an ultimate load capacity of 400 kips (1779.3 kN). At the load and support points of the member, so as to prevent crushing or localized failure of the specimen, an attempt was made to spread the load as much as possible. The load spreading was accomplished through the use of 8 in (203.2 mm) by ¾ in (19.0 mm) plywood boards and 6 in (152.4

mm) by 1 in (25.4 mm) steel plates. In each case the plywood was directly against the specimen and the steel plate was between the plywood and the steel roller. Figure 5.2 illustrates one of the support points of the specimens. Instrumentation of the beams consisted of eight linear variable differential transformer (LVDT) transducers placed one on either side of the section at each support point, at the mid-point, and at one quarter-point of the beam. Additional instrumentation consisted of strain gages bonded to the core material and to the top and bottom faces of the section at mid-span; the data from the strain gages are not presented herein. Figure 5.3 illustrates the test setup for the SF-2-1 and SF-2-2 specimens.

Figure 5.2 Specimen Support Detail

Measurements of the cross section were taken to better approximate the moment of inertia; the dimensions of the two specimens, which were approximated as I-beams for calculation purposes are outlined in Figure 5.4. The area and moment of inertia for specimen SF-2-1 were 76.66 in^2 (494.57 cm^2) and 5949.62 in^4 (247641.88 cm^4), respectively; these values for specimen SF-2-2 were 74.86 in^2 (482.97 cm^2) and 5632.89 in^4 (234458.58 cm^4), respectively.

Figure 5.3 Flexural Test Setup – SF-2-1 and SF-2-2

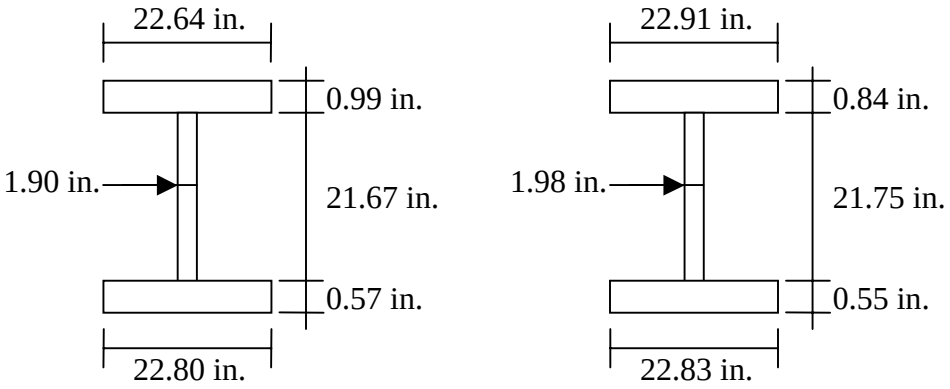

Note: 1 in. = 25.4 mm

Figure 5.4 Specimen Dimensions – St. Francis Street

Based on simple beam theory and a failure criterion of a maximum fiber stress of 9825 psi (67.76 MPa), the failure load for both of the specimens was approximated at 150 kips (667 kN). The maximum stress failure criterion of approximately 9825 psi (67.76 MPa) was based on previous testing conducted by the manufacturer; it was also used during the design phase of the project as mentioned in Section 3. Another failure criteria

prescribed by the manufacturer indicated a span-to-deflection ratio of approximately 100, which would have placed the failure load as high as 240 kips (1068 kN).

The predicted ultimate load was determined based on the manufacturer's estimate of the effective modulus of elasticity of the panels, as outlined in Appendix D. The specimens were tested to failure through the application of quasi-static load cycles. First the specimen was loaded to up to approximately 20 percent of its predicted ultimate capacity and unloaded to approximately 5000 lb (22.24 kN); this cycling was repeated up to approximately 35 percent and 50 percent of the ultimate capacity and then the beam was loaded up to failure. Figure 5.5 illustrates the load-deflection diagram for the failure load cycle only. It should be noted that the dashed line represents the theoretical behavior, the line outlined with points represents the experimental behavior of the SF-2-1 specimen and the solid line represents the experimental behavior of specimen SF-2-2. Good agreement between design and experimental material properties is exhibited for both specimens.

Failure of specimen SF-2-1 was observed at approximately 194 kips (862.99 kN). The corresponding mid-span deflection was 1.33 in (33.78 mm), which yields a span-to-deflection ratio of approximately 115. Additionally, the maximum bottom fiber stress at failure was approximately 12,500 psi (86.21 MPa), 30 percent higher than the design failure limit.

Failure of specimen SF-2-2 occurred at approximately 288 kips (1281.1 kN). The mid-span deflection exhibited at failure was 1.81 in (45.98 mm); the equivalent span-to-deflection ratio is approximately 86. Additionally, the maximum bottom fiber stress at

failure was approximately 95 percent greater than the design failure limit, 19,100 psi (131.7 MPa).

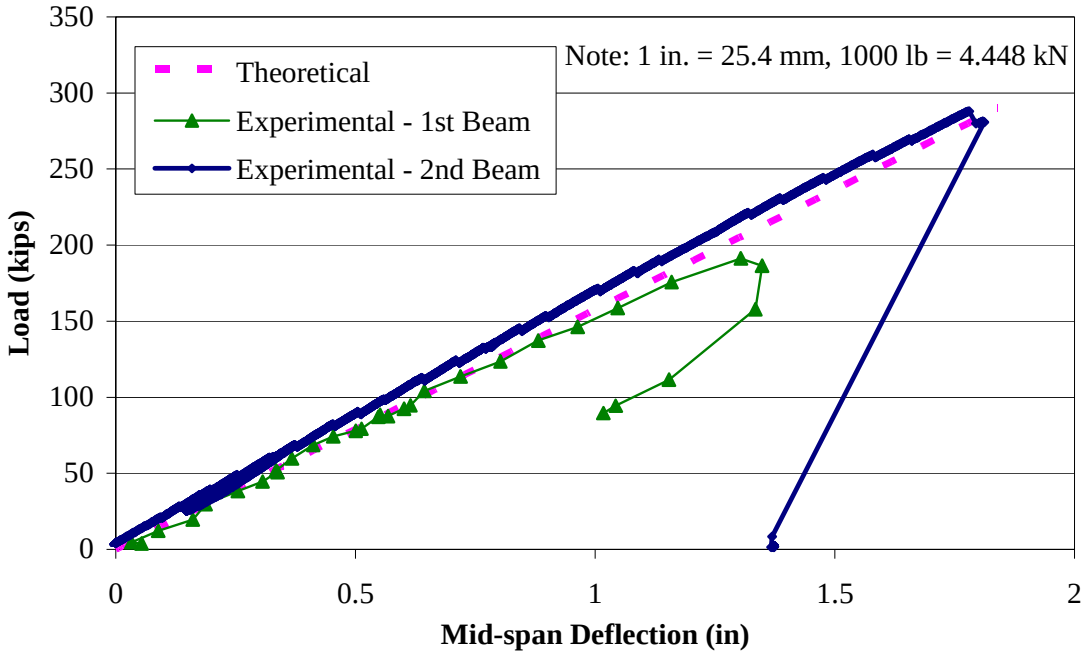

Figure 5.5 Load vs. Deflection Results – SF-2-1 and SF-2-2

The failure mode anticipated, based on experience from previous testing conducted by the manufacturer (Nagy et al., 1996; Nagy and Kunz, 1998), was delamination between the top face and the core material. However, the failure mode exhibited by specimen SF-2-1 was delamination of the bottom face from the core material. This failure initiated at one end of the beam and progressed toward mid-span as the load was increased. It should be noted that buckling of the core material was also observed, however no delamination of the core layers from one another was noted. Figure 5.6 illustrates the failure mode.

(a) Delamination (b) Buckling of the Core

Figure 5.6 Failure Mode of Specimen SF-2-1

Failure of specimen SF-2-2 was exhibited by delamination of the core from the top and bottom face. Lateral expansion of the core material was observed on one end of the panel around the one-quarter span point on both sides of the panel. The core delaminated completely form the top and bottom faces on one side of the panel, which combined with delamination between layers of the core, resulted in the complete detachment of several layers of the core from between the faces. The failure mode is illustrated in Figure 5.7.

The load versus deflection behavior of the specimens was analyzed to determine the modulus of elasticity of the panels. An overall modulus of elasticity for the panels was determined based on simple beam theory; Equation 5.1 defines the relationship between load and deflection for the case where two-point loads are applied symmetrically.

$$\Delta_{max} = \frac{Pa}{24EI}\left(3l^2 - 4a^2\right) \quad \textbf{(5.1)}$$

where P is the magnitude of one of the applied loads, a is the distance from the support to the point of load application, l is the span length, E is the modulus of elasticity of the material and I is the moment of inertia of the section. When simplified in this manner, the modulus value calculated will take into consideration the deflections due to bending and shear. The results indicate modulus of elasticity values of 3.78×10^6 psi (26.06 GPa) and 4.36×10^6 psi (30.06 GPa) for specimens SF-2-1 and SF-2-2, respectively.

(a) Lateral Expansion (b) Complete Detachment

Figure 5.7 Failure Mode of Specimen SF-2-2

5.3. ENVIRONMENTAL CONDITIONING RESISTANCE.

The GFRP laminates and sandwich panels, utilizing an isophthalic polyester resin, were subjected to environmental conditions designed to simulate their in-situ environments. Three different conditioning regimens were utilized.

One series consisted of combined environmental conditioning. The environmental conditioning of the specimens consisted of a series of freeze-thaw, high temperature, and high relative humidity cycles. This environmental conditioning was performed in an environmental chamber to duplicate seasonal effects in the mid-west United States. Table 5.2 details the temperature and humidity information for each of the cycle types along with the total number of cycles to which the specimens were exposed. The second exposure regime consisted of immersion in a 140°F (60°C) saline solution for 42 days. The saline solution contained 15 percent sodium chloride (NaCl) by weight and 85 percent potable water. The third set of conditioning consisted of exposure to ambient conditions in the laboratory for the duration of the other two conditioning regimens.

Table 5.2 Environmental Chamber Cycles

Cycles	Temperature Range (ºF)	Total Number of Environmental Cycles
Freeze-Thaw	-4 to 40	200
High Temperature	80 to 120	480
High Relative Humidity (60% – 100%)	60	160
High Relative Humidity (60% – 100%)	80	80

Note: °F=1.8*°C+32

The tensile properties of the single-ply GFRP laminates were measured after conditioning and compared to that of the control specimens. For the GFRP sandwich panels, a set of three small-scale panels representing the St. Johns Street Bridge panels were used. A comparison between the ultimate load, stress, span-to-deflection ratio, and failure mode is presented.

5.3.1. FRP Laminate Characterization. In order to compare the tensile properties of the constituent materials of the FRP composite deck panels subjected to the aforementioned environmental conditioning, a set of coupon-sized specimens of the single ply FRP laminates were tested. Recall that an Instron 4485 testing machine was utilized during the testing of the six 1.5 in (38.1 mm) by 15 in (381.0 mm) specimens. The thickness of the laminates was 0.06 in (1.5 mm). It should be noted that prior to both of the exposure regimens, the edges of the laminates were sealed using a silicone gel to prevent unwanted moisture ingress from occurring.

Like the control specimens, a set of six coupon-sized specimens was tested after environmental conditioning in the environmental chamber. The results are outlined in Table 5.3. The failure mode exhibited by the specimens was the desired mode of rupture of the fibers discussed previously for the control specimens.

Table 5.3 Tensile Test Results - GFRP Laminates - Environmentally Conditioned

Specimen	Failure Load (lb)	Tensile Strength (ksi)	Tensile Modulus (ksi)
EC1	3928	43.6	2362.2
EC2	3853	42.8	2534.3
EC3	3649	40.5	2332.6
EC4	4057	45.1	2535.5
EC5	3866	43.0	2137.8
EC6	4027	44.7	2263.2
Average	3897	43.3	2360.9

Note: 1 psi = 6.89 kPa, 1000 lb = 4.448 kN

The average results indicate that the ultimate failure load was 3897 lb (17.33 kN), the ultimate tensile strength of the specimens was 43.3 ksi (298.5 MPa) and the tensile modulus of elasticity was 2360.9 ksi (16.28 GPa). The standard deviation for the tensile

strength and tensile modulus were 1.63 ksi (11.25 MPa) and 155.37 ksi (1.07 GPa), respectively. Compared to the results from the control specimens the residual tensile strength was approximately 100.7 percent, while the residual tensile modulus was approximately 104.6 percent.

A set of six coupon-sized specimens was also tested after conditioning in a saline solution at 140ºF (60ºC) for 42 days; the results are summarized in Table 5.4. Again, the failure mode exhibited by the specimens was the desired mode of rupture of the fibers discussed previously for the control specimens.

Table 5.4 Tensile Test Results - GFRP Laminates - Saline-Conditioned

Specimen	Failure Load (lb)	Tensile Strength (ksi)	Tensile Modulus (ksi)
S1	3571	39.7	2499.0
S2	4145	46.1	2263.4
S3	3755	41.7	2168.3
S4	3842	42.7	2191.6
S5	3104	34.5	2126.2
S6	2964	32.9	2304.5
Average	3563	39.6	2258.8

Note: 1 psi = 6.89 kPa, 1000 lb = 4.448 kN

The average results indicate that the ultimate failure load was 3563 lb (15.85 kN), the ultimate tensile strength of the specimens was 39.6 ksi (273.03 MPa) and the tensile modulus of elasticity was 2258.8 ksi (15.57 GPa). The standard deviation for the tensile strength and tensile modulus were 5.03 ksi (34.65 MPa) and 134.21 ksi (0.92 GPa), respectively. Compared to the results from the control specimens the residual tensile strength was approximately 92.1 percent, while the residual tensile modulus was approximately 100.1 percent.

Table 5.5 summarizes the comparison of the conditioned specimens to the control specimens. Figure 5.8 illustrates the change in tensile stress and tensile modulus exhibited by the FRP laminates. The results will be compared to those from the environmental conditioning of entire FRP panels discussed later in this Section.

Table 5.5 Summary of Tensile Test Results - GFRP Laminates

	Load (lb)	Stress (ksi)	E (ksi)
Control	3739	42.98	2265.5
Percent Residual		100.0	100.0
Environmental Cycles	3897	43.3	2360.9
Percent Residual		100.7	104.6
42 days Saline Conditioning	3563	39.6	2258.8
Percent Residual		92.1	100.1

Note: 1 psi = 6.89 kPa, 1000 lb = 4.448 kN

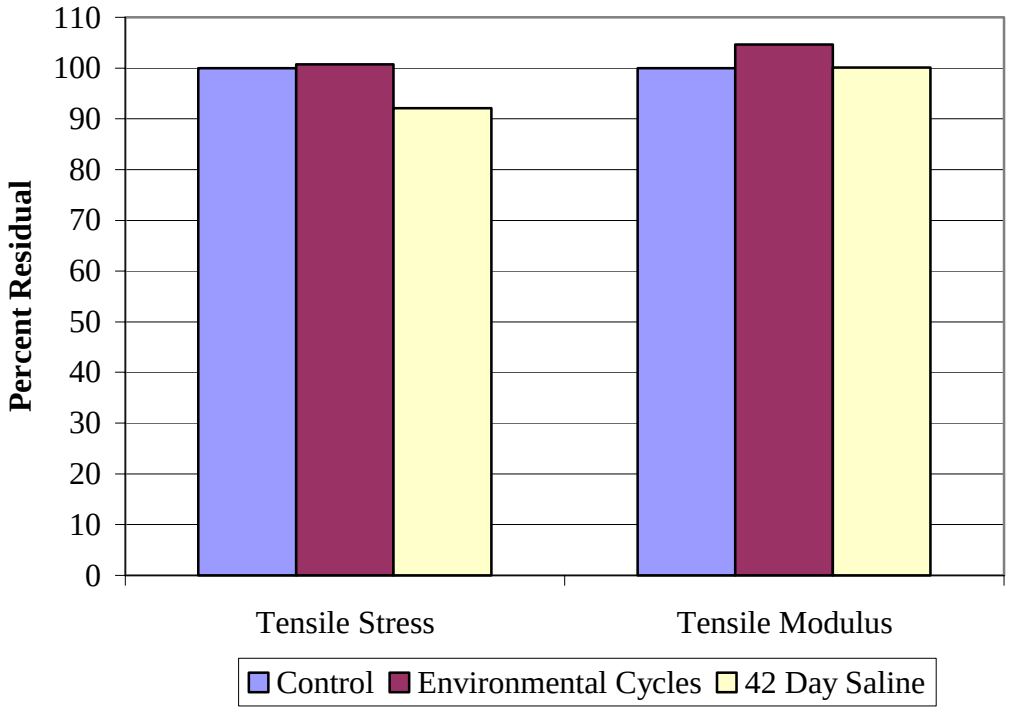

Figure 5.8 Summary of FRP Laminate Results

As illustrated by the results in Table 5.5 and Figure 5.8, approximately 8 percent degradation occurred in the strength of laminate, whereas no degradation in the modulus of the laminates was exhibited. However, based on the standard deviation of the data sets noted previously, in should be noted that the changes in tensile strength and modulus are generally within one standard deviation of the average.

5.3.2. FRP Panel Characterization. For the GFRP sandwich panels, small-scale beams measuring approximately 5.125 inches (130.2 mm) deep, 9 inches (228.6 mm) wide, and 3 feet (0.9 m) long, were tested in four-point bending. Two of the specimens were subjected to a predetermined sequence of environmental conditioning, while the remaining specimen was designated as the control specimen and remained in the laboratory under ambient conditions. One specimen was exposed to the aforementioned conditioning in an environmental chamber, while the exposure regime for the second specimen consisted of immersion in a 140°F (60°C) saline solution for 42 days. A comparison between the ultimate load and failure mode of the two conditioned specimens and the control specimen is presented. For the specimen subjected to the environmental cycles, nothing was done to the specimen prior to conditioning. However, for the specimen immersed in the saline solution, small 0.31-in (7.94-mm) holes were drilled approximately at the neutral axis through the entire width of the specimen; this was done in order to create the worst-case scenario of flooding of the entire core.

After conditioning of all of the specimens was completed, testing of all three specimens was conducted on one day. The specimens were tested under four-point bending with equal loads applied 12.5 in (317.5 mm) from each support, leaving a 8-in (203.2-mm) constant moment region in the center of the beam. The span-to-depth ratio

for the specimens was approximately 2.6. A picture of the test setup is illustrated in Figure 5.9. Loading of the specimens was performed by an MTS880 universal testing machine; loading was conducted using a constant displacement rate until failure of the specimen occurred. It should be noted that similar measures to those noted for the SF-2 specimens to distribute the load were taken for these specimens as well.

Figure 5.9 Test Setup for the Small-Scale Beam GFRP Sandwich Panel Specimens

Manual lay-up is utilized for the manufacturing of the specimens; each of the specimens had slightly different dimensions. The moment of inertia values for the small-scale beams were approximated as 42.68 in^4 (1776.48 cm^4), 32.84 in^4 (1366.9 cm^4), and 38.91 in^4 (1620.81 cm^4) for the control, environmental cycle, and saline exposed specimens, respectively. In order to normalize the results for all three specimens, Figure 5.10 illustrates the load divided by the moment of inertia of the specimen plotted versus mid-span deflection up to failure.

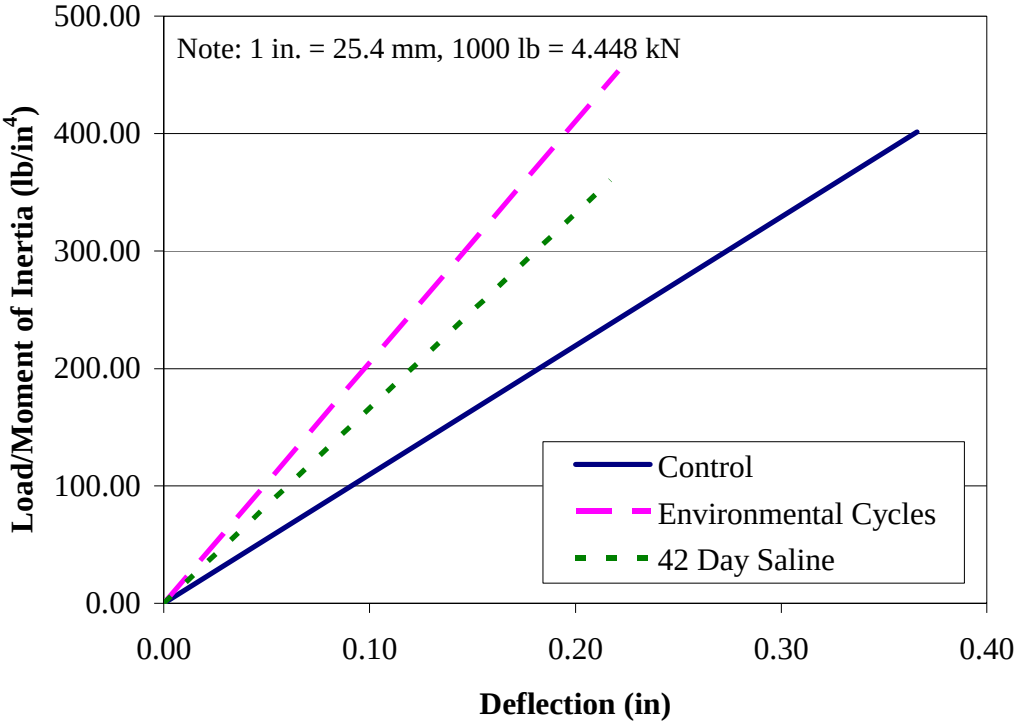

Figure 5.10 Normalized Load versus Mid-span Deflection for the Small-Scale GFRP Sandwich Panel Specimens

Failure of the control specimen occurred at a load of approximately 17.13 kips (76.21 kN). Failure loads for the environmental cycle and saline exposed specimens were 14.89 kips (66.25 kN) and 14.01 kips (62.33 kN), respectively. These failure loads correspond to failure stress values of approximately 6220 psi (42.89 MPa), 7010 psi (48.33 MPa), 5610 psi (38.68 MPa) for the control, environmental cycle, and saline exposed specimens, respectively. Furthermore, it should be noted that the span-to-deflection ratio values at failure for the three specimens were 234, 204, and 259, respectively.

The same trends exhibited in the testing of the GFRP laminates are reiterated by the results of the small-scale beam testing. The ultimate normalized load exhibited by the environmental cycle exposed specimen is approximately 13 percent higher than that

exhibited by the control specimen and for the saline exposed specimen the normalized load is approximately 10 percent lower than the control. Furthermore, the stiffness exhibited by both conditioned specimens is higher than that exhibited by the control specimen.

Failure of all three panels occurred by delamination of the core from the top and bottom faces of the panel on only one end of the panel. In the case of the control and environmental cycle exposed specimens, lateral expansion of the core material occurred whereby one side of the core material bulged out approximately 0.5 in (12.7 mm) at approximately one-quarter of the span. Figure 5.11 illustrates the failure mode exhibited by the control and environmental cycle exposed specimens. It should be noted that the variability in the manufacturing process could have influenced both the failure load and the failure mode of the specimens tested.

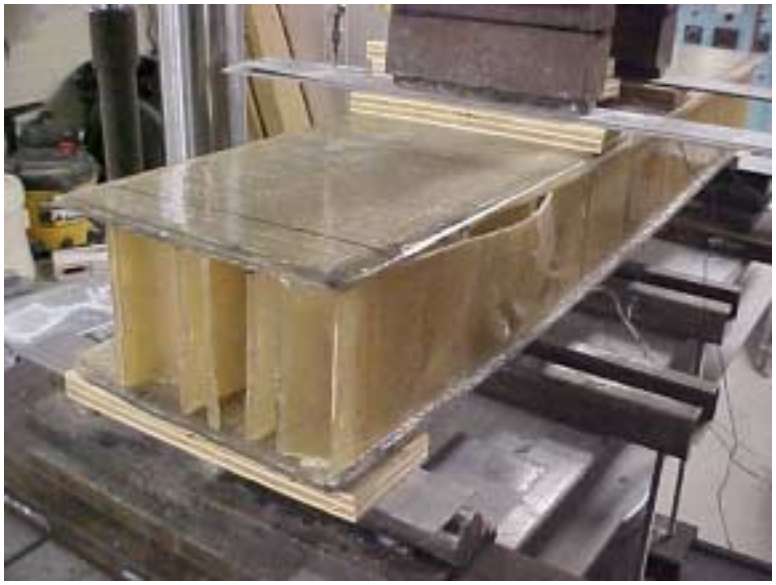

Figure 5.11 Failure Mode of the Small-Scale GFRP Sandwich Panel Specimens

Again, the load versus deflection behavior of the specimens was analyzed to determine the modulus of elasticity of the panels. An overall modulus of elasticity for the panels was determined according to Equation 5.1 based on simple beam theory. This modulus value will take into consideration the deflections due to bending and shear. The results indicate a modulus of elasticity values of 1.51×10^6 psi (10.41 GPa), 2.82×10^6 psi (19.44 GPa), and 2.28×10^6 psi (15.72 GPa) for the control, environmental cycle, and saline exposed specimens, respectively.

5.4. DISCUSSION AND SUMMARY OF RESULTS

Based on the results of the testing conducted on the SF-2 specimens, it is possible that the variability in the manufacturing process could have affected the results of the flexural testing. The difference in the failure load and failure mode of the two, seemingly identical, specimens can be explained once the method of fabrication used for the panels is considered. Appendix A outlines the basic steps of the manual lay-up process. Utilizing manual lay-up for the panels, the core materials are laid into the bottom face of the panel while it is still wet. The process utilized by KSCI uses only weights to ensure contact of the core to the face materials in this particular situation. To the best of the authors' knowledge, the set of weights utilized for this purpose is not standard. At a minimum, it is recommended that a standard load per unit area be applied to the panels to ensure bonding of the core to the bottom face. Further assurance could be provided by implementing vacuum-assisted curing, whereby the panels themselves would be sealed in a constant pressure vacuum bag during the curing process. This could ensure consistent,

more thorough contact of the core materials with the face materials and would decrease the variability in the panels.

When exposed to accelerated aging or a saline solution at an elevated temperature the tensile strength of the GFRP laminates was not adversely affected. In fact in most cases, the modulus and strength of the laminates increased due to the conditioning. The flexural behavior of GFRP sandwich panel beams exposed to accelerated aging in an environmental chamber or exposed to a saline solution at an elevated temperature is different from the behavior of the control specimen. The modulus of both conditioned specimens was higher than that of the control specimen and the strength of the environmentally conditioned specimen was higher than that of the control, while the strength of the saline conditioned specimen was lower.

The same trends exhibited in the testing of the GFRP laminates are reiterated by the results of the small-scale beam testing. The ultimate normalized load exhibited by the environmental cycle exposed specimen is approximately 13 percent higher than that exhibited by the control specimen and for the saline exposed specimen the normalized load is approximately 10 percent lower than the control. Furthermore, the stiffness exhibited by both conditioned specimens is higher than that exhibited by the control specimen.

The increase in modulus of the laminates and the FRP panels following conditioning is assumed to be due to the post-curing of the resin when exposed to the elevated temperatures. One factor affecting the rate and, therefore, degree of curing of a resin is the ambient temperature. When FRP materials are cured at room temperature for an insufficient period of time, there can exist within the resin unlinked polymers.

Exposure to an elevated temperature (i.e., a temperature above the curing temperature) can facilitate the linking of these polymers, causing additional curing of the resin and therefore increasing the stiffness of the FRP material. Investigations into the magnitude of change in the tensile properties of the FRP materials are recommended (CERF, 2001).

Comparison of failure stress values and span-to-deflection ratios at failure is outlined in Table 5.6 for all five of the FRP panels tested. It is evident that the structure of the member affects the performance. Recall that the SF-2 specimens are approximately 4.5 times as deep as the other specimens; additionally the panels are constructed with faces and core material of different thickness/depth. It appears that the failure stress of 9825 psi (67.74 MPa) and span-to-deflection ratio of 100 recommended by the manufacturer may not be conservative for all panel configurations. It is recommended that the manufacturer reconsider their recommendations and adopt a conservative failure stress and span-to-deflection ratio. These values could be dependent on various panel structure parameters (e.g., face thickness, core depth, etc.).

Table 5.6 Comparison of Failure Stress and Deflection Ratio – FRP Panels

Specimen	Maximum Stress at Failure (psi)	Span-to-deflection ratio at failure
SF-2-1	12500	115
SF-2-2	19100	86
Small-scale, control	6220	234
Small-scale, environmental	7010	204
Small-scale, saline	5610	259

Note: 1 psi = 6.89 kPa

A comparison of the average modulus values for the panels illustrates the same trend of property variation based on panel structure; Table 5.7 details such a comparison. With respect to the conservative nature of the design recommendations made by KSCI, recall from Section 3 that the modulus value utilized in the design of the bridges was 1.94×10^6 psi (13.38 GPa). This value would be conservative for all specimens tested with the exception of the small-scale control specimen.

Table 5.7 Comparison of Modulus of Elasticity – FRP Panels

Specimen	Average Modulus of Elasticity (psi)
SF-2-1	3.78×10^6
SF-2-2	4.36×10^6
Small-scale, control	1.51×10^6
Small-scale, environmental	2.82×10^6
Small-scale, saline	2.28×10^6

Note: 1 psi = 6.89 kPa

If the modulus values calculated for the panels are compared to the properties exhibited by the laminates, the similarity between the properties of the small-scale panels and the laminates can be observed. Table 5.8 illustrates a summary of the results for the GFRP laminates.

Of additional interest is a comparison of the failure stress of the FRP laminates and the FRP panels. The average failure stress of the FRP laminates was 42.98 ksi (296.3 MPa), while the highest failure stress of the FRP panels, as exhibited by specimen SF-2-

2, was 19.10 ksi (131.7 MPa); the failure stress exhibited by specimen SF-2-2 was approximately 45 percent of that exhibited by the FRP laminates. An even more marked difference in failure stress is noted when the failure stress of the small-scale control specimen is considered. With a failure stress of 6.22 ksi (42.9 MPa), the small-scale control specimen exhibits a stress approximately 15 percent of that exhibited by the FRP laminates. Recall again that the manufacturer recommended a failure stress of 9825 psi (67.74 MPa) and designed the panels utilizing a factor of safety of 3.0, for a maximum allowable stress of 3275 psi (22.58 MPa). Overall, the difference in performance of the FRP laminates and the FRP panels is based on the structure of the panels, particularly the connection of the core to the faces and the manufacturing process; again the panel configuration is identified as a variable for panel performance.

Table 5.8 Comparison of Modulus of Elasticity – GFRP Laminates

Specimen	Average Modulus of Elasticity (psi)
Control	2.26×10^6
Environmental	2.36×10^6
Saline	2.26×10^6

Note: 1 psi = 6.89 kPa

Examination of the failure mode of the five FRP panel specimens tested, it seems that the typical failure occurs by lateral expansion of the core at one-quarter span and delamination of the core material from the top and/or bottom face of the panels. These results are consistent with the failure of the panels outlined by Nagy et al. (1996).

6. FRP-RC LABORATORY EXPERIMENTATION

The first series of experiments was conducted on the FRP reinforcing bars. Next, in order to compare the behavior of FRP-RC to that of steel-reinforced concrete (steel-RC), testing was conducted on two bridge panels. Testing to determine the flexural and shear capacity of the panels was conducted on an identical FRP-RC bridge panel in the laboratory; results in terms of a load-deflection diagram, ultimate load, and the failure mode of the beam are noted herein. The outcomes of these laboratory tests were compared to the testing results of a steel-RC panel with the same ultimate capacity that was tested in an identical fashion. Comparisons will be drawn between the theoretical and experimental flexural and shear behavior of the FRP-RC panel and the steel-RC panel, with consideration given to several factors utilized in design. Finally, a discussion of the durability of the GFRP bars compares the virgin properties of the GFRP bars to the properties of environmentally conditioned specimens.

6.1. FRP REINFORCING BAR CHARACTERIZATION

It was necessary to verify the tensile strength and tensile modulus of elasticity of the FRP reinforcing bars used for the Walters Street Bridge panels. A series of two each of the 3/8-in (9.5-mm) GFRP, 1/2-in (12.7-mm) GFRP, and 3/8-in (9.5-mm) CFRP bars was tested using a Tinius-Olsen universal testing machine.

To avoid failure of the specimen at the grips due to the relatively low transverse strength of the FRP materials, the ends of the specimens were encased in steel pipe using an expansive grout. A gripping length of 15 in (38.1 cm) was used based on work

conducted by Micelli et al. (2001). Furthermore, an overall specimen length of $40d_b$ plus two times the gripping length, where d_b is the diameter of the bar, was used based on provisional specifications for FRP bars testing that are under review by ACI Committee 440K (2002 Draft). For the first portion of each test, an extensometer was attached to the bar to monitor the deformation under load, thus allowing for determination of the tensile elastic modulus of the bar. See Figure 6.1 for a picture of the extensometer as it was attached during testing.

Figure 6.1 Extensometer Utilized During Tensile Testing

Once the load on the bar reached approximately 50 percent of the expected ultimate load capacity, the extensometer was removed to prevent damage to the instrument during failure. A typical stress versus strain plot from the tensile testing is illustrated in Figure 6.2; the solid line represents the experimental data, while the dashed line represents the expected behavior up to failure. As expected, in all cases linear-elastic

behavior was exhibited until failure and the ultimate load capacity of each bar was recorded.

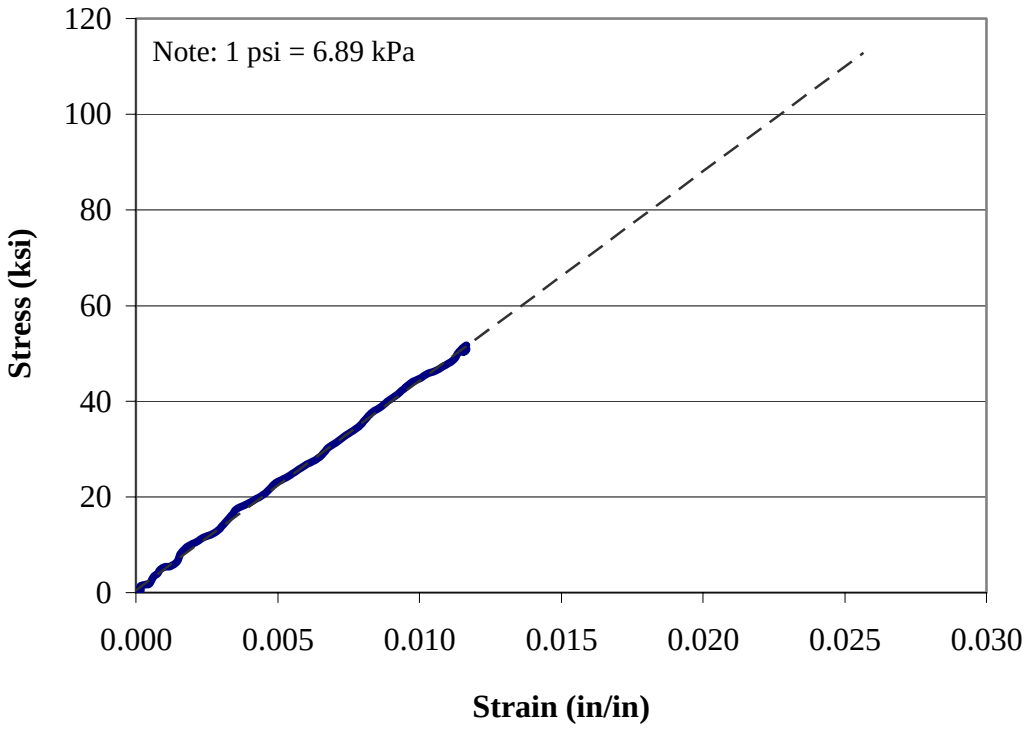

Figure 6.2 FRP Bar – Typical Tensile Test Result

Table 6.1 details the results of the tests conducted. Table 6.2 compares the results of the testing along with the properties reported by the manufacturer; the measured values reported in Table 6.2 are average values obtained from the results of the two specimens tested. For all three types of bars, the measured tensile strength exceeded the tensile strength recommended by the manufacturer. The CFRP bars exhibited a similar trend during testing demonstrating a higher tensile modulus of elasticity than the manufacturer's specifications. On the other hand, the GFRP bars exhibited a modulus of elasticity lower than that recommended by the manufacturer.

Table 6.1 Tensile Test Results – GFRP Bars

	Failure Stress (ksi)	Modulus of Elasticity (Msi)
CFRP - 3/8 in	308	15842
	317	17409
Mean	312.5	16625.5
Standard Deviation	6.4	1108 .4
Coefficient of Variation	1.9%	6.7%
GFRP - 3/8 in	129	5358
	124	5442
Mean	126.5	5400
Standard Deviation	3.5	59.4
Coefficient of Variation	2.7%	1.0%
GFRP - 1/2 in	114	5167
	114	5311
Mean	114	5239
Standard Deviation	0	101.8
Coefficient of Variation	0.0%	1.9%

Note: 1 psi = 6.89 kPa, 1 in. = 25.4 mm

Table 6.2 Comparison of Tensile Properties – GFRP Bars

	Manufacturer's Values		Percent Difference	
Bar Type	**Tensile Strength (ksi)**	**Tensile Modulus (ksi)**	**In tensile strength**	**In tensile modulus**
CFRP 3/8 in	270	15200	+15.9%	+9.4%
GFRP 3/8 in	113	6000	+12.4%	-10%
GFRP 1/2 in	105	6000	+8.6%	-12.7%

The failure mode exhibited by the bars was rupture of the fibers and is illustrated in Figure 6.3. This is the desired failure mode for the bars, which was exhibited in each of the tests.

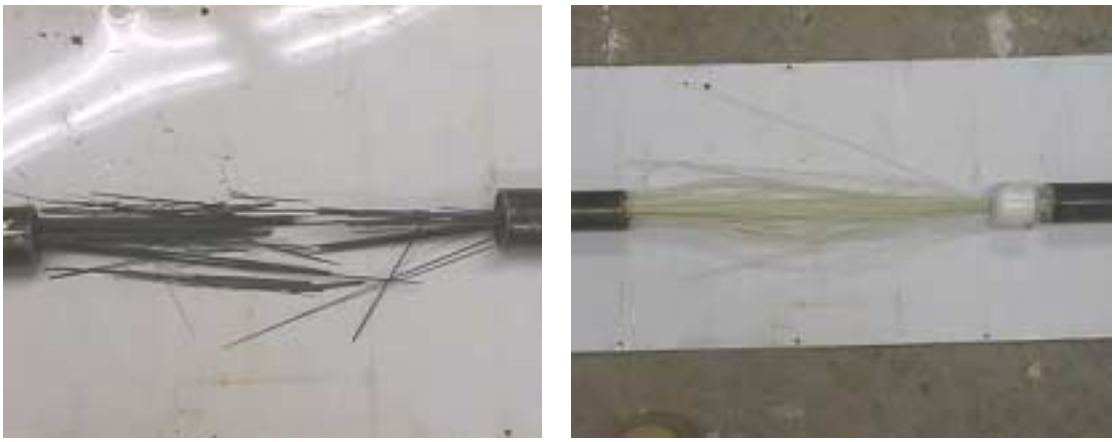

(a) CFRP Bar (b) GFRP Bar

Figure 6.3 Failure Mode of the FRP Bars

6.2. FRP-RC PANEL FLEXURAL AND SHEAR BEHAVIOR

In order to compare the behavior of FRP-RC to that of steel-RC, testing was conducted on two bridge panels. Comparisons will be drawn between the theoretical and experimental flexural and shear behavior of the FRP-RC panel and the steel-RC panel.

Design of the FRP-RC panels outlined previously was conducted according to ACI 440 guidelines (2001). Design of the steel-RC panel was conducted in the traditional manner, according to ACI 318 guidelines, such that the ultimate capacity, M_n, of the panel was approximately equal to the ultimate moment capacity of the FRP-RC panel. The steel-RC panel was under-reinforced indicating that failure would be defined by yielding of the steel followed by crushing of the concrete. The reinforcement in the steel-

reinforced panel consisted of eight 7/8-in (22.2-mm) bars for the tensile longitudinal reinforcement, three 1/2-in (12.7-mm) bars for the compressive longitudinal reinforcement and two 3/8-in (9.5-mm) bars for the shear reinforcement. Figure 6.4 illustrates the layout of the steel reinforcement in the panel. The design compressive strength of the concrete for the steel-RC panel was 4000 psi (27.6 MPa) and steel reinforcement with a yield strength of 60 ksi (413.7 MPa) was utilized; it should be underlined that a bi-linear constitutive model was assumed for the steel, neglecting any strain hardening that may occur.

Figure 6.4 Steel Reinforcement Layout

Verification of the yield strength of the steel reinforcement was also conducted in the laboratory. The yield strength of the steel was reported at 60 ksi (414 MPa) by the manufacturer and the average strength determined from the three specimens tested was 60.4 ksi (416 MPa). Verification of the concrete strength was also conducted by coring cylinders from the tested RC panels. For the four concrete cylinders tested from each of the panels, the average compressive strength values were 3960 psi (27.3 MPa) and 3260 psi (22.5 MPa) for the steel-RC and FRP-RC panels, respectively.

6.2.1. Flexural Testing. In order to verify the design of the FRP-RC panels used for the Walters Street Bridge flexural testing was conducted. One representative specimen was tested in four-point bending to evaluate its load-deflection behavior. Recall that the panels are 2.83 ft (0.9 m) wide, 24 ft (7.3 m) long, and 1 ft (0.3 m) deep. The laboratory specimen was identical to the bridge panels, except that it was not skewed. Additionally, to serve as a comparison, one bridge panel was designed with steel reinforcement to approximately the same ultimate moment capacity, and the panel was tested in the same manner. The test schematic is illustrated in Figure 6.5.

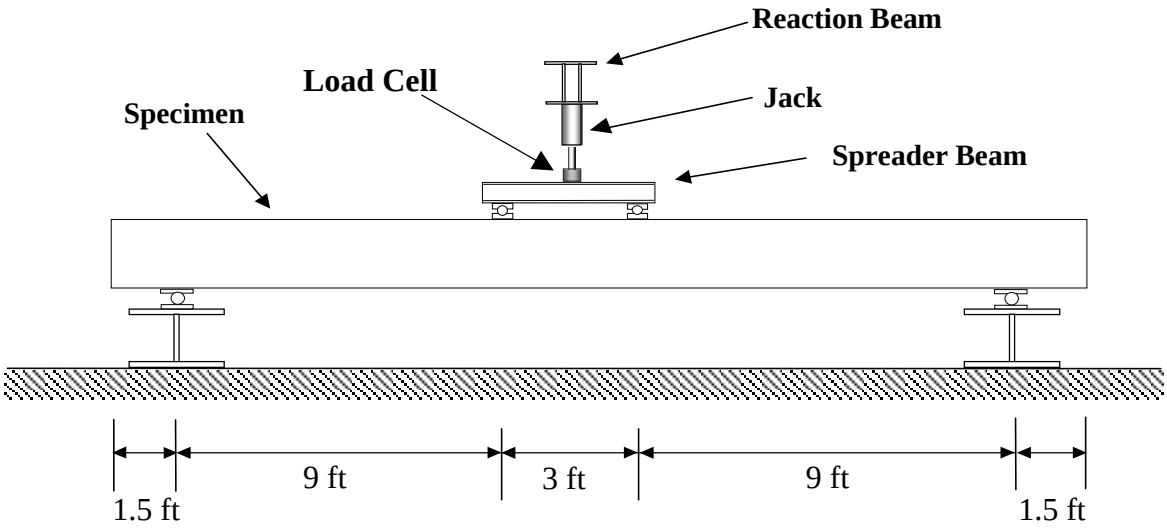

Figure 6.5 Test Schematic for the RC Specimens

The 24–ft (7.32-m) specimens were tested over a clear span of 21 ft (6.4 m) with equal loads applied 9 ft (2.74 m) from each support, leaving a constant-moment region 3 ft (0.91 m) in length. In addition to the LVDT transducers, string transducers, and electrical resistance strain gages installed to the exterior of the specimens in the

laboratory, electrical resistance strain gages were installed on the reinforcing bars prior to casting of the panels. Strain gages were located on several of the tension reinforcement and compression reinforcement bars at mid-span and on the shear stirrups at 20 in (0.51 m) and 30 in (0.76 m) from one end of the panel. Figure 3.7 illustrates the FRP reinforcement layout; the strain gages were located on the first, second, and third bars from the left of the compression reinforcement and on the first, fourth and ninth bars from the left of the tensile reinforcement. It should be noted that the strain gages on the compression and tension reinforcement were at approximately the same lateral location. The test setup for the flexural testing is illustrated in Figure 6.6. Note the string transducers located at mid-span, as well as the LVDT transducers located at the supports, the quarter-span locations and mid-span.

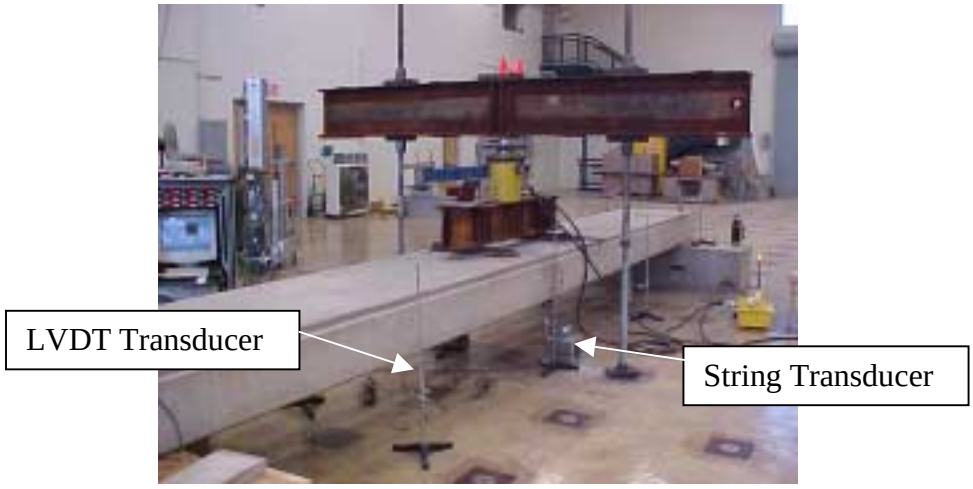

Figure 6.6 Test Setup for Flexural Testing

Based on simple beam theory and a failure criterion of a maximum concrete strain of 0.003, the failure load was approximated at 47 kips (210 kN) for both the steel-RC and

FRP-RC sections. Recall that the design of the FRP-RC panel was conducted such that the section would be over-reinforced and the design of the steel-RC panel was conducted such that the section would be under-reinforced. The panels were tested to failure through the application of quasi-static load cycles. Several load cycles were conducted within each of the moment-curvature diagram regions (e.g., up to cracking, yielding of the steel, etc.). Each load cycle proceeded up to the desired load followed by unloading to approximately 5 kips (22.24 kN); during the final load cycle the specimen was taken to failure. The results of these tests are summarized herein in terms of the moment-curvature diagrams, load-deflection diagrams, plots of strain versus load and observed failure modes.

Figure 6.7 illustrates the moment-curvature relationships for the steel-RC and FRP-RC panels. For each panel the experimental envelope is plotted along with the theoretical relationship, which is tri-linear in the case of the steel-RC panel and bi-linear in the case of the FRP-RC panel. For the tri-linear moment-curvature relationship for the steel-RC panel, the cracking, yield and ultimate moment and curvature values were calculated. For the bi-linear moment-curvature relationship for the FRP-RC panel, the cracking and ultimate moment and curvature values were calculated. Both theoretical relationships were based on the following assumptions:

- Plane sections remain plane, that is, the concrete and reinforcement strain values are proportional to their distance from the neutral axis
- The tensile strength of the concrete is ignored.
- A parabolic stress distribution in the concrete was utilized.
- The ultimate concrete compressive strain is 0.003.

- There is perfect bond between the reinforcement and the concrete.

As mentioned in the outline of the design of the panels, specific to the reinforcement utilized, it was assumed that the FRP reinforcement exhibits linear-elastic behavior until failure and no strain hardening of the steel reinforcement was considered.

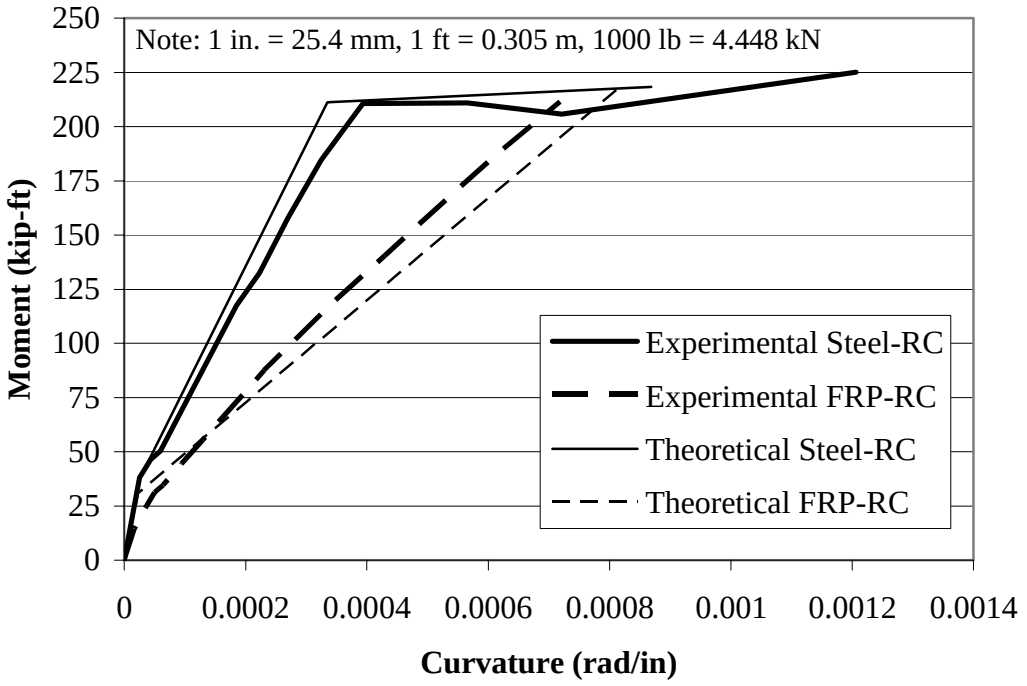

Figure 6.7 Experimental and Theoretical Moment-Curvature Relationships for the Steel-RC and FRP-RC Panels

Failure of both panels was predicted at and occurred at approximately 220 kip-ft (298 kN-m). It should be noted that for the FRP-RC panel, the difference between the initial slope of the experimental curves and the initial slope of the theoretical curves is due to the presence of a crack near mid-span that had occurred during shipment. Very good agreement was observed between the theoretical and experimental stiffness values for both of the panels.

The load-deflection diagrams for the steel-RC and FRP-RC panels are illustrated in Figure 6.8. For the steel-RC section, the envelope of the experimental results is plotted against the theoretical load-deflection relationship, which is obtained via double-integration of the tri-linear approximation of the moment-curvature relationship. For the FRP-RC section, the envelope of the experimental results is plotted against the theoretical load-deflection relationship, which is obtained via double-integration of the bi-linear approximation of the moment-curvature relationship. Furthermore, the predicted load-deflection relationship for the FRP-RC panel as calculated utilizing the ACI 440 guidelines (2001) is presented. Utilizing the modified Branson's equation presented by ACI, the effective moment of inertia of the section was determined for various levels of applied moment and used to calculate the deflection of the panel. The modified Branson's equation is as follows:

$$I_e = \left(\frac{M_{cr}}{M_a}\right)^3 \beta_d I_g + \left[1 - \left(\frac{M_{cr}}{M_a}\right)^3\right] I_{cr} \le I_g \qquad \textbf{(6.1)}$$

$$\beta_d = \alpha_b \left[\frac{E_f}{E_s} + 1\right] \qquad \textbf{(6.2)}$$

where M_{cr} is the cracking moment of the section, M_a is the moment applied to the section, β_d is a modification factor based on the ratio of the modulus of the FRP reinforcement to that of steel reinforcement defined by Equation 6.2, I_g is the gross moment of inertia of the section, I_{cr} is the cracked moment of inertia of the section, α_b is a bond-dependent coefficient taken to be 0.5 in this case, E_f is the longitudinal modulus of elasticity of the FRP reinforcement, and E_s is the modulus of elasticity of the steel reinforcement. As the ACI provisions intend to limit the deflections at service load levels, the ACI predicted

load-deflection relationship is plotted up to the load that would induced the service moment in the panel. This is done by equating the two conditions where the maximum positive moment would be induced at mid-span; the loading of the panels and the bridge have slightly different configurations.

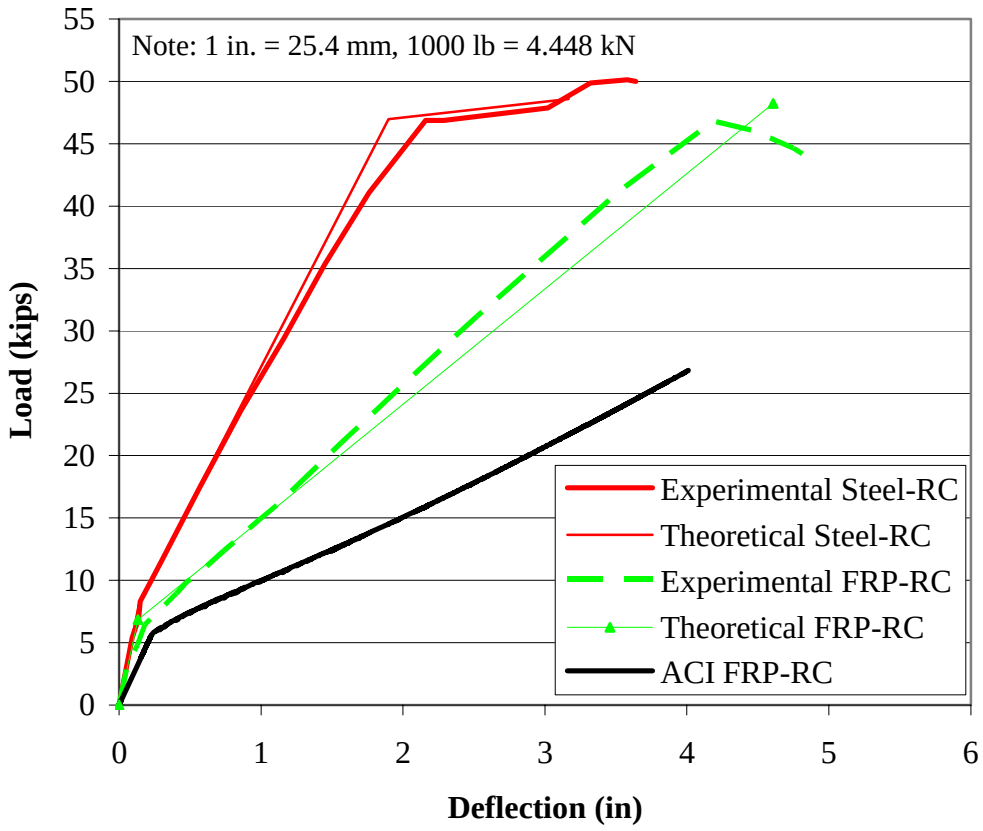

Figure 6.8 Experimental and Theoretical Load-Deflection Relationships for the Steel-RC and FRP-RC Panels

Failure of the steel-RC panel occurred at a load of approximately 50 kips (222.4 kN) and was characterized by yielding of the tensile reinforcement followed by crushing of the concrete just outside the area of load application. Failure of the FRP-RC panel occurred at approximately 47 kips (209.1 kN), as indicated by shear cracking and crushing of the concrete. Failure of the steel-RC and FRP-RC panels during the flexural

capacity tests is illustrated in Figure 6.9 and Figure 6.10, respectively. The shear cracking of the FRP-RC panel in Figure 6.10 is highlighted with lines to make it more visible.

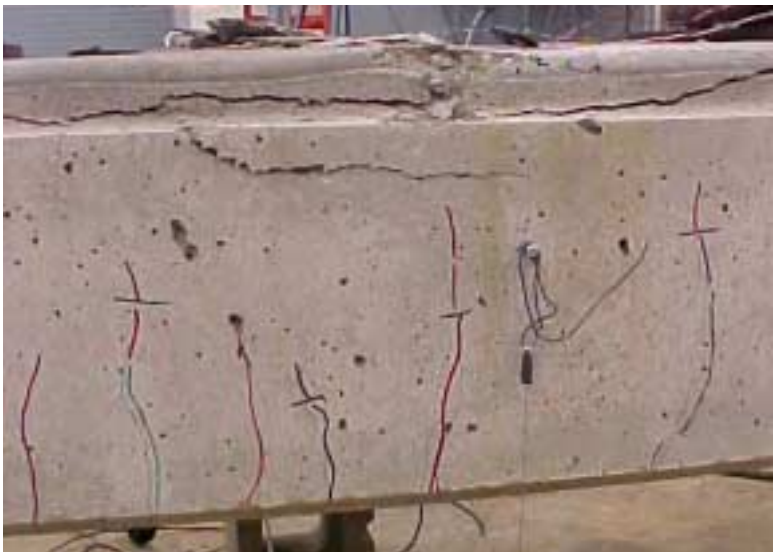

Figure 6.9 Failure of the Steel-RC Panel During the Flexural Testing

Figure 6.10 Failure of the FRP-RC Panel During Flexural Testing

A comparison of the load-deflection curves of the FRP-RC and steel-RC panels confirms that the FRP-RC section is less stiff than the steel-RC section; however both sections reached the predicted failure load. For both sections, the slope of the experimental curve is nearly identical to the theoretical curve obtained from the moment-curvature relationship; however the ACI 440 theoretical curve exhibits a much lower stiffness than the other two curves for the FRP-RC section. A comparison of the ACI 440 theoretical deflection, a value of approximately 4.1 in (103.4 mm) at the service load level, and the experimental deflection, a value of approximately 2.1 in (52.9 mm) at the same load level, indicates that the experimental deflection is approximately 50 percent of the theoretical deflection as predicted by the ACI 440 guidelines (2001). If the same comparison is drawn between the predicted deflection of the steel-RC panel based on the Branson equation and the experimental deflection, the ratio of experimental to theoretical deflection is also approximately 50 percent. The fact that the same level of conservatism is exhibited by both the Branson equation and the modified Branson equation lends confidence to the adoption of the modified Branson equation in the ACI 440 guidelines (2001).

Figure 6.11 through Figure 6.13 illustrate the load versus strain in the tensile reinforcement, the strain in the compression reinforcement, and the compressive strain in the concrete, respectively for the FRP section. Three electrical resistance strain gages at different lateral positions were located at each depth, with their specific locations detailed previously. It should be noted that one of the gages on the compression reinforcement failed to work properly. The trends exhibited in these plots are further examined by considering several normalized parameters: strain in the tensile reinforcement divided by

ultimate strain at rupture, compressive strain in the concrete, and depth of the neutral axis divided by entire section depth.

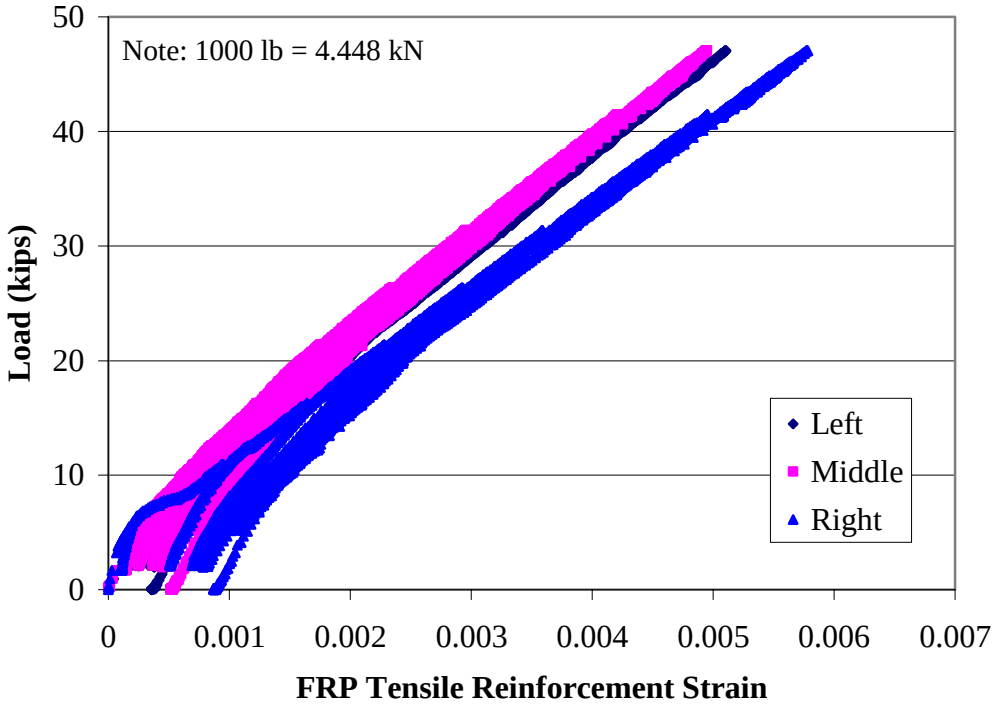

Figure 6.11 Load versus Strain in the Tensile Reinforcement – FRP-RC Panel

Strain in the tensile reinforcement increases bi-linearly until panel failure at a strain of approximately 0.005. Rupture of the CFRP reinforcement would occur at an ultimate strain of approximately 0.015. Failure of the panel occurred when the strain in the CFRP reinforcement was approximately 33 percent of the ultimate strain at rupture indicating a stress in the tensile reinforcement of roughly 80 ksi (552 MPa). The maximum compressive strain in the concrete at failure was approximately 0.002, or nearly 66 percent of the theoretical maximum concrete compressive strain, which is generally taken to be 0.003. The location of the neutral axis was determined by examination of the strain in the concrete and FRP reinforcement in the panel. The

location of the neutral axis of the section at failure, expressed as a percentage of the section depth, was approximately 0.223. The theoretical location at failure of the panel was 0.213, which is very close to the experimental failure ratio.

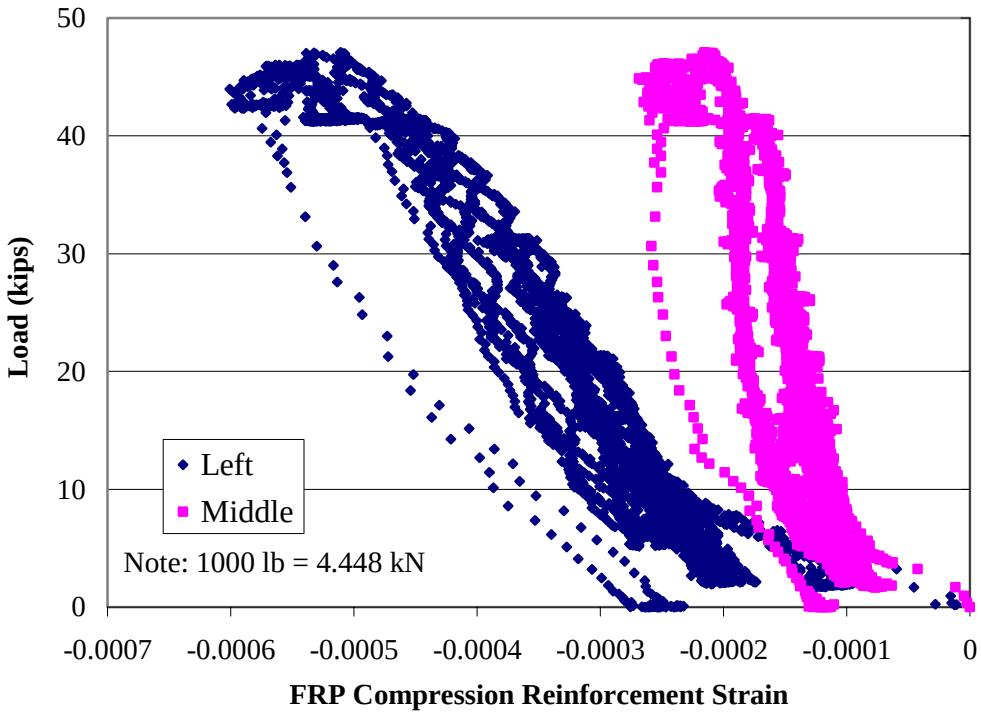

Figure 6.12 Load versus Strain in the Compression Reinforcement – FRP-RC Panel

6.2.2. Shear Testing. Following the flexural capacity testing, the same two panels were also tested to determine their shear capacity. The portion of the panels that were unaffected by the flexural testing were re-tested in three-point bending with a clear span of 7 ft (2.13 m). Figure 6.14 illustrates the test setup; note that the load was applied at mid-span. Instrumentation for the shear capacity tests consisted of string transducers and LVDT transducers. Furthermore, for the FRP-RC panel the strain gages located on

the shear stirrups 20 in (0.51 m) and 30 in (0.76 m) from the end of the panel measured strain in the FRP stirrups at shear failure of the panel.

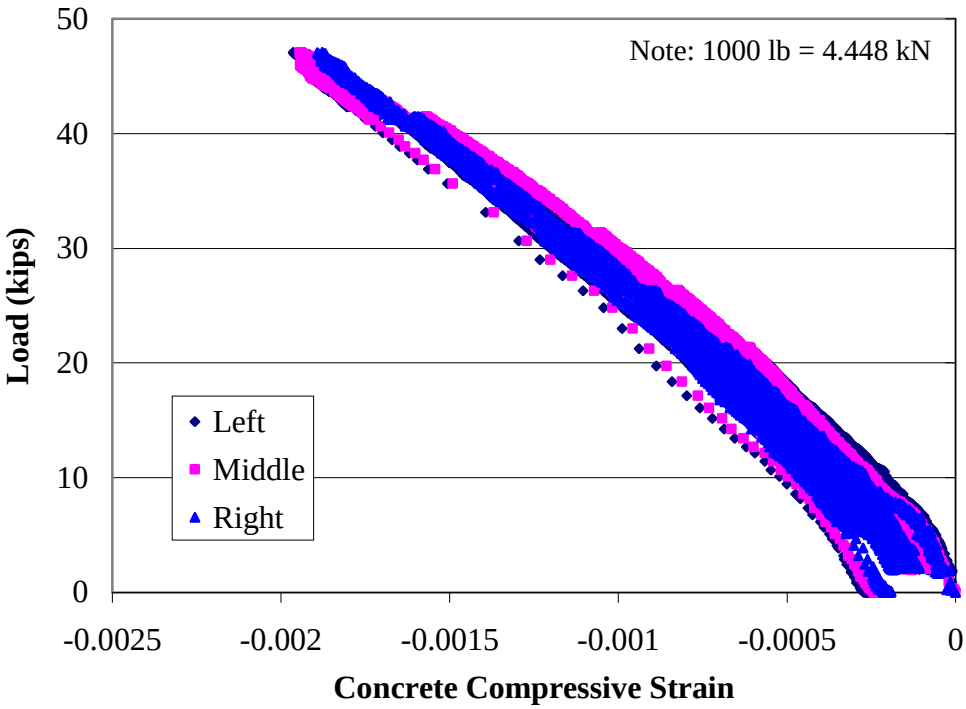

Figure 6.13 Load versus Compressive Strain in Concrete – FRP-RC Panel

Figure 6.14 Test Setup for Shear Testing

Utilizing the material properties obtained from the laboratory characterization and the ACI guidelines for FRP- and steel-RC, the ultimate shear capacity of the steel-RC and FRP-RC panels was predicted at approximately 70.7 kips (314.5 kN) and 30.8 kips (137 kN), respectively. The concrete contribution to the shear capacity is approximated for the steel-RC by

$$2\sqrt{f_c'}bd \quad \textbf{(6.3)}$$

and for the FRP-RC by

$$\frac{\rho_f E_f}{\rho_s E_s}\left(2\sqrt{f_c'}bd\right) \quad \textbf{(6.4)}$$

In the above relationships f'c denotes the concrete compressive strength, b denotes the width of the panel, and d denotes the depth to the centroid of the reinforcing bars. The reinforcement contribution to the shear capacity is approximated for the steel-RC by

$$\frac{A_v f_y d}{s} \quad \textbf{(6.5)}$$

and for the FRP-RC by

$$\frac{A_{fv} f_{fv} d}{s} \quad \textbf{(6.6)}$$

In the above relationships A_v and A_{fv} denote the area of shear reinforcement for the steel and FRP, f_y is the yield stress of the steel shear reinforcement, f_{fv} is the design stress level for the FRP shear reinforcement, and s denotes the spacing of the shear reinforcement. It should be underlined that the strain in the FRP shear reinforcement is limited to 0.002 by the ACI 440 guidelines (2001). For the steel-RC panel, the concrete contribution to the shear strength is 43.6 kips (193.9 kN) and the reinforcement contribution is 27.1 kips

(120.4 kN); for the FRP-RC section these values are 21.3 kips (94.7 kN) and 9.5 kips (42.3 kN), respectively.

Figure 6.15 illustrates the experimental load-deflection relationships obtained during the shear capacity testing. Failure of the steel-RC panel occurred at approximately 130 kips (580 kN), while failure of the FRP-RC panel occurred at approximately 118 kips (525 kN). The steel-RC and FRP-RC shear capacity predictions were very conservative, due in part to the factor of two assumed for the contribution of the concrete to the shear capacity, the ratio used in Equation 6.3 to reduce the concrete contribution to the shear capacity of the FRP-RC panel, and the limit of 0.002 on the strain in the FRP shear reinforcement. The ratio between experimental and predicted shear capacities was 1.84 for the steel-RC and 3.83 for the FRP-RC.

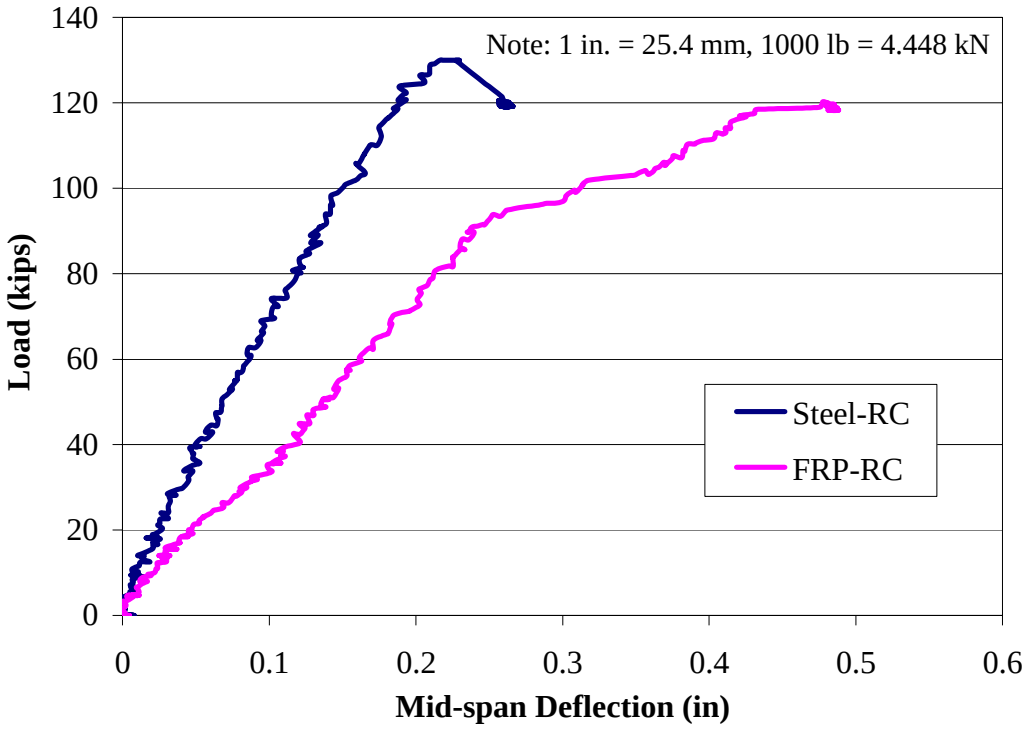

Figure 6.15 Experimental Load-Deflection Relationships for the Shear Testing of the Steel-RC and FRP-RC Panels

Failure of the steel-RC and FRP-RC panels during the shear capacity tests is illustrated in Figure 6.16 and Figure 6.17, respectively. In Figure 6.16, a line to make it more visible highlights the shear crack in the steel-RC section. With regard to Figure 6.17, the vertical dashed lines represent the location of the instrumented stirrups located approximately 20 in (0.51 m) and 30 in (0.77m) from the end of the panel. Although it is not visible in the figures, crushing of the concrete did occur at failure.

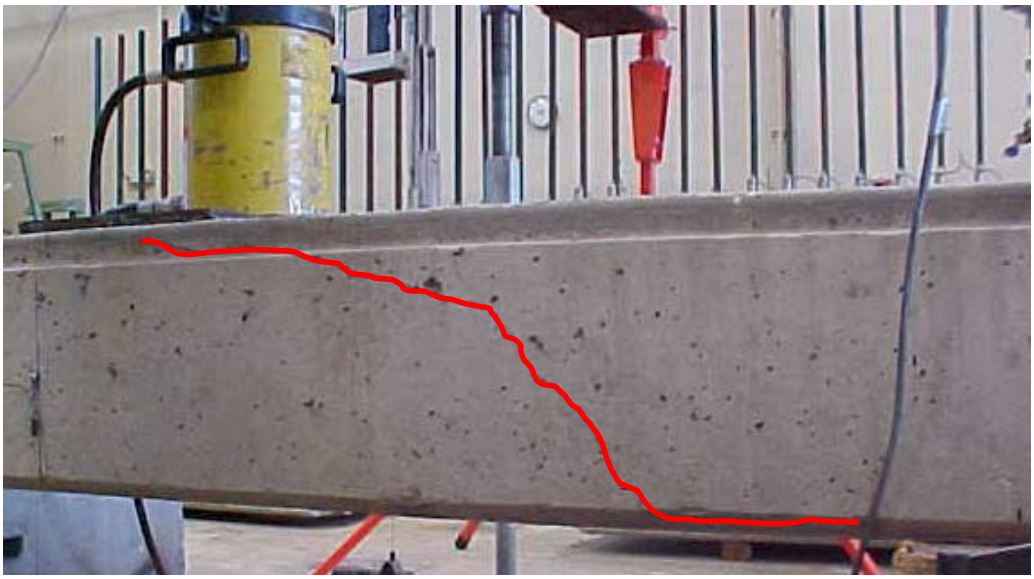

Figure 6.16 Shear Failure of the Steel-RC Panel

Strain readings from the shear stirrups are illustrated in Figure 6.18. Due to the testing configuration, the shear stirrups were located 2 in (50.8 mm) and 12 in (0.30 m) from the support. The two instrumented stirrups located 12-in (0.30-m) from the center of the support both experienced significant levels of strain. The stirrup in the right side of the panel exhibited more strain than that on the left side; however this is consistent with the shear cracking exhibited by the panel.

Figure 6.17 Shear Failure of the FRP-RC Panel

Figure 6.18 indicates the very conservative ACI 440 limit for the strain in the shear stirrups of 0.002, or 2000 με, (marked on the figure by a dashed vertical line). The maximum strain experienced by the shear stirrups was roughly 0.0065, or 6500 με, corresponding to roughly one-third the ultimate strain at rupture and a stress of approximately 36 ksi (250 MPa). Rupture of the FRP stirrups was not observed.

6.3. ENVIRONMENTAL CONDITIONING RESISTANCE

The GFRP bars utilizing a urethane-modified vinyl ester resin were subjected to environmental conditions designed to simulate their in-situ environments. The tensile and interlaminar shear properties of GFRP bars subjected to each of these conditions were determined and are compared to the properties of the control specimens.

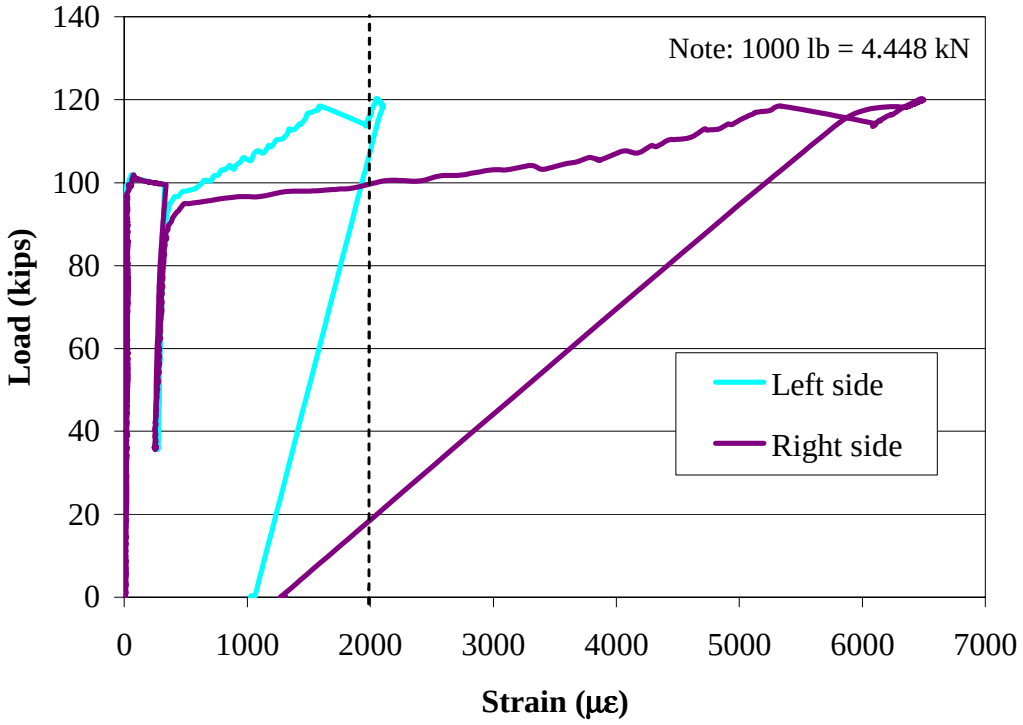

Figure 6.18 Strain in FRP Stirrups 12 in (0.3 m) from the Support – Shear Testing

6.3.1. Tensile Strength. To replicate the exposure of the GFRP bars to an alkaline environment such as would be encountered when used as reinforcement for concrete, a solution containing calcium, sodium and potassium hydroxides was formulated. The following percentages by weight were dissolved in distilled water to produce a solution with a pH of 12.6,

$$0.012\%\ Ca(OH)2 + 0.073\%\ Na(OH) + 0.103\%\ K(OH) \quad \textbf{(6.7)}$$

To accelerate absorption, the bars were immersed in the alkaline solution at an elevated temperature of 140°F (60°C). The following correlation between exposure to an alkaline solution at elevated temperature developed by Litherland et al. was reported by Vijay et al. (1999)

$$\frac{N}{C} = 0.098\, e^{0.0558T} \quad \textbf{(6.8)}$$

where N is the predicted age in natural days, C is the number of days of exposure to the alkaline solution at an elevated temperature, T, in Fahrenheit. For this research program, specimens were conditioned for 42 days, which should correspond to natural aging of 28 years.

The same testing procedure outlined for the unconditioned bars, outlined in Section 6.1, was utilized for the conditioned bars as well. Three bars of each type were tested, with the results detailed in Table 6.3 and Table 6.4.

Three specimens for each GFRP bar diameter were tested with the results summarized in Table 6.3 and Table 6.4 for the 3/8-in (9.5-mm) GFRP and 1/2-in (12.7-mm) GFRP bars, respectively.

Table 6.3 Tensile Test Results - 3/8 in GFRP Bars - Alkaline-Conditioned

Specimen	Failure Load (lb)	Tensile Strength (ksi)	Tensile Modulus (ksi)
M3-A1	10925	98.9	4618.6
M3-A2	11775	106.6	4392.5
M3-A3	10480	94.6	5123.7
Average	11060	100.0	4711.6

Note: 1 psi = 6.89 kPa, 1 in. = 25.4 mm, 1000 lb = 4.448 kN

The average results for the indicate that the ultimate failure load was 11060 lb (49.20 kN), indicating an ultimate tensile strength of 100.0 ksi (689.48 MPa) and a tensile modulus of elasticity of 4711.6 ksi (32.48 GPa). The standard deviation for the tensile strength and tensile modulus were 6.08 ksi (41.9 MPa) and 374.4 ksi (2.6 GPa), respectively.

The average results indicate that the ultimate failure load was 20450 lb (90.97 kN), indicating an ultimate tensile strength of 104.2 ksi (718.43 MPa) and a tensile modulus of elasticity of 4849.3 ksi (33.43 GPa). The standard deviation for the tensile strength and tensile modulus were 1.13 ksi (7.8 MPa) and 645.8 ksi (4.5 GPa), respectively.

Table 6.4 Tensile Test Results - 1/2 in GFRP Bars - Alkaline-Conditioned

Specimen	Failure Load (lb)	Tensile Strength (ksi)	Tensile Modulus (ksi)
M4-A1	20700	105.4	5585.6
M4-A2	20275	103.3	4378.9
M4-A3	20375	103.8	4583.3
Average	20450	104.2	4849.3

Note: 1 psi = 6.89 kPa, 1 in. = 25.4 mm, 1000 lb = 4.448 kN

Compared to the results from the control specimens the residual tensile strength for the 3/8-in (9.5-mm) GFRP and 1/2-in (12.7-mm) GFRP bars was approximately 78.8 percent and 91.4 percent, respectively. For the tensile modulus these values are 87.3 percent and 92.6 percent, respectively. Figure 6.19 illustrates the change in tensile stress and tensile modulus exhibited by the GFRP bars. It should be noted that the failure mode for the conditioned bars was the same as it was for the control bars.

Residual values of tensile strength and modulus can be compared to the recommendations put forth by ACI (2001), which outline an environmental reduction factor, C_E, to be used to account for the long-term tensile strength of the bars. For GFRP bars exposed to earth and weather, this factor is equal to 0.7. For both diameters of

GFRP bar the results indicate that the factor of 0.7 is conservative. Recall that the conditioning was approximated to represent natural aging of 28 years.

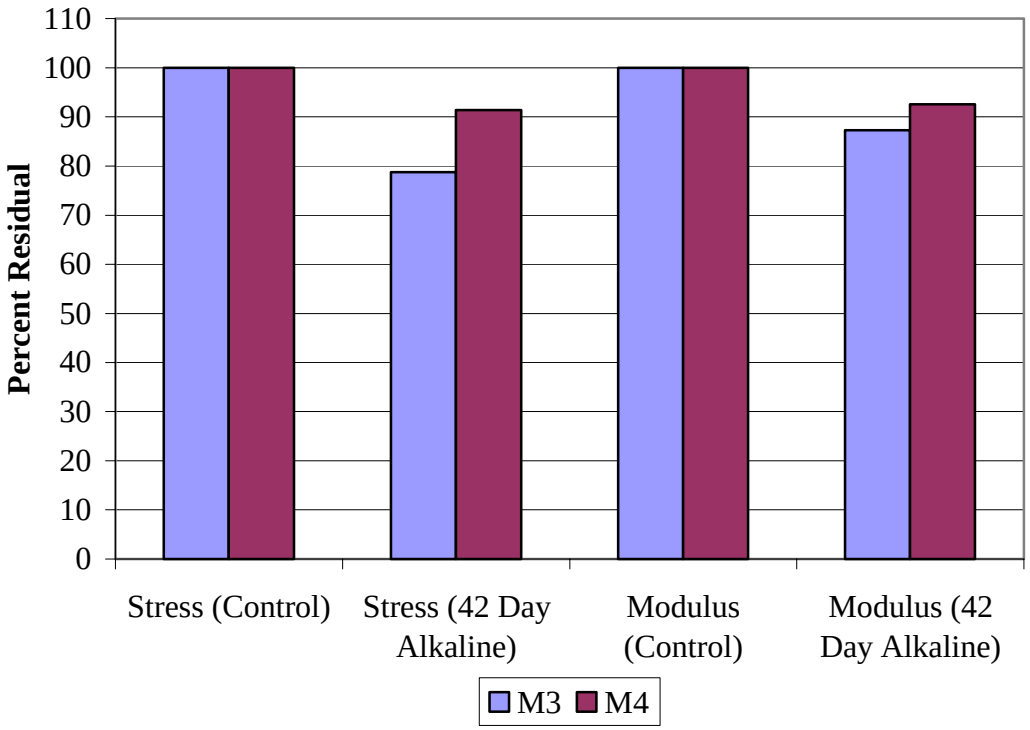

Figure 6.19 Residual Tensile Properties for GFRP Bars

6.3.2. Interlaminar Shear Strength. In addition to the aforementioned alkaline solution, the interlaminar shear strength specimens were also subjected to a second conditioning scheme, consisting of the combined environmental conditioning outlined for the FRP panels in Section 5.3.

The interlaminar shear properties of GFRP bars subjected to these conditions were determined and are compared to the properties of control specimens. ASTM standard test method D4475 was utilized to determine the apparent horizontal shear

strength, or interlaminar shear strength, of the GFRP bars. Specimens were evaluated prior to any conditioning, after 4 cycles of exposure in the environmental chamber, and after 21 and 42 days of exposure to the alkaline solution. Prior to conditioning the specimens were cut to the recommended length, four times the diameter of the given bar, and the ends of the specimens were sealed with silicone to prevent unwanted absorption of moisture. A minimum of six specimens of each type were evaluated under three-point bending over a span length of three times the diameter of the given bar. ASTM D4475 dictates that the loading rate of the specimens should be 0.05 in (1.3 mm) per minute. The failure load, P, and the diameter, d_b, of the bar are used to calculate the interlaminar shear strength, S, of the bar using the following equation:

$$S = 0.849\frac{P}{d_b^{\,2}} \qquad \textbf{(6.9)}$$

It should be noted that the interlaminar shear strength values obtained via this test are to be used only for comparative purposes, whereby the change in properties of bars subjected to different exposure regimens can be identified. A typical load versus mid-span deflection curve is illustrated in Figure 6.20; the curve is for one of the M4 control specimens.

Failure for nearly all of the specimens was indicated by a combination of vertical (parallel to the loading head of the machine) and horizontal (perpendicular to the loading head of the machine) cracking that propagated along the longitudinal axis of the bar. Figure 6.20 contains a picture of the failed specimen as well, illustrating the failure mode described.

Table 6.5 through Table 6.12 detail the failure load and interlaminar shear strength values for each type of bar. Specimen identification consists of the bar type,

either M3, or M4, followed by the conditioning regimen; “C” for control, “EC” for four environmental cycles, or “21A” or “42A” for 21 and 42 days of alkaline conditioning, respectively. Figure 6.21 illustrates a summary of the comparison between the conditioned specimens to the control specimens for both the 3/8 in GFRP and 1/2 in GFRP bars.

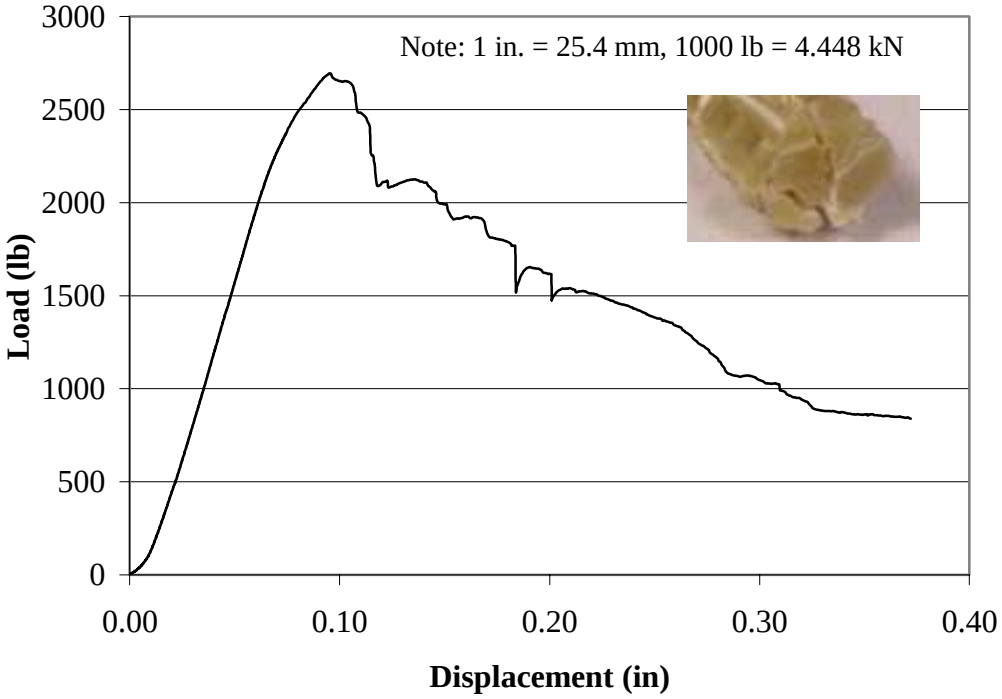

Figure 6.20 Typical Load versus Mid-span Deflection Curve for Interlaminar Shear Strength Tests

The exposure to the environmental cycles appears to have no effect on the interlaminar shear strength. However, the results indicate that the alkaline conditioning conducted causes more degradation in the 1/2-in (12.7-mm) GFRP bars than the 3/8-in (9.5-mm) GFRP bars. Residual properties of approximately 65 percent were recorded for

the 1/2-in (12.7-mm) GFRP bars, while for the 3/8-in (9.5-mm) GFRP bars the values were greater than 100 percent, indicating an increase in performance.

Table 6.5 Interlaminar Shear Strength - 3/8 in GFRP Bars - Control

Specimen	Failure Load (lb)	Interlaminar Shear Strength (psi)
M3-C1	1582.8	9555.9
M3-C2	1366.4	8249.4
M3-C3	1630.6	9844.5
M3-C4	1186.0	7160.3
M3-C5	1078.1	6508.8
M3-C6	1154.9	6972.5
Average	1333.1	8048.6

Note: 1 psi = 6.89 kPa, 1 in. = 25.4 mm, 1000 lb = 4.448 kN

Table 6.6 Interlaminar Shear Strength - 3/8 in GFRP Bars – Environmentally Conditioned

Specimen	Failure Load (lb)	Interlaminar Shear Strength (psi)
M3-EC1	1513.0	9134.5
M3-EC2	1251.5	7555.7
M3-EC3	1148.5	6933.9
M3-EC4	1553.3	9377.8
M3-EC5	1491.0	9001.7
M3-EC6	1554.9	9387.4
Average	1418.7	8565.2

Note: 1 psi = 6.89 kPa, 1 in. = 25.4 mm, 1000 lb = 4.448 kN

In addition to the interlaminar shear testing conducted on the short FRP bars specimens, gravimetric measurements were also taken for each group of specimens every seven days during the conditioning. The fluid content was measured as follows:

$$M_t = \frac{W - W_d}{W_d} \quad \textbf{(6.10)}$$

where M_t equals the percentage of fluid content at time t, W_d is the weight of the dry specimen at the initiation of the test, and W is the weight of the moist specimen after some time, t, of conditioning. Although no specific calculations of the diffusivity of the materials were performed, Figure 6.22 illustrates the change in weight as a function of time (i.e., the square root of the time in minutes).

Table 6.7 Interlaminar Shear Strength - 3/8 in GFRP Bars – 21 day Alkaline-Conditioned

Specimen	Failure Load (lb)	Interlaminar Shear Strength (psi)
M3-21A1	1590.3	9601.2
M3-21A2	1535.6	9270.9
M3-21A3	1566.2	9455.7
M3-21A4	1560.8	9423.1
M3-21A5	1255.8	7581.7
M3-21A6	1332.6	8045.4
M3-21A7	994.9	6006.5
M3-21A8	1439.5	8690.7
M3-21A9	1482.4	8949.7
Average	1417.6	8558.3

Note: 1 psi = 6.89 kPa, 1 in. = 25.4 mm, 1000 lb = 4.448 kN

Table 6.8 Interlaminar Shear Strength - 3/8 in GFRP Bars – 42 day Alkaline-Conditioned

Specimen	Failure Load (lb)	Interlaminar Shear Strength (psi)
M3-42A1	1590.9	9604.8
M3-42A2	1507.1	9098.9
M3-42A3	1396.0	8428.1
M3-42A4	1504.4	9082.6
M3-42A5	1429.8	8632.2
M3-42A6	1521.1	9183.4
M3-42A7	1420.7	8577.2
M3-42A8	1293.4	7808.7
M3-42A9	1421.2	8580.3
Average	1453.8	8777.3

Note: 1 psi = 6.89 kPa, 1 in. = 25.4 mm, 1000 lb = 4.448 kN

Table 6.9 Interlaminar Shear Strength - 1/2 in GFRP Bars - Control

Specimen	Failure Load (lb)	Interlaminar Shear Strength (psi)
M4-C1	2481.9	8428.5
M4-C2	2575.8	8747.4
M4-C3	2657.7	9025.5
M4-C4	2754.4	9353.9
M4-C5	2379.9	8082.1
M4-C6	2694.0	9148.8
Average	2590.6	8797.7

Note: 1 psi = 6.89 kPa, 1 in. = 25.4 mm, 1000 lb = 4.448 kN

Table 6.10 Interlaminar Shear Strength - 1/2 in GFRP Bars – Environmentally Conditioned

Specimen	Failure Load (lb)	Interlaminar Shear Strength (psi)
M4-EC1	2622.8	8907.0
M4-EC2	2140.9	7270.5
M4-EC3	2405.4	8168.7
M4-EC4	2739.6	9303.7
M4-EC5	2625.5	8916.2
M4-EC6	2685.9	9121.3
Average	2536.7	8614.6

Note: 1 psi = 6.89 kPa, 1 in. = 25.4 mm, 1000 lb = 4.448 kN

Table 6.11 Interlaminar Shear Strength - 1/2 in GFRP Bars – 21 day Alkaline-Conditioned

Specimen	Failure Load (lb)	Interlaminar Shear Strength (psi)
M4-21A1	1665.0	5654.3
M4-21A2	2147.7	7293.6
M4-21A3	1260.1	4279.3
M4-21A4	1311.2	4452.8
M4-21A5	1856.1	6303.3
M4-21A6	1637.6	5561.3
M4-21A7	1819.1	6177.6
M4-21A8	1653.7	5616.0
M4-21A9	1514.1	5141.9
Average	1651.6	5608.9

Note: 1 psi = 6.89 kPa, 1 in. = 25.4 mm, 1000 lb = 4.448 kN

Table 6.12 Interlaminar Shear Strength - 1/2 in GFRP Bars – 42 day Alkaline-Conditioned

Specimen	Failure Load (lb)	Interlaminar Shear Strength (psi)
M4-42A1	1362.2	4626.0
M4-42A2	2136.9	7256.9
M4-42A3	2140.9	7270.5
M4-42A4	1363.8	4631.5
M4-42A5	1507.7	5120.1
M4-42A6	1894.2	6432.7
M4-42A7	1692.3	5747.1
M4-42A8	1780.4	6046.2
M4-42A9	1616.1	5488.3
Average	1721.6	5846.6

Note: 1 psi = 6.89 kPa, 1 in. = 25.4 mm, 1000 lb = 4.448 kN

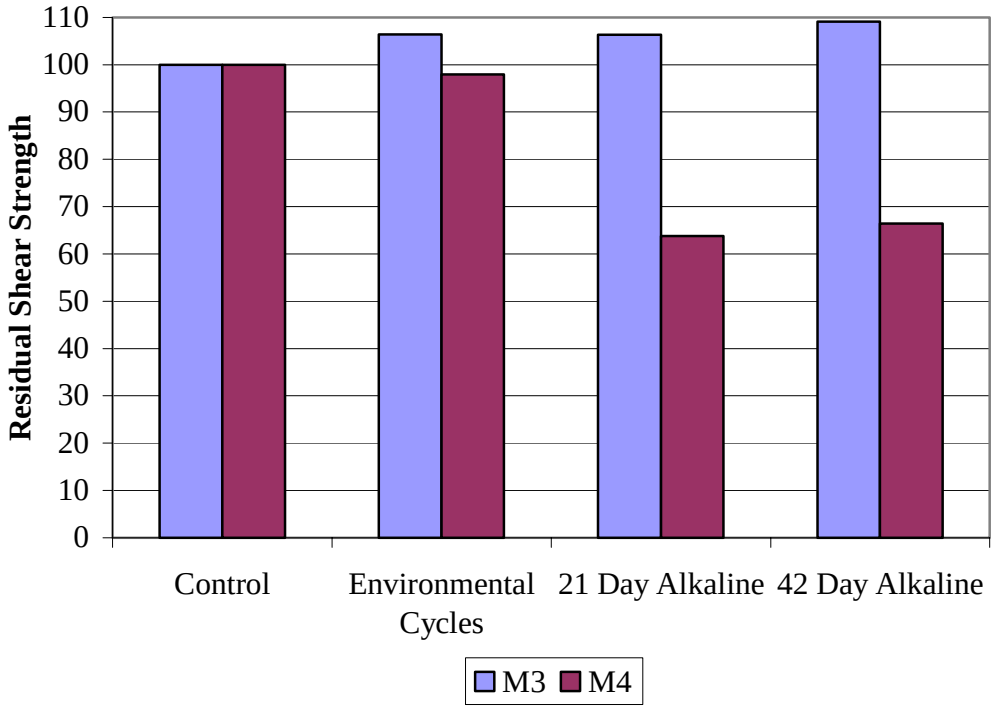

Figure 6.21 Residual Interlaminar Shear Strength of Conditioned 3/8 in and 1/2 in GFRP Bars

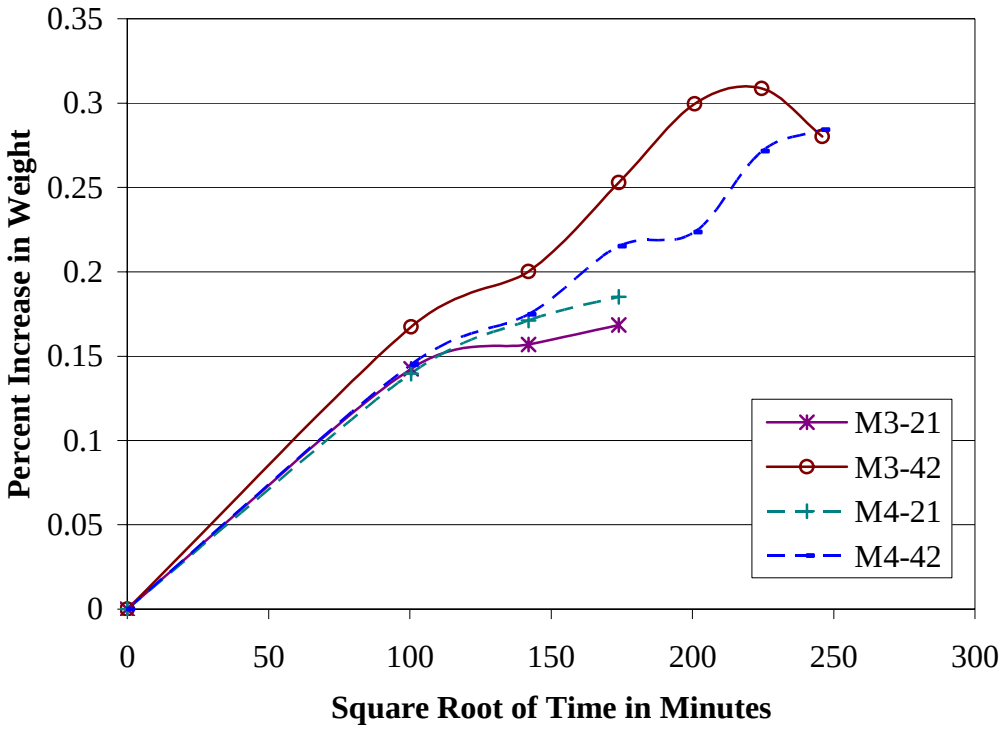

Figure 6.22 Weight Increase with Time

Consistent absorption rates are exhibited by the bars tested in this study and the maximum amount of absorption is approximately 0.3 percent. This value is equal to that reported by the manufacturer for absorption tests conducted in a similar solution at 140ºF (60ºC) for 49 days.

6.4. DISCUSSION AND SUMMARY OF RESULTS

For material characterization of the FRP bars, the measured tensile strength exceeded the tensile strength recommended by the manufacturer. The CFRP bars exhibited a similar trend during testing demonstrating a higher tensile modulus of

elasticity than the manufacturer's specifications. On the other hand, the GFRP bars exhibited a modulus of elasticity lower than that recommended by the manufacturer.

Laboratory testing exhibited good agreement between the experimental and theoretical stiffness values based on moment-curvature predictions. A summary of the test results is outlined in Table 6.13. The flexural capacity of both the FRP-RC panel and the steel-RC panel were predicted very accurately by their respective design guidelines. The failure mode exhibited by the panels was also as expected based on design assumptions. The shear capacity predictions for both the steel-RC and FRP-RC panels were very conservative. Recall, the ratio between experimental and predicted shear capacities was 1.84 for the steel-RC and 3.83 for the FRP-RC. This is due in part to the factor of two assumed for the contribution of the concrete to the shear capacity, the ratio used to reduce the concrete contribution to the shear capacity of the FRP-RC panel, and the limit of 0.002 on the strain in the FRP shear reinforcement.

The experimental deflection of the FRP-RC panel in the laboratory was approximately 50 percent of the theoretical deflection as predicted by ACI 440 guidelines (2001), which use the modified Branson equation, indicating that the ACI 440 flexural design guidelines are conservative. The same level of conservatism is exhibited by the ACI 318 guidelines, which use the Branson equation, lending credibility to the adoption of the modified Branson equation by ACI 440.

The exposure to the environmental cycles appears to have no effect on the interlaminar shear strength. However, the results indicate that the alkaline conditioning conducted causes more degradation in the 1/2-in (12.7-mm) GFRP bars than the 3/8-in (9.5-mm) GFRP bars. Residual properties of approximately 65 percent were recorded for

the 1/2-in (12.7-mm) GFRP bars, while for the 3/8-in (9.5-mm) GFRP bars the values were greater than 100 percent, indicating an increase in performance. Further durability testing of GFRP bars needs to be conducted in order to validate this trend.

Both tensile strength and tensile modulus of GFRP bars are affected by exposure to an alkaline solution at an elevated temperature. Degradation was generally within the recommended reduction factors offered by ACI (2001).

Table 6.13 Summary of Flexural and Shear Testing Results

FRP-RC			
	Experimental	**Predicted**	**Ratio**
Flexural Capacity (kips)	47 kips	48 kips	0.98
Deflection at Service Moment (in)	2.0 in	4.0 in	0.50
Shear Capacity (kips)	118 kips	30.8 kips	3.83
Steel-RC			
	Experimental	**Predicted**	**Ratio**
Flexural Capacity (kips)	50 kips	48 kips	1.04
Deflection at Service Moment (in)	1.0 in	2.1 in	0.48
Shear Capacity (kips)	130 kips	70.7 kips	1.84

Note: 1 in. = 25.4 mm, 1000 lb = 4.448 kN

7. FIELD EVALUATION

While the main goal of the laboratory experimentation and the field evaluation is very similar, that is to characterize the behavior of the structure being analyzed; both provide information that the other cannot. The field evaluation outlined herein will provide information about the interaction of the bridge panels, both FRP and RC, with one another and with the supporting bridge girders, if applicable. Further information will be obtained regarding the stiffness of the panels, which will then be compared to the result of the laboratory experimentation. However, unlike the testing procedures for the laboratory experimentation, the bridges will not be loaded to failure and no proof of the ultimate capacity of the structures will be available. Since the primary focus of the field evaluation will vary based on the structure type, this section will be organized on that basis.

Although in-situ bridge load testing is recommended by AASHTO (2000) as an "effective means of evaluating the structural performance of a bridge," no guidelines currently exist for bridge load test protocols. In each case the load test objectives, load configuration, instrumentation type and placement, and analysis techniques are to be determined by the organization conducting the test.

For this study, the prescribed or assumed design factors for each of the bridges will be compared to those exhibited by the performance of the bridge; these design factors include the wheel load distribution factor and the impact load factor. In the case of the girders the AASHTO factors are prescribed, while for the FRP panels and the FRP-RC panels assumptions regarding their behavior are utilized to determine potentially

appropriate factors based on existing AASHTO guidelines for other materials. The validity of these assumptions will be explored. Furthermore, comparisons will be drawn between the design values for deflection and those experienced by the structures during testing; verification of the design methodology will be conducted through this process.

It should also be noted that in an effort to monitor the long-term performance of the bridge in-situ, additional field load tests will be conducted annually for two more years. The deflection from year-to-year will be compared and any degradation will be quantified. The annual load test will also be combined with an inspection of the visible bridge components for possible wear and degradation.

The load tests of all four bridges were conducted utilizing the same loading truck and with the tests conducted on four consecutive days (October 1 through October 4, 2001). Loading of the bridge was accomplished with a loaded tandem-axle dump truck placed at various locations on the bridge. The total weight of the truck was 47,880 lb (212.98 kN) with 14,880 lb (66.19 kN), 16,380 lb (72.86 kN), and 16,620 lb (73.93 kN), on each of the three axles from the front to the rear of the truck, respectively.

Table 7.1 Truck Axle Spacing

	Center-to-center spacing (ft)	**Out-to-out spacing (ft)**
WIDTH		
Front axle	6.63	7.51
Middle axle	6.14	7.91
Rear axle	6.14	7.91
LENGTH		
Front axle to Middle axle	15.09	
Middle axle to Rear axle	4.43	

Note: 1 ft = 0.305 m

For each of the bridges, the instrumentation layout was designed to gain the maximum amount of information about the structure. It was assumed that the bridges acted symmetrically, therefore instrumentation was concentrated on one half of the bridge in each case. The details will be presented separately for each of the bridges as each is configured in a different manner.

7.1. ST. JOHNS STREET BRIDGE

The main research objectives for the testing of this bridge are to determine the load distribution between the girders, examine the overall performance of the bridge, and determine the load distribution from panel to panel. Further assessment of the load distribution from panel to panel and the stiffness of the panels, in terms of the modulus of elasticity, will be conducted during the presentation of the results of the in-situ testing of the St. Francis Street Bridge. Due to the steel diaphragms connecting the girders together, the interaction of panels and girders cannot be quantified with the tests performed. It should be noted that, to a certain extent, guidance regarding the in-situ bridge load testing of the St. Johns Street and Jay Street Bridges, specifically instrumentation location, was taken from Reising et al. (2001) and Chajes et al. (2001) as mentioned in the Section 1.3.

Instrumentation utilized during the testing included direct current variable transformer (DCVT) transducers, which were installed underneath the bridge to monitor deflection of the bridge panels. Nine DCVT transducers were located at mid-span and three were located in the lateral center between Girder 5 and Girder 6 at various longitudinal positions of interest. Figure 7.1 illustrates the layout of the DCVT

transducers. The deflection of both the FRP panels and the steel girders was monitored; in two locations DCVT transducers were located on the steel girder and on the FRP panel adjacent to the girder flange in order to measure any separation that might be occurring. It should be noted that the DCVT transducers denoted in black were recorded continuously during the testing, however the DCVT transducers denoted in grey were only recorded periodically at pertinent times.

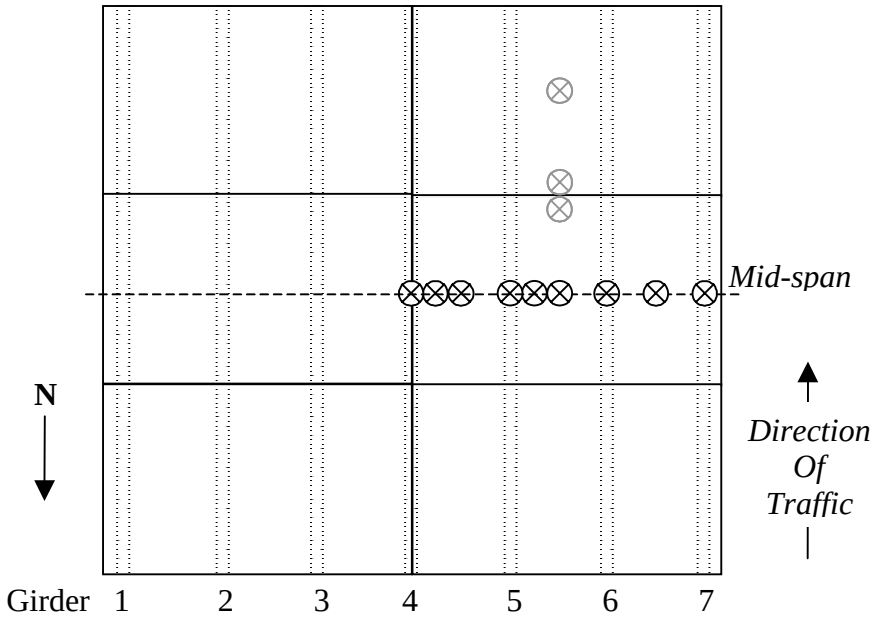

Figure 7.1 Layout of the DCVT Transducers – St. Johns Street

Several passes of the truck were made, each at a different transverse position on the bridge. Figure 7.2 illustrates the lateral location of the first four truck passes. Additional passes were made at 20 mph (32 kph) at the same location as Pass 4 as were three passes that were symmetric to Passes 1 through 3. Assuming that the bridge behaved symmetrically, the measurements from the symmetric load passes were used to

complete the deflected shapes for Passes 1 through 3. During each pass the truck was stopped at five longitudinal locations. Table 7.2 details the location of the truck stops. Due to the axle loads and axle spacing of the loading truck, truck location 3 corresponds to the worst-case loading condition. A picture of the bridge during the load test is shown in Figure 7.3.

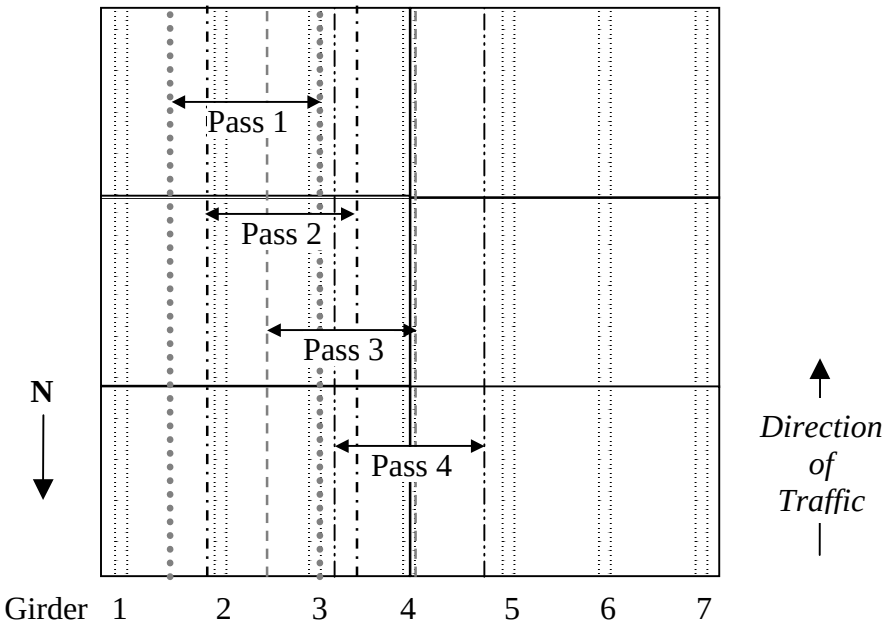

Figure 7.2 Lateral Location of Truck Passes 1 through 4 – St. Johns Street

The results of the load test for Passes 1 through 4 are presented in Figure 7.4 through Figure 7.7, respectively. It should be noted that the illustration at the bottom of each figure depicts the layout of the girders and panels and the lateral location of the tandem axles on the bridge for each pass. Furthermore, the dashed portion of the curve is taken from the abovementioned symmetric pass for each of the passes. For each of the figures, the progression of the deflected shape from the top curve to the bottom curve is

consistent with the level of moment induced by each loading position. Stop 5 generates the least moment in the bridge; followed by Stop 1; Stops 2 and 4, which are nearly identical; and Stop 3, which produces the largest bending moment.

Table 7.2 Longitudinal Truck Locations – St. Johns Street

Stop	Truck Position
1	Middle and rear axles of the truck centered longitudinally on the northern two panels, approximately 4.42 ft (1.35 m) onto the bridge from the north end
2	Middle and rear axles of the truck centered longitudinally on the joint between the northern two panels and the center two panels, approximately 8.83 ft (2.69 m) onto the bridge from the north end
3	Middle and rear axles of the truck centered longitudinally on the center two panels, approximately 13.25 ft (4.04 m) onto the bridge from the north end (i.e., at mid-span)
4	Middle and rear axles of the truck centered longitudinally on the joint between the center two panels and the southern two panels, approximately 17.67 ft (5.38 m) onto the bridge from the north end
5	Middle and rear axles of the truck centered longitudinally on the southern two panels, approximately 22.08 ft (6.73 m) onto the bridge from the north end

Figure 7.3 In-situ Bridge Load Test – St. Johns Street

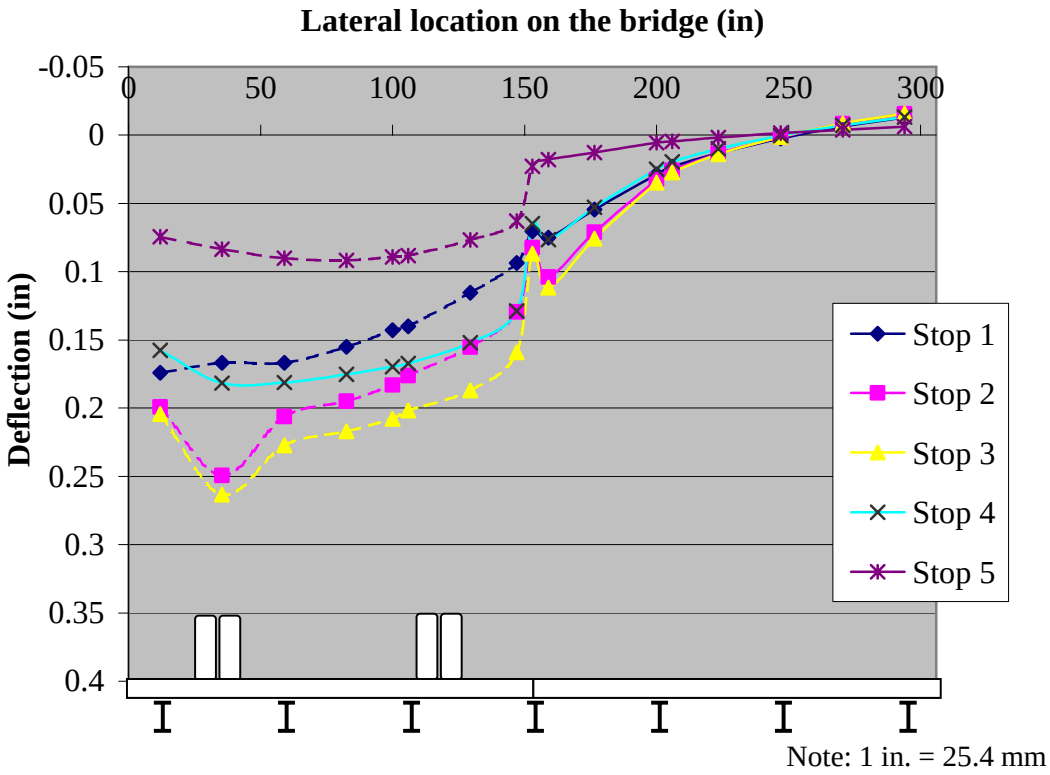

Figure 7.4 Deflected Shape – Pass 1 – St. Johns Street

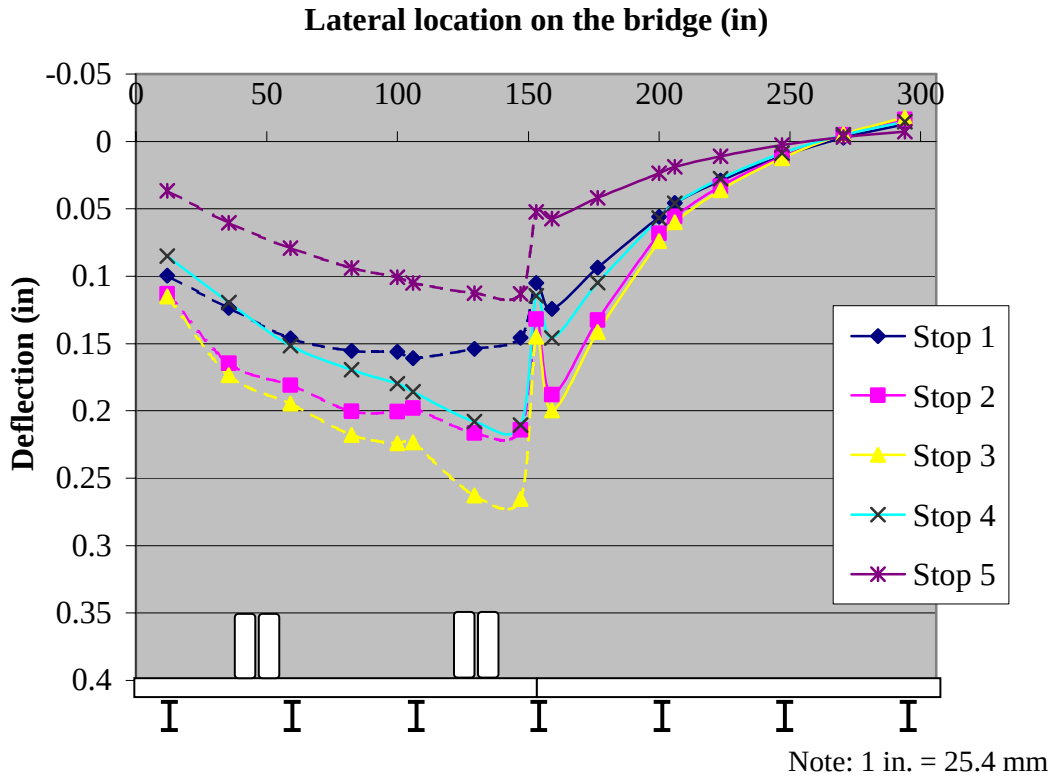

Figure 7.5 Deflected Shape – Pass 2 – St. Johns Street

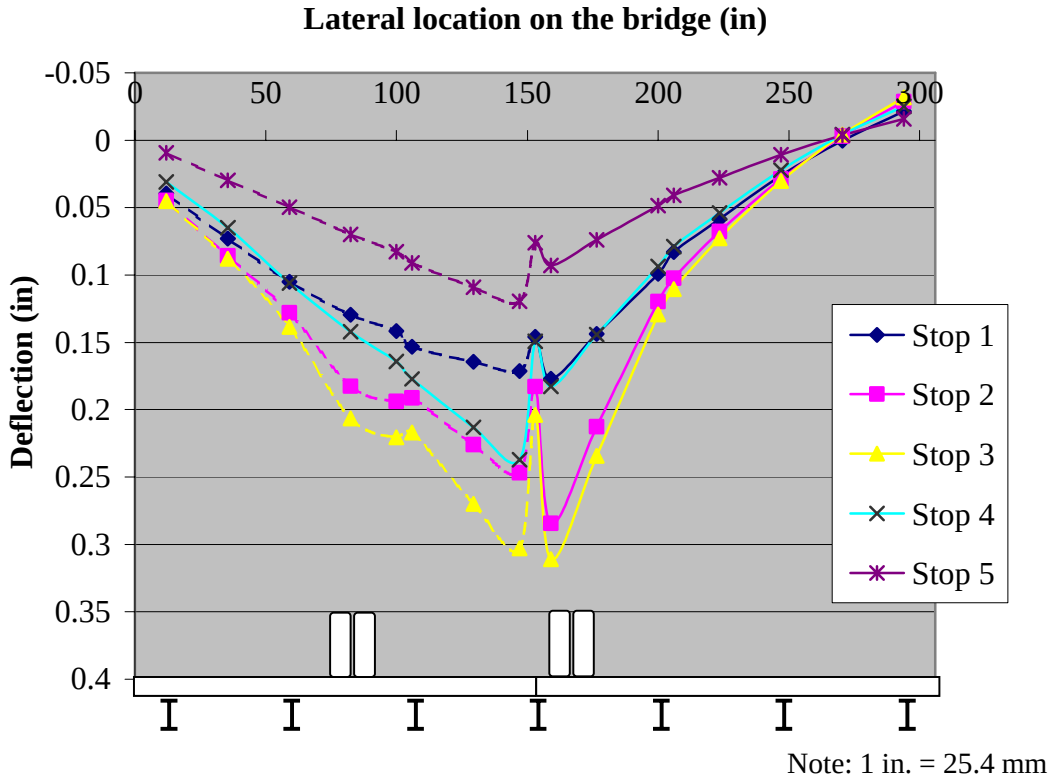

Note: 1 in. = 25.4 mm

Figure 7.6 Deflected Shape – Pass 3 – St. Johns Street

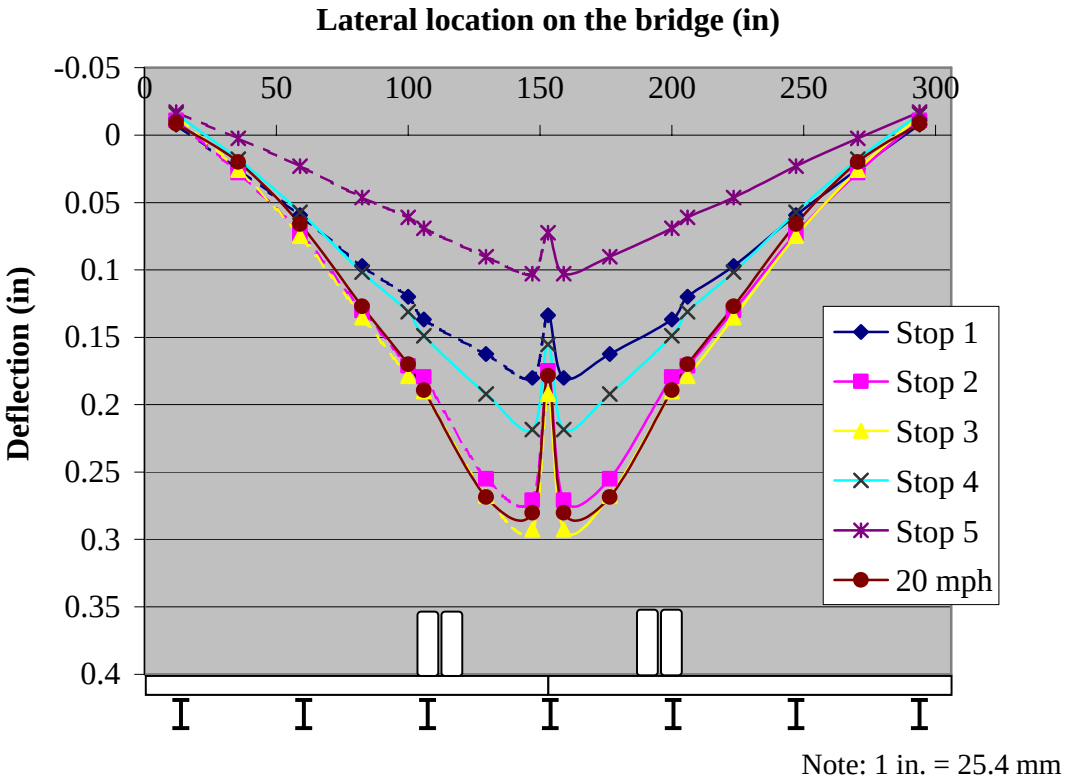

Note: 1 in. = 25.4 mm

Figure 7.7 Deflected Shape – Pass 4 and 20 mph Pass – St. Johns Street

A preliminary examination of the data indicates that the readings are accurate. The consistency of the readings from stop to stop and from pass to pass lends credence to their validity. The curves also exhibit, in general, a smooth transition from point to point.

One point of interest was the connection of the panels to the girders. To investigate the ability of the connections to prevent panel movements, in two mid-span locations DCVT transducers were located on the girders and on the panel immediately next to the girder flange. Examination of Figure 7.4 through Figure 7.7 reveals that the readings taken next to the girders indicate a larger or approximately equal deflection to the deflection experienced by the girder; these results confirm that separation between the panels and the girders is minimal, if any.

Due to the fact that deflection readings were taken on both the panels and the girders, Figure 7.4 through Figure 7.7 are not as clear as they could be. A more simple view of the load test results is presented in Figure 7.8, which illustrates only the deflection of the girders for Stop 3 of each of the passes conducted and the 20-mph pass, and Figure 7.9, which illustrates the deflection for Stop 3 of Pass 4 for the girders and the panels separately.

A comparison of Figure 7.4 through Figure 7.8 illustrates that as the load progresses from Pass 1 through Pass 4 that the maximum deflection experienced by the bridge decreases slightly due to the fact that a larger number of girders are engaged in sharing the load. A comparison of the maximum deflection of the girders during Pass 1 to the maximum deflection of the girders during Pass 4 confirms a decrease in deflection of approximately 15 percent.

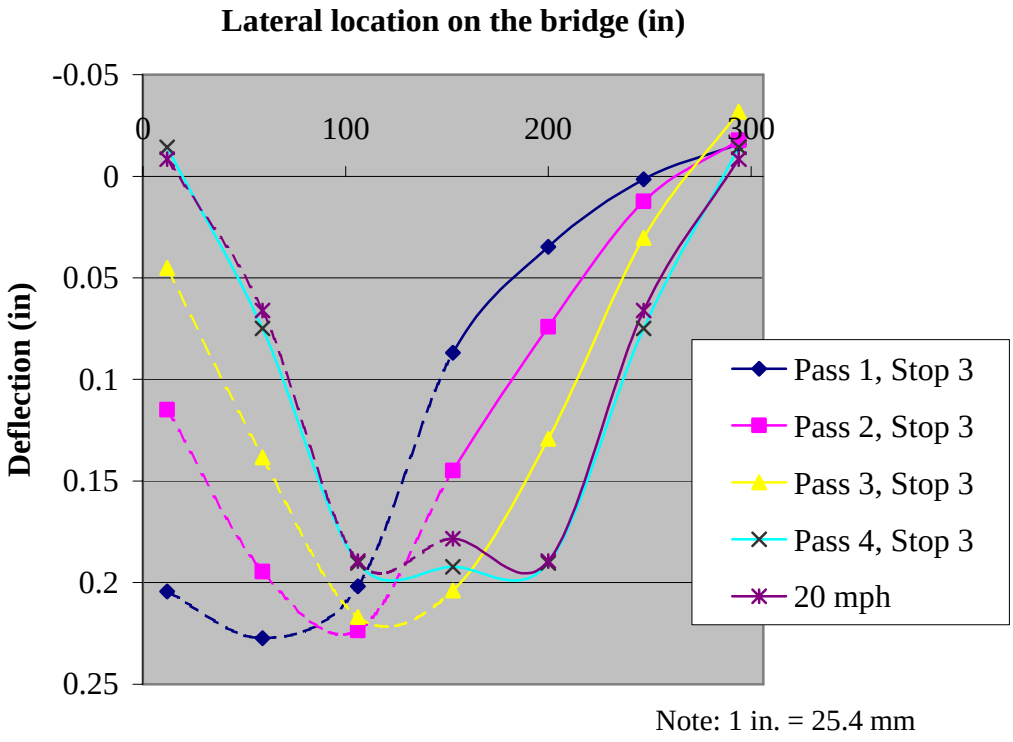

Figure 7.8 Deflected Shape – Girders Only – St. Johns Street

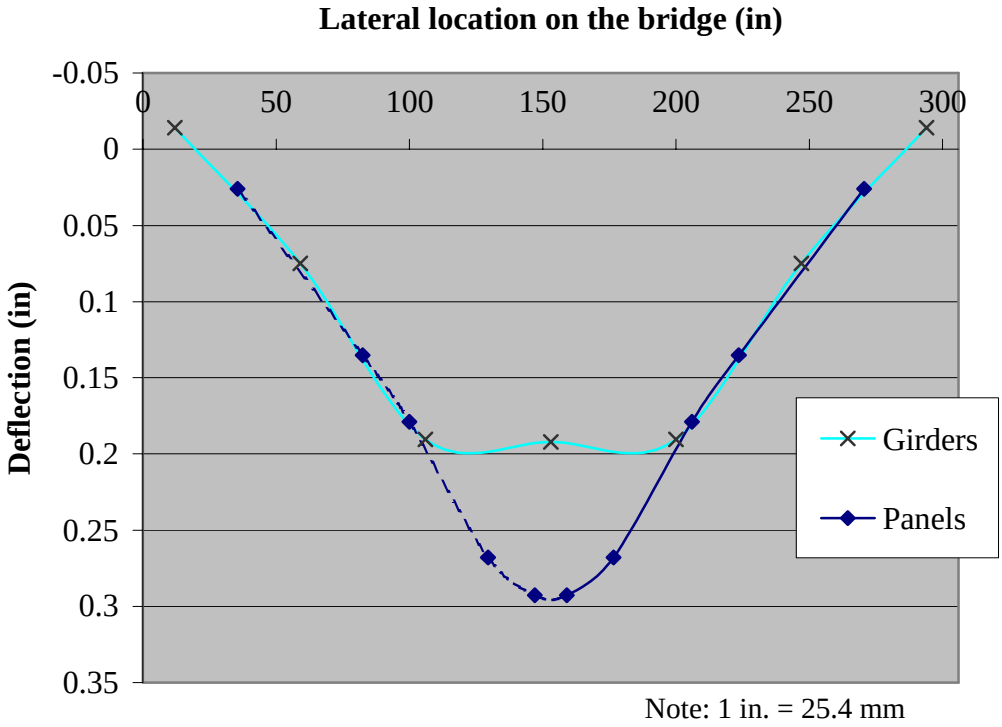

Figure 7.9 Deflected Shape – Stop 3, Pass 4 – St. Johns Street

The impact factor for the live load was examined by conducting a pass in the same location as Pass 4 at a speed of approximately 20 mph (32 kph) (see Figure 7.7). The live load impact factor was computed as the ratio of the deflection obtained at 20 mph (32 kph) to the deflection obtained at Stop 3. The seven values, one for each girder, were averaged to obtain a live load impact factor of -0.06. Compared to the computed AASHTO live load impact factor for this bridge, which is 0.30, the AASHTO guidelines appear to be conservative. The fact that the impact factor is nearly zero indicates that the deflections during Stop 3 of Pass 4 are nearly identical to the deflections experienced during the 20-mph pass.

Distribution of load between girders was also examined by comparing the deflection of the girders. If the relationship between load and deflection is assumed to be linear then they are related by a single constant; this is a valid assumption because the design of the steel girders was conducted in the elastic range. Under this assumption the ratio of the deflection of one girder to the sum of the deflections of the girders will be equal to the load on one girder divided by the total load on the bridge. It should be noted that only positive, or downward, deflections were considered in light of the fact that a negative, or upward, deflection would yield a negative wheel load distribution factor. The physical significance of a negative distribution factor would be that an upward load would be applied to the panel, causing the sum of the positive load ratios carried by the panels to be greater than unity.

Equations 7.1 and 7.2 outline these relationships where P_n is the load carried by panel *n*, x is the constant relating load to deflection for the given material and loading

configuration, and Δ_n is the deflection of panel *n*. A comparison of these ratios quantifies the lateral distribution of load between the panels.

$$P_n = x\Delta_n \quad \textbf{(7.1)}$$

$$Ratio\ of\ \ load\ on\ each\ \ panel = \frac{P_n}{\sum P_n} = \frac{x\Delta_n}{\sum x\Delta_n} = \frac{\Delta_n}{\sum \Delta_n} \quad \textbf{(7.2)}$$

Figure 7.10 illustrates the load distribution as a percentage of the total load on the bridge for Passes 1 through 4. There is a clear progression of the peak load percentage from one side of the bridge toward the center as the load moves from Pass 1 to Pass 4. As was also exhibited in the plots of the deflected shape, it is observed that as the loading truck goes from Pass 1 through Pass 4 the peak load percentage decreases slightly as the number of girders sharing a larger portion of the load increases.

It is desirable to determine the load carried by the girder as a fraction of one wheel line load so that the values can be readily compared to the AASHTO wheel load distribution factors. Equation 7.2 outlines the calculations with respect to the total load on the bridge. Since the load on one wheel load line is equal to half of the total load on the bridge, it follows that the percentages in Figure 7.10 must be multiplied by two. The maximum distribution factor for the St. Johns Street Bridge would come from Girder 2 with a value of 0.60. When compared to the AASHTO distribution factor, 1.096, utilized in the design (recall Section 3.1) the conservative nature of the AASHTO guidelines is exhibited. Furthermore, Figure 7.11 illustrates the load distribution as a percent of the total load on the bridge for Pass 4 and the pass at 20 mph (32 kph). Although the total load experienced by the bridge is different in the case of the 20-mph (32-kph) pass due to impact, the percentage of load carried by each respective girder is very similar.

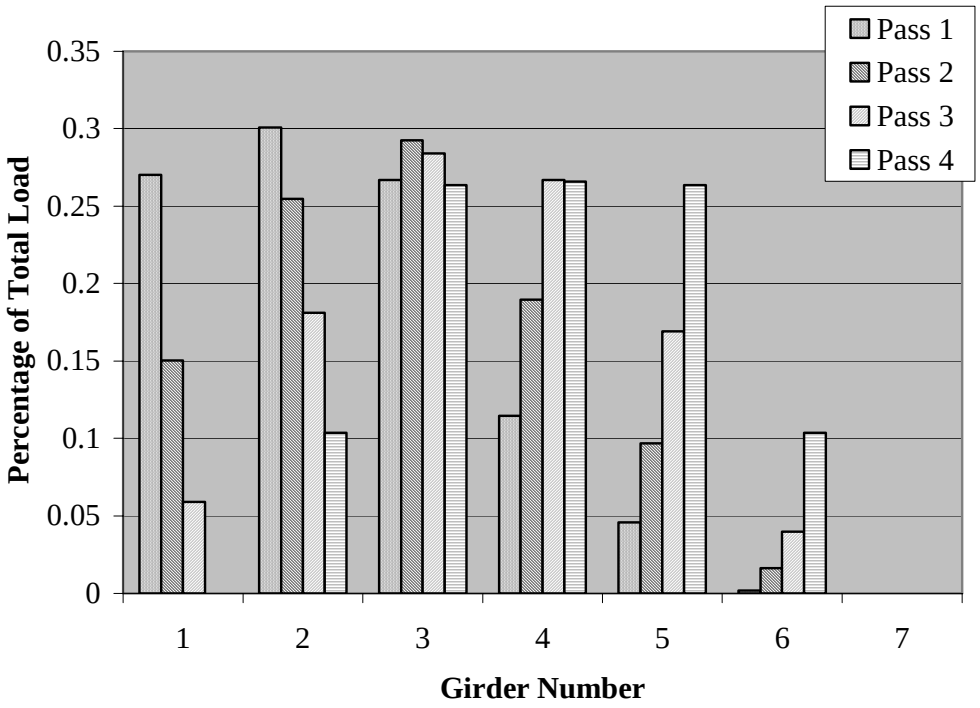

Figure 7.10 Percentage of Load Carried per Panel as a Percentage of Total Load on the Bridge – Passes 1 through 4 – St. Johns Street

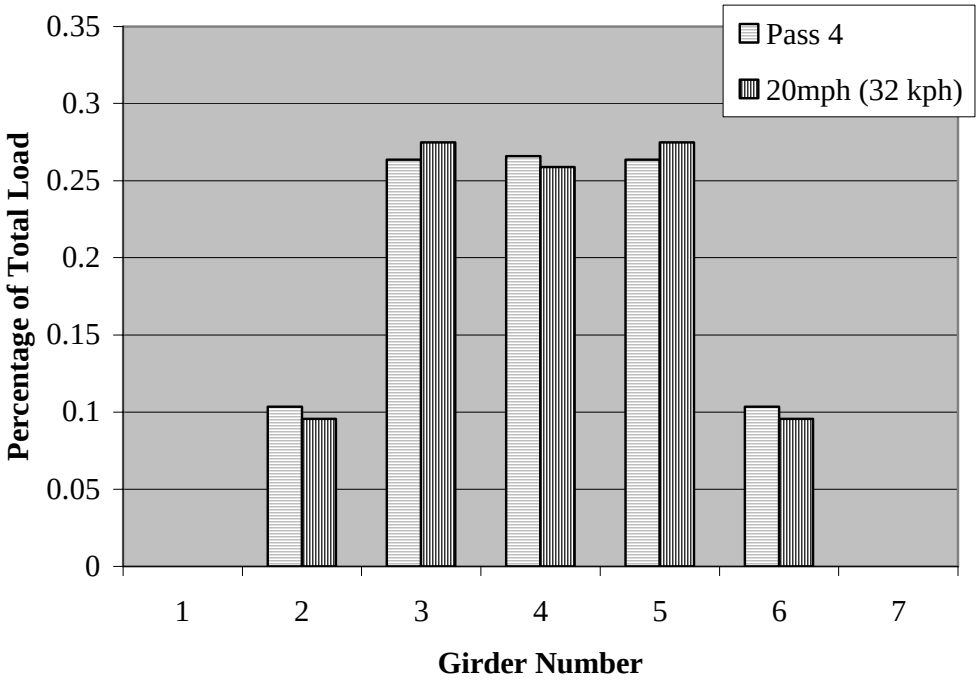

Figure 7.11 Percentage of Load Carried per Panel as a Percentage of Total Load on the Bridge – Pass 4 and 20mph Pass – St. Johns Street

Due to the lateral load distribution between panels and girders, the theoretical deflection is difficult to determine, therefore a direct comparison will not be drawn. It is known however that the bridge panels themselves were designed to meet the AASHTO deflection requirement of span length divided by 800, which in this case, with a span length equal to 25.6 ft (7.80 m), corresponds to a deflection of 0.384 in (9.75 mm). The maximum observed deflection for the girders during the static load passes was 0.227 in (5.77mm), yielding a span-to-deflection ratio of approximately 1350 or approximately 60 percent of the allowable deflections. Moreover, Figure 7.12 illustrates the predicted deflection of the bridge for the design loading condition of one truck in each of the two lanes. The principle of superposition was utilized assuming linear-elastic behavior of the bridge, yielding a maximum deflection of roughly 0.229 in (5.82 mm) for a span-to-deflection ratio of approximately 1340, or roughly 60 percent of the allowable deflection.

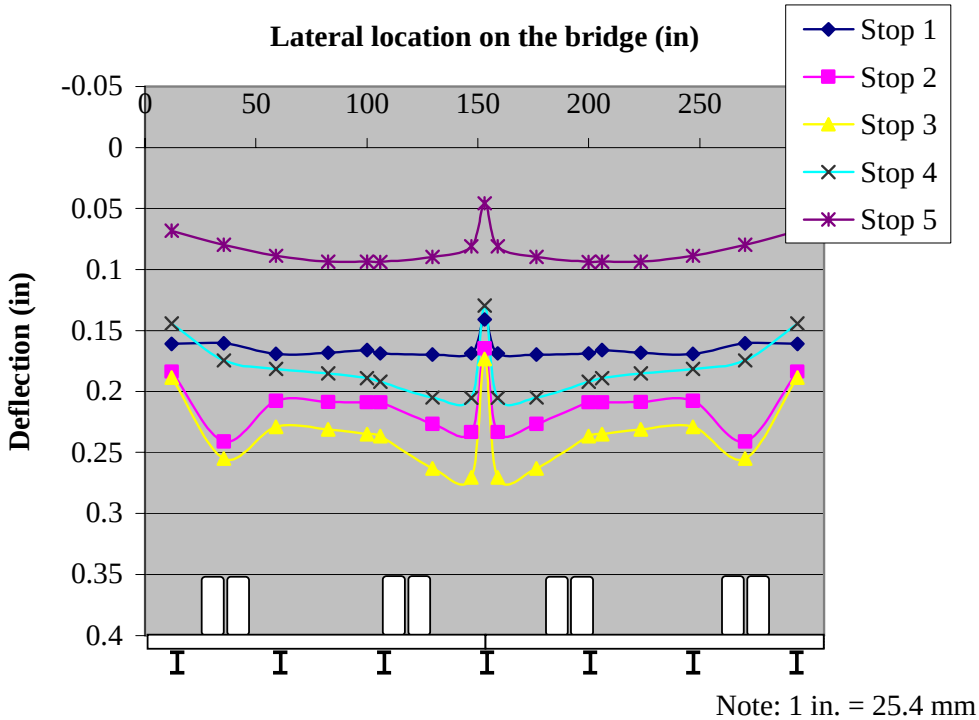

Note: 1 in. = 25.4 mm

Figure 7.12 Deflected Shape – Superposition of Pass 1 – St. Johns Street

7.2. JAY STREET BRIDGE

The main research objectives for the testing of this bridge are the same as those outlined for the St. Johns Street Bridge, to determine the load distribution between the girders, examine the overall performance of the bridge, and determine the load distribution from panel to panel. Twelve DCVT transducers were located at mid-span. Figure 7.13 illustrates the layout of the DCVT transducers; the DCVT transducers denoted in black were recorded continuously during the testing, however the DCVT transducers denoted in grey were only recorded periodically at pertinent times. Again, the deflection of both the FRP panels and the steel girders was monitored and in four locations DCVT transducers were located on the steel girder and on the FRP panel adjacent to the girder flange in order to measure any separation that might be occurring.

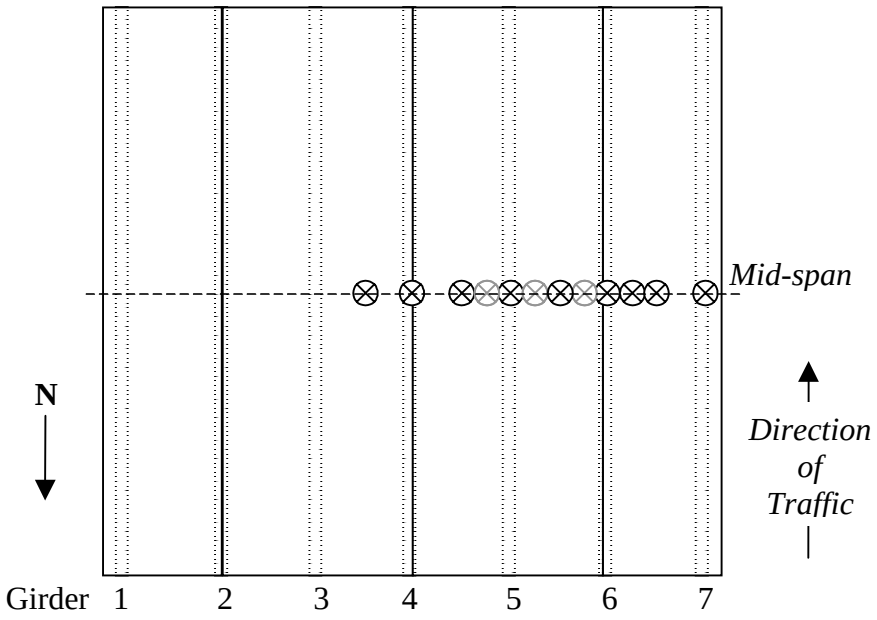

Figure 7.13 Layout of the DCVT Transducers – Jay Street

Figure 7.14 illustrates the lateral location of the first four truck passes. Additional passes were made at 20 mph (32 kph) at the same location as Pass 4 as were three passes that were symmetric to Passes 1 through 3. Assuming that the bridge behaved symmetrically, the measurements from the symmetric load passes were used to complete the deflected shapes for Passes 1 through 3. During each pass the truck was stopped at five longitudinal locations. Table 7.3 details the location of the truck stops. Due to the axle loads and axle spacing of the loading truck, truck location 3 corresponds to the worst-case loading condition. A picture of the bridge during the load test is shown in Figure 7.15.

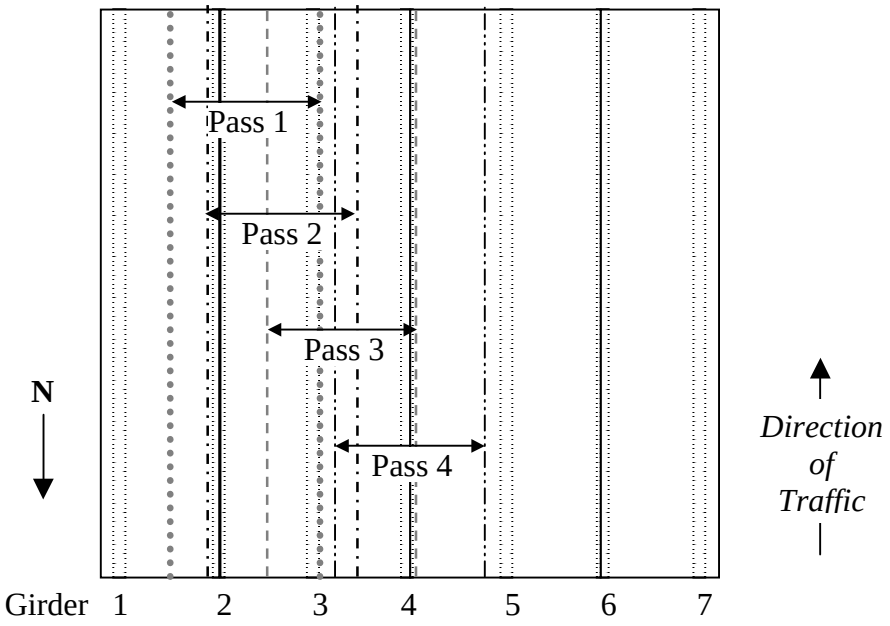

Figure 7.14 Lateral Location of Truck Passes 1 through 4 – Jay Street

The results of the load test for Passes 1 through 4 are presented in Figure 7.16 through Figure 7.19, respectively. It should be noted that the illustration at the bottom of

each figure depicts the layout of the girders and panels and the lateral location of the tandem axles on the bridge for each pass. Furthermore, the dashed portion of the curve is taken from the abovementioned symmetric pass for each of the passes. For each of the figures, the progression of the deflected shape from the top curve to the bottom curve is consistent with the level of moment induced by each loading position. Stop 5 generates the least moment in the bridge; followed by Stop 1; Stops 2 and 4, which are nearly identical; and Stop 3, which produces the largest bending moment.

Table 7.3 Longitudinal Truck Locations – Jay Street

Stop	Truck Position
1	Middle and rear axles of the truck centered approximately 2.5 ft (0.76 m) onto the bridge from the north end
2	Middle and rear axles of the truck centered approximately 7.5 ft (2.29 m) onto the bridge from the north end
3	Middle and rear axles of the truck centered approximately 12.5 ft (3.81 m) onto the bridge from the north end (i.e., at mid-span)
4	Middle and rear axles of the truck centered approximately 17.5 ft (5.33 m) onto the bridge from the north end
5	Middle and rear axles of the truck centered approximately 22.5 ft (6.86 m) onto the bridge from the north end

Figure 7.15 In-situ Bridge Load Test – Jay Street

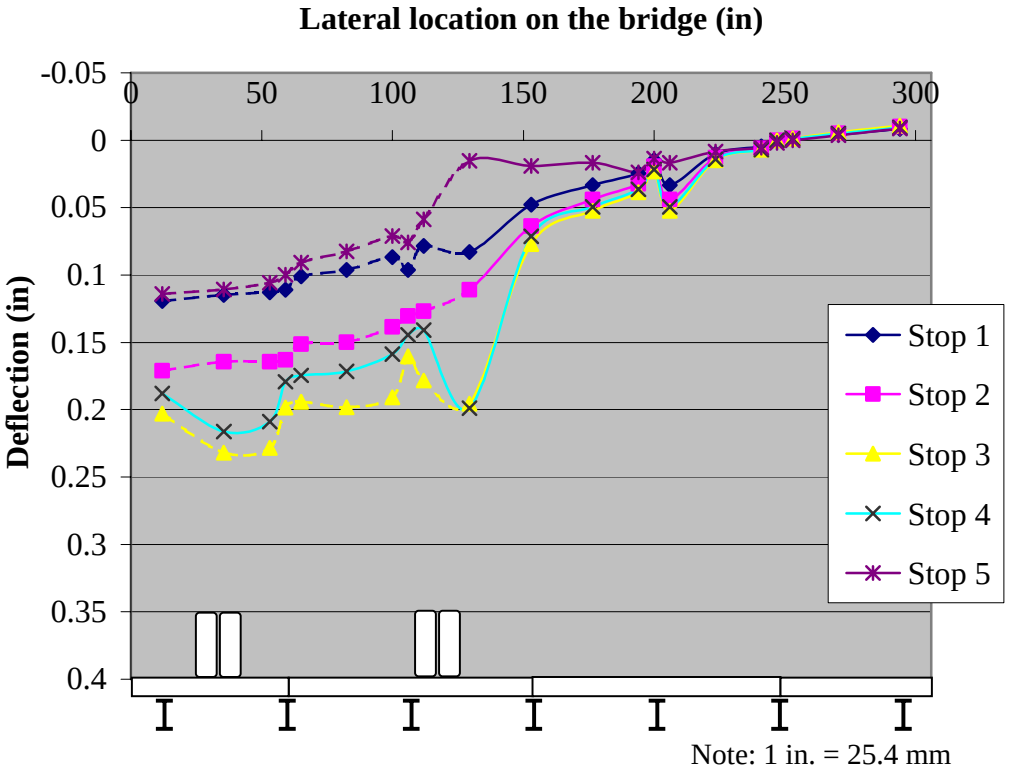

Figure 7.16 Deflected Shape – Pass 1 – Jay Street

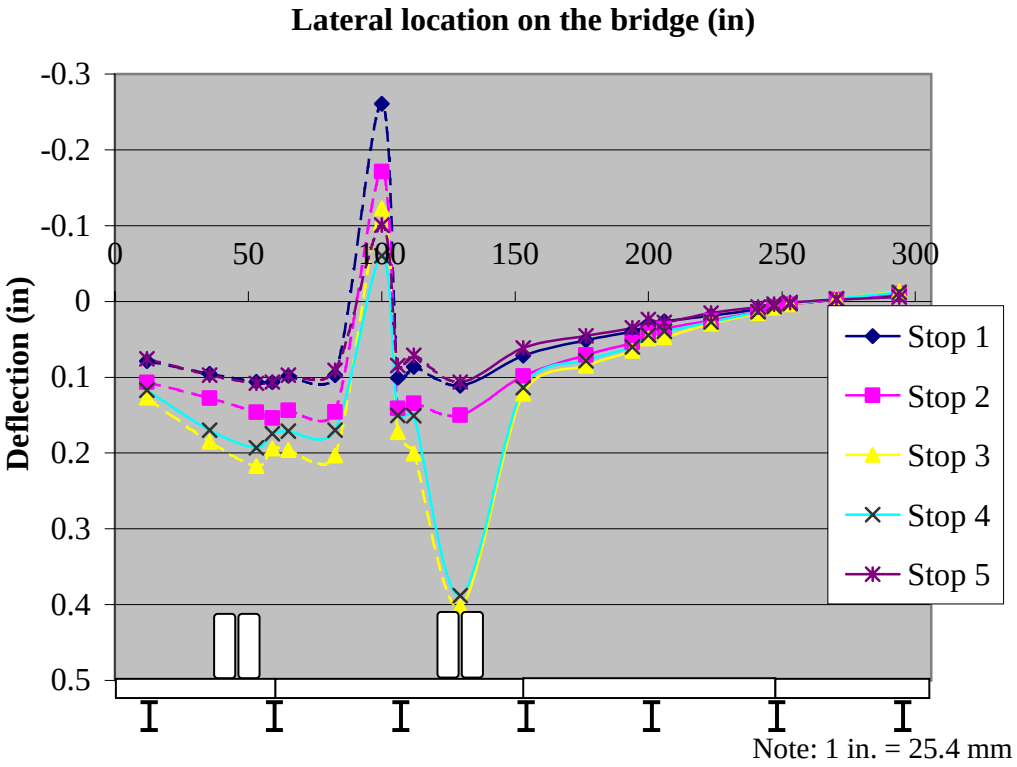

Figure 7.17 Deflected Shape – Pass 2 – Jay Street

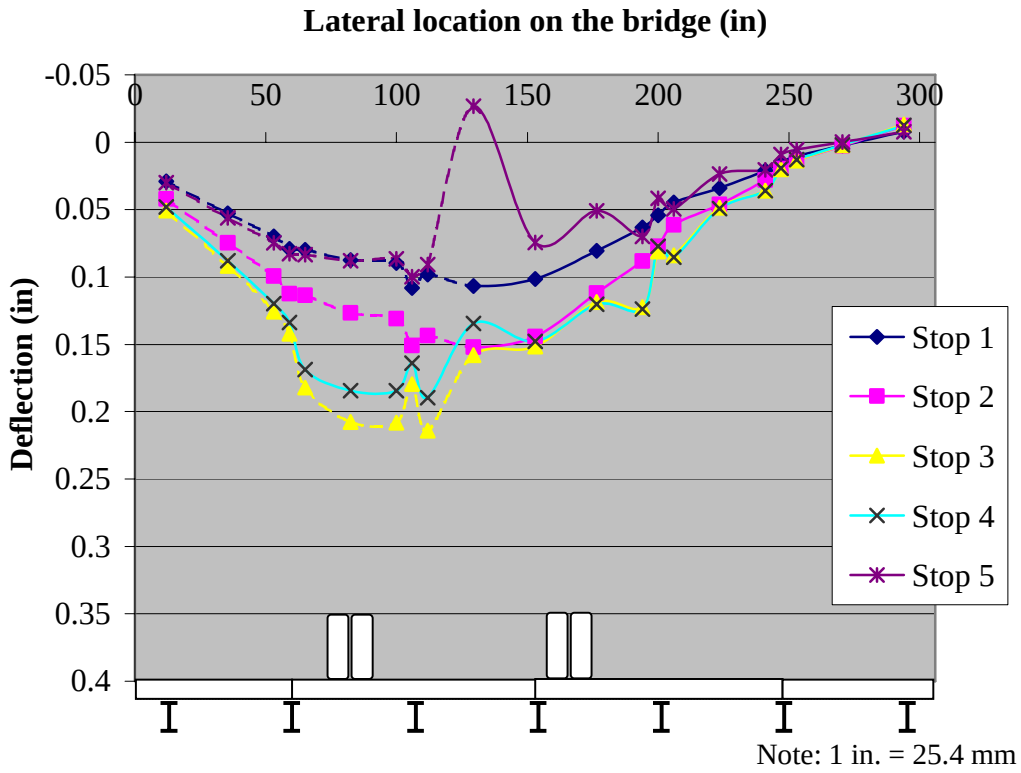

Figure 7.18 Deflected Shape – Pass 3 – Jay Street

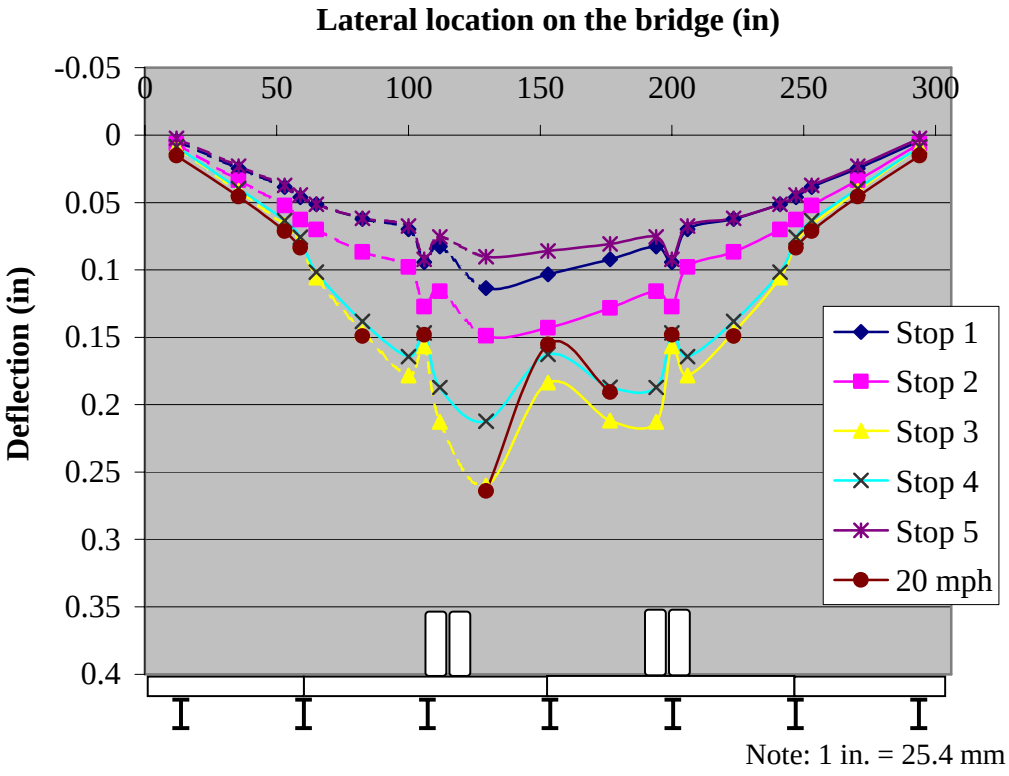

Figure 7.19 Deflected Shape – Pass 4 and 20 mph Pass – Jay Street

A preliminary examination of the data indicates that the readings may not be accurate. The lack of consistency of the readings from stop to stop and from pass to pass lends uncertainty to their validity. The seemingly sporadic readings for a few of the DCVT transducers will be compared to the results obtained in future load tests to establish their accuracy. The analysis of these results is presented for completeness, although their validity is in question.

One point of interest was the connection of the panels to the girders. To investigate the ability of the connections to prevent panel movements, in two locations at mid-span DCVT transducers were located on the girders and on the panel immediately next to the girder flange. Examination of Figure 7.16 through Figure 7.19 reveals that there are several locations where the readings taken next to the girders indicate a smaller deflection then the deflection experienced by the girder; these results strongly suggest that separation between the panels and the girders is occurring. This is primarily occurring in the locations were the panels are not connected to the girders; recall from the design and installation of the bridges that where there is no panel joint the panels are not attached to the girders.

Due to the fact that deflection readings were taken on both the panels and the girders, Figure 7.16 through Figure 7.19 are not as clear as they could be. A more simple view of the load test results is presented in Figure 7.20, which illustrates only the deflection of the girders for Stop 3 of each of the passes conducted and the 20-mph pass, and Figure 7.21, which illustrates the deflection for Stop 3 of Pass 4 for the girders and the panels separately.

A comparison of Figure 7.16 through Figure 7.20 illustrates that as the load progresses from Pass 1 through Pass 4 that the maximum deflection experienced by the bridge decreases slightly due to the fact that a larger number of girders are engaged in sharing the load. A comparison of the maximum deflection of the girders during Pass 1 to the maximum deflection of the girders during Pass 4 confirms a decrease in deflection of approximately 11 percent.

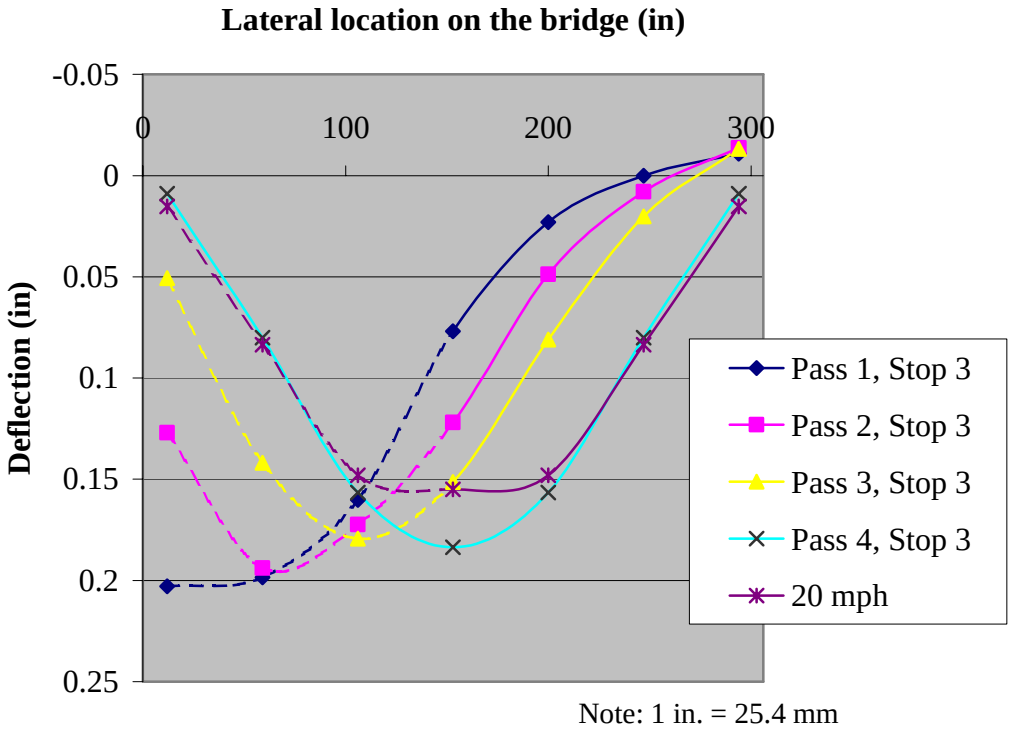

Figure 7.20 Deflected Shape – Girders Only – Jay Street

The impact factor for the live load was examined by conducting a pass in the same location as Pass 4 at a speed of approximately 20 mph (32 kph) (see Figure 7.19). The live load impact factor was computed as the ratio of the deflection obtained at 20 mph (32 kph) to the deflection obtained at Stop 3. The seven values, one for each girder, were averaged to obtain a live load impact factor of -0.04. Compared to the computed

AASHTO live load impact factor for this bridge, which is 0.30, the AASHTO guidelines appear to be conservative. The fact that the impact factor is nearly zero indicates that the deflections during Stop 3 of Pass 4 are nearly identical to the deflections experienced during the 20-mph pass.

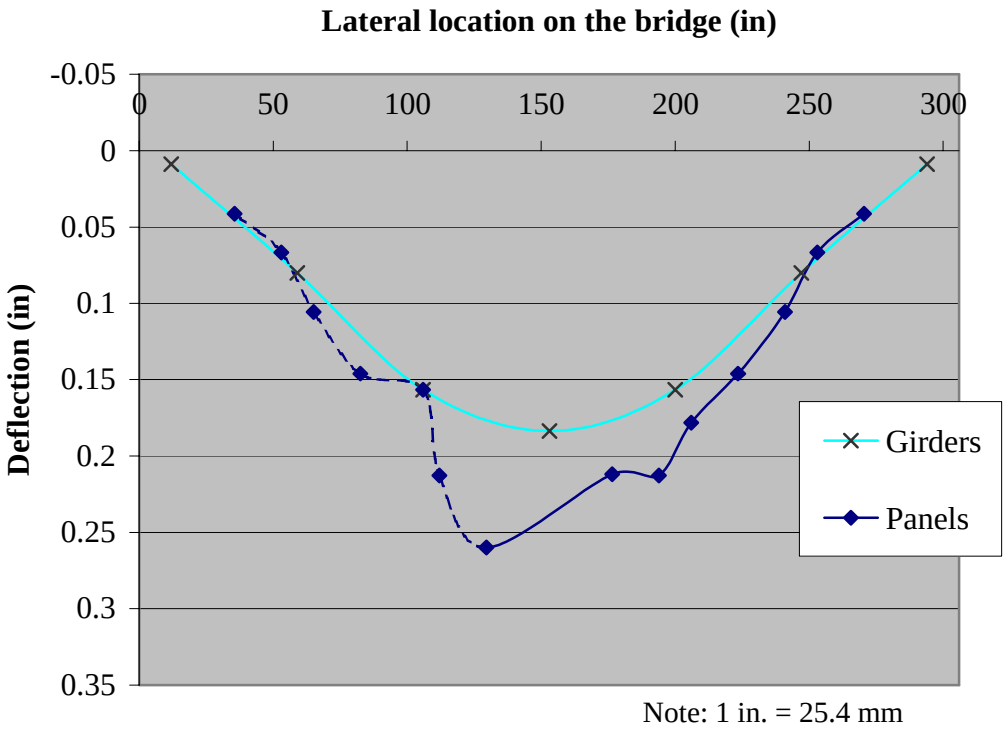

Figure 7.21 Deflected Shape – Stop 3, Pass 4 – Jay Street

Distribution of load between girders was also examined by comparing the deflection of the girders. Again, if the relationship between load and deflection is assumed to be linear then they are related by a single constant and the ratio of the deflection of one girder to the sum of the deflections of the girders will be equal to the load on one girder divided by the total load on the bridge. A comparison of these ratios quantifies the lateral distribution of load between the panels.

Figure 7.22 illustrates the load distribution as a percentage of the total load on the bridge for Passes 1 through 4. There is a clear progression of the peak load percentage from one side of the bridge toward the center as the load moves from Pass 1 to Pass 4. As was also exhibited in the plots of the deflected shape, it is observed that as the loading truck goes from Pass 1 through Pass 4 the peak load percentage decreases slightly as the number of girders sharing a larger portion of the load increases.

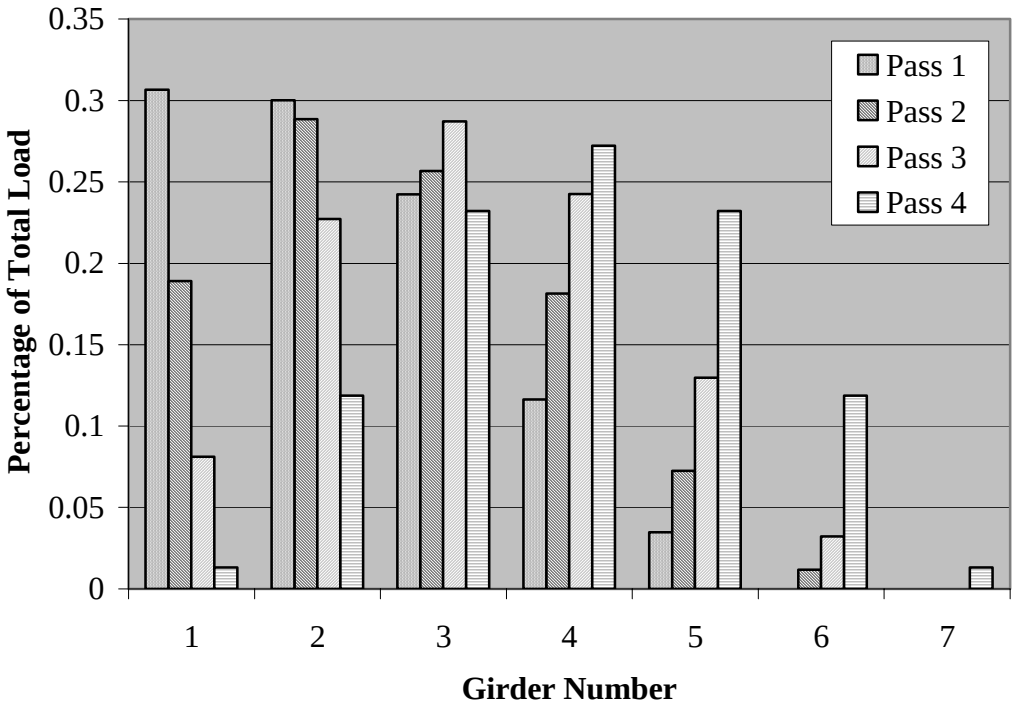

Figure 7.22 Percentage of Load Carried per Panel as a Percentage of Total Load on the Bridge – Passes 1 through 4 – Jay Street

Again, since the load on one wheel load line is equal to half of the total load on the bridge, it follows that the percentages in Figure 7.22 must be multiplied by two to obtain the load carried by the girder as a fraction of one wheel load. The maximum distribution factor for the Jay Street Bridge would come from Girder 1 with a value of

0.613. When compared to the AASHTO distribution factor, 1.096, utilized in the design (recall Section 3.2) the conservative nature of the AASHTO guidelines is exhibited.

Figure 7.23 illustrates the load distribution as a percent of the total load on the bridge for Pass 4 and the pass at 20 mph (32 kph). Although the total load experienced by the bridge is different in the case of the 20-mph (32-kph) pass due to impact, the percentage of load carried by each respective girder is very similar.

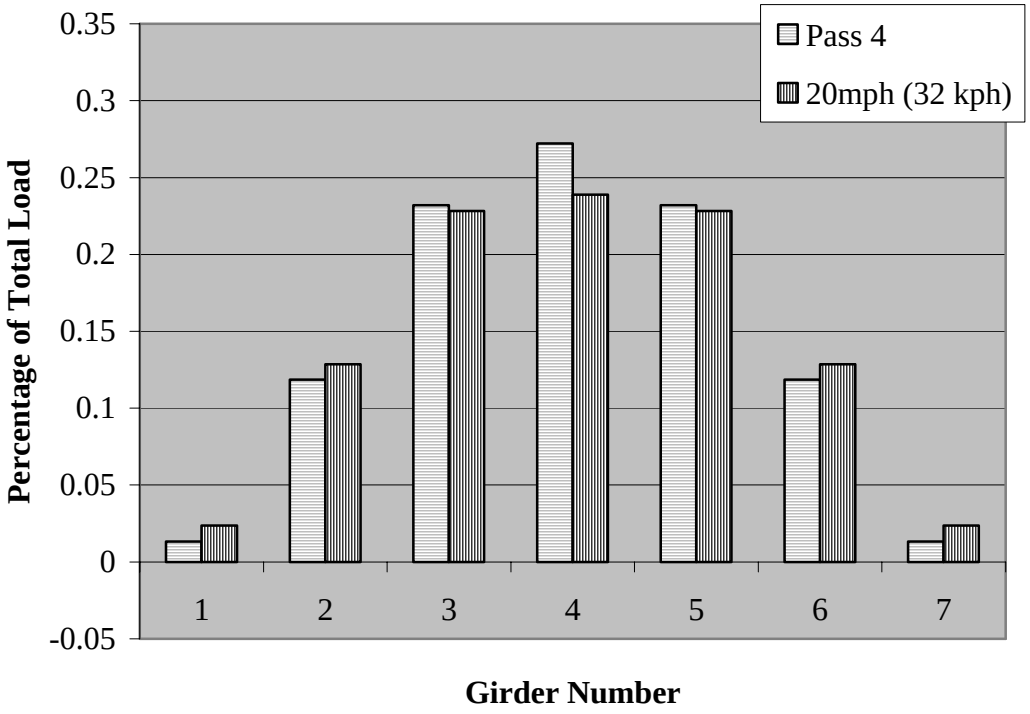

Figure 7.23 Percentage of Load Carried per Panel as a Percentage of Total Load on the Bridge – Pass 4 and 20mph Pass – Jay Street

Due to the lateral distribution of load between panels and girders, the theoretical deflection is difficult to determine, therefore a direct comparison will not be drawn. It is known however that the bridge panels themselves were designed to meet the AASHTO

deflection requirement of span length divided by 800, which in this case, for a span length equal to 25.83 ft (7.87 m), corresponds to a deflection of 0.388 in (9.84 mm). The maximum observed deflection for the girders during the static load passes was 0.203 in (5.15 mm), yielding a span-to-deflection ratio of approximately 1530 or approximately 50 percent of the allowable deflections. Moreover, Figure 7.24 illustrates the predicted deflection of the bridge for the design loading condition of one truck in each of the two lanes. The principle of superposition was utilized assuming linear-elastic behavior of the bridge. The maximum deflection in this case is roughly 0.199 in (5.04 mm) for a span-to-deflection ratio of approximately 1560, or still roughly 50 percent of the allowable deflection.

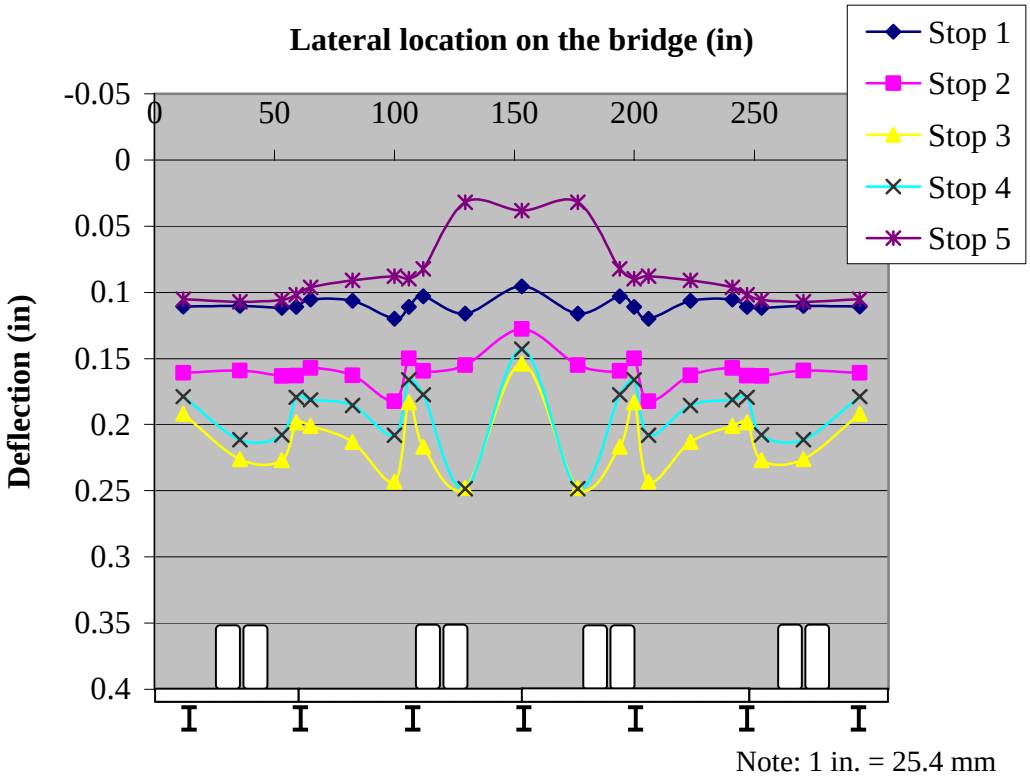

Figure 7.24 Deflected Shape – Superposition of Pass 1 – Jay Street

7.3. ST. FRANCIS STREET BRIDGE

The main research objectives in testing this bridge were to determine the load distribution from panel to panel and the stiffness of the panels. Nine DCVT transducers were located at mid-span and three were located near the supports. Figure 7.25 illustrates the layout of the DCVT transducers; the DCVT transducers denoted in black were recorded continuously during the testing and the DCVT transducers denoted in grey were only recorded periodically at pertinent times.

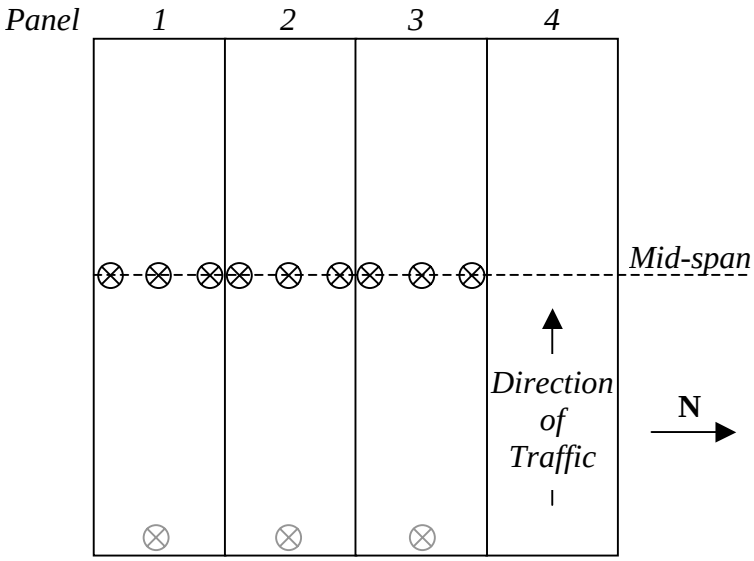

Figure 7.25 Layout of the DCVT Transducers – St. Francis Street

Figure 7.26 illustrates the lateral location of the first four truck passes. Additional passes were made at 20 mph (32 kph) at the same location as Pass 4 as were three passes that were symmetric to Passes 1 through 3. Assuming that the bridge behaved symmetrically, the measurements from the symmetric load passes were used to complete the deflected shapes for Passes 1 through 3. During each pass the truck was stopped at

five longitudinal locations. Table 7.4 details the location of the truck stops. Due to the axle loads and axle spacing of the loading truck, truck location 3 corresponds to the worst-case loading condition. A picture of the bridge during the load test is shown in Figure 7.27.

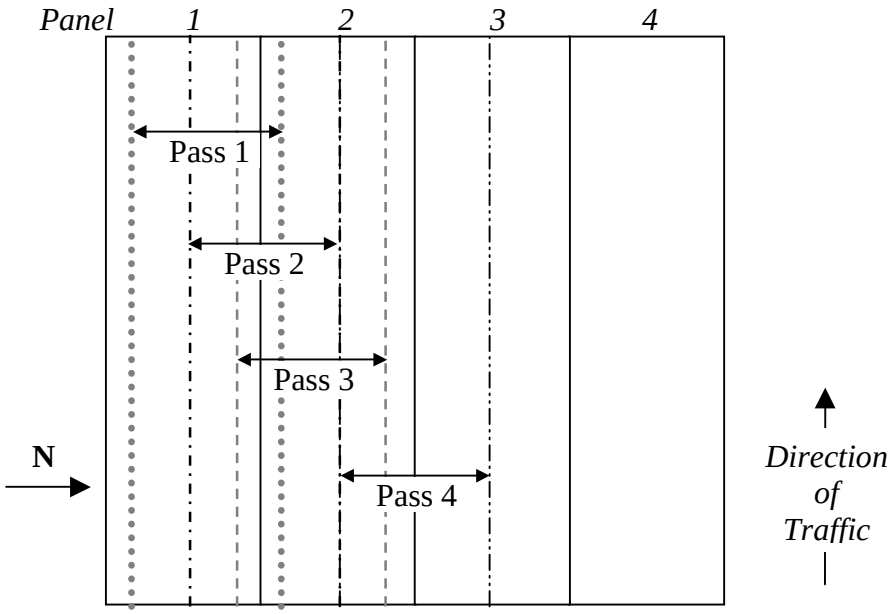

Figure 7.26 Lateral Location of Truck Passes 1 through 4 – St. Francis Street

Table 7.4 Longitudinal Truck Locations - St. Francis Street

Stop	Truck Position
1	Middle and rear axles of the truck centered approximately 2 ft (0.61 m) onto the bridge from the east end
2	Middle and rear axles of the truck centered approximately 7 ft (2.13 m) onto the bridge from the east end
3	Middle and rear axles of the truck centered approximately 12 ft (3.66 m) onto the bridge from the east end (i.e., at mid-span)
4	Middle and rear axles of the truck centered approximately 17 ft (5.18 m) onto the bridge from the east end
5	Middle and rear axles of the truck centered approximately 22 ft (6.71 m) onto the bridge from the east end

Figure 7.27 In-situ Bridge Load Test – St. Francis Street

The results of the load test for Passes 1 through 4 are presented in Figure 7.28 through Figure 7.31, respectively. It should be noted that the illustration at the bottom of each figure depicts the layout of each of the four panels and the lateral location of the tandem axles on the bridge for each pass. Furthermore, the dashed portion of the curve is taken from the abovementioned symmetric pass for each of the passes. For each of the figures, the progression of the deflected shape from the top curve to the bottom curve is consistent with the level of moment induced by each loading position. Stop 5 generates the least moment in the bridge; followed by Stop 1; Stops 2 and 4, which are nearly identical; and Stop 3, which produces the largest bending moment.

A preliminary examination of the data indicates that the readings are accurate. The consistency of the readings from stop to stop and from pass to pass lends credence to their validity. The curves also exhibit, in general, a smooth transition from point to point.

Each of the passes exhibits negative, or upward, deflection of the unloaded edge panels. On the whole, the negative deflection is of the greatest magnitude for Stop 1,

which induces a relatively small amount of moment in the panels, and is of the smallest magnitude for Stop 3, which generated the highest amount of moment in the panels. This can be explained by considering the possible two-way action exhibited by the panels. When the moment is small (e.g., Stop 1) the movement at mid-span, where the deflections were measured, is due almost exclusively to the two-way action and is upward. As the moment on the bridge increases (e.g., Stop 3) the deflections at mid-span are due primarily to the bending moment causing downward movement at mid-span; while the upward deflections due to the two-way action of the bridge are still occurring their relative magnitude to the downward deflections due to longitudinal bending is very small and the net deflection is positive (downward), or is at least less negative.

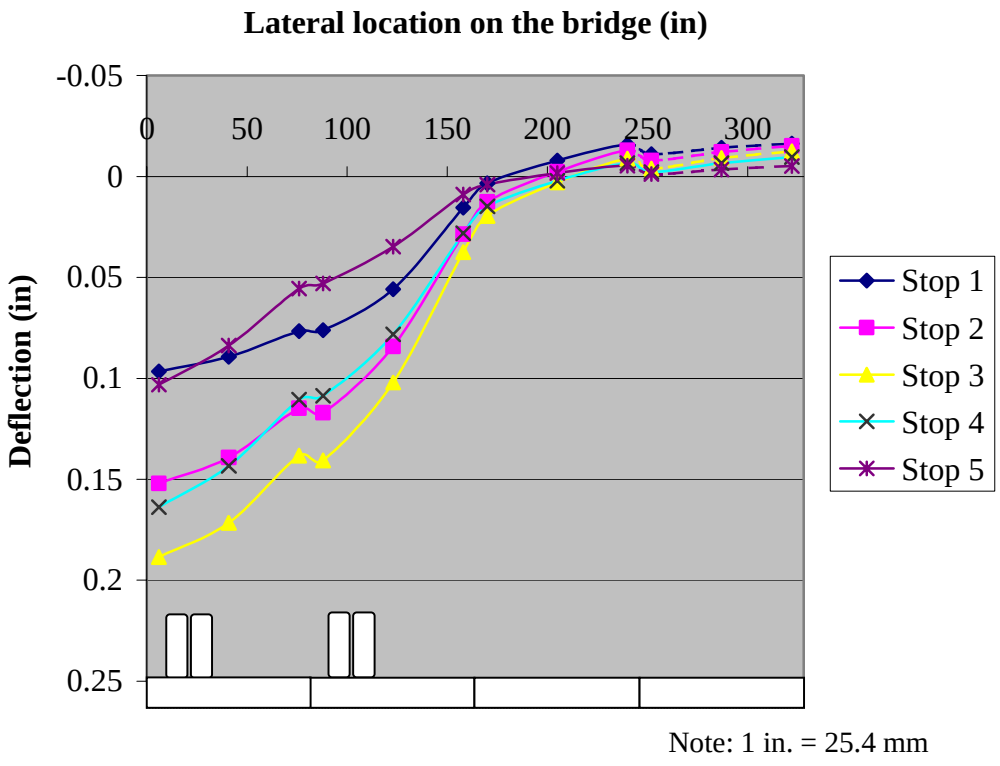

Figure 7.28 Deflected Shape – Pass 1 – St. Francis Street

A comparison of Figure 7.28 through Figure 7.31 illustrates that as the load progresses from Pass 1 through Pass 4 that the maximum deflection experienced by the bridge decreases due to the fact that even though the degree of a lateral load distribution is small, a larger number of panels are engaged in sharing the load and the rigidity of the edge panels influences the deflection when the center panels are loaded. A comparison of the maximum deflection during Pass 1 to the maximum deflection during Pass 4 confirms a decrease in deflection of approximately 35 percent.

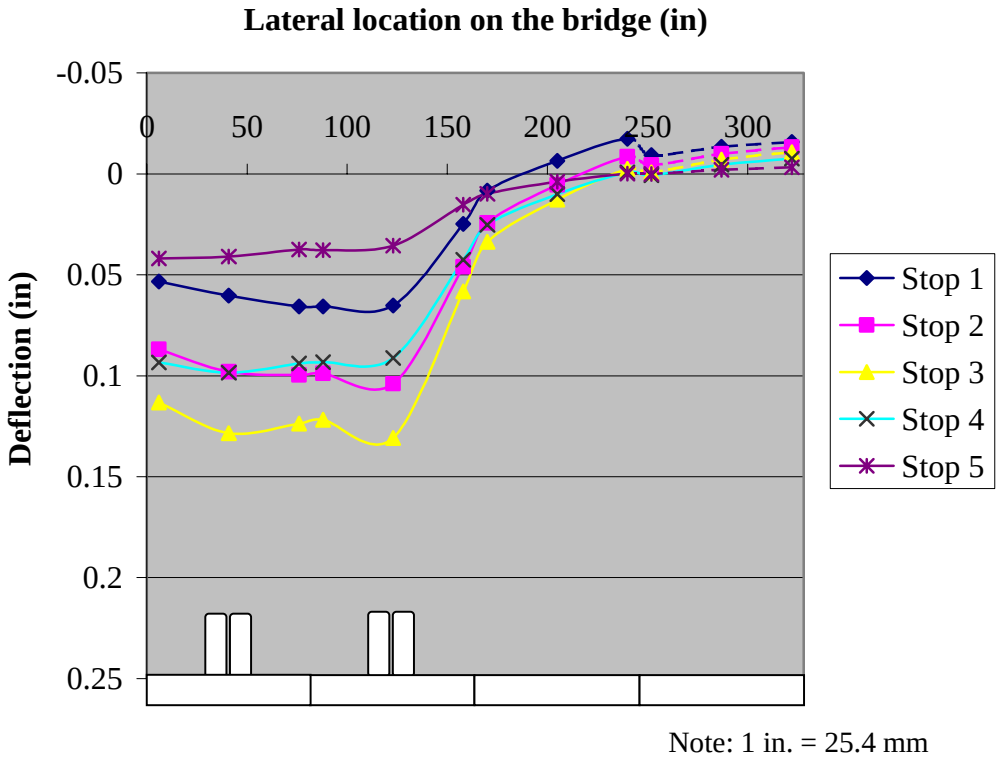

Note: 1 in. = 25.4 mm

Figure 7.29 Deflected Shape – Pass 2 – St. Francis Street

The impact factor for the live load was examined by conducting a pass in the same location as Pass 4 at a speed of approximately 20 mph (32 kph) (see Figure 7.31). The live load impact factor was computed as the ratio of the deflection obtained at 20

mph (32 kph) to the deflection obtained at Stop 3. The four values, one for the lateral center of each panel, were averaged to obtain a live load impact factor of 0.64. Following AASHTO recommendations for multi-beam concrete decks a live load impact factor of 0.3 would be calculated. A comparison of these two values seems to suggest that appropriate guidelines for FRP panel need to be developed for use by AASHTO and other design guidelines.

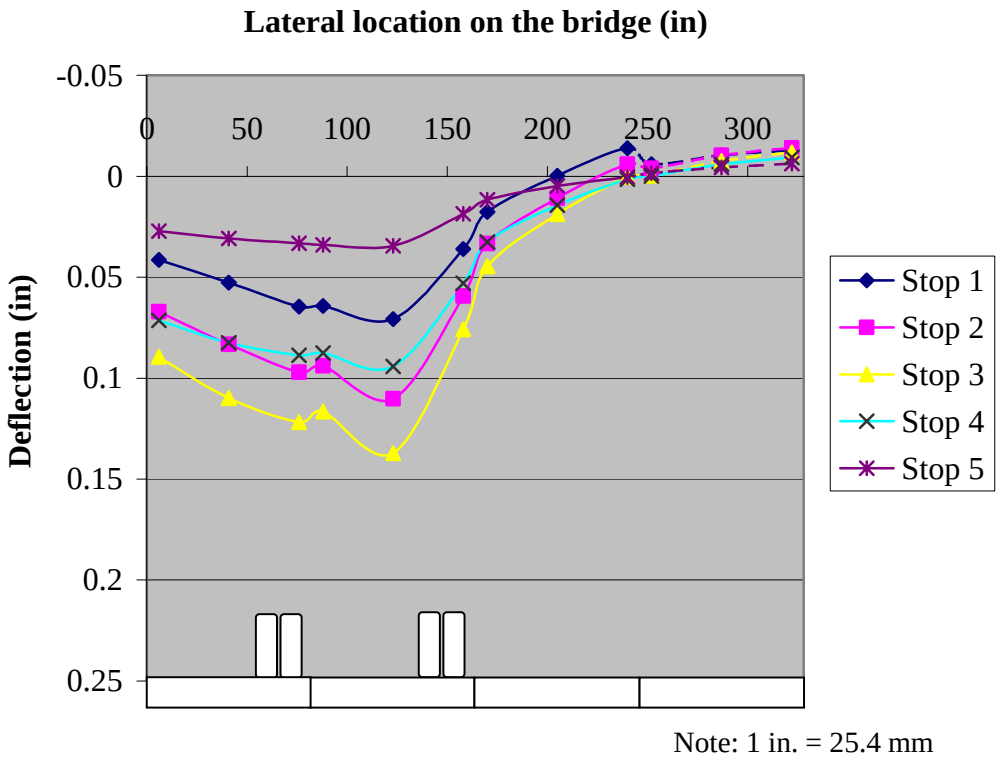

Figure 7.30 Deflected Shape – Pass 3 – St. Francis Street

Distribution of load between panels was also examined by comparing the deflection of the bridge panels. Again, the relationship between load and deflection is assumed to be linear then they are related by a single constant; this is a valid assumption due to the linear-elastic behavior exhibited by FRP materials. Under this assumption, a

comparison of the ratio of the deflection of one panel to the sum of the deflections of the panels quantifies the lateral distribution of load between the panels.

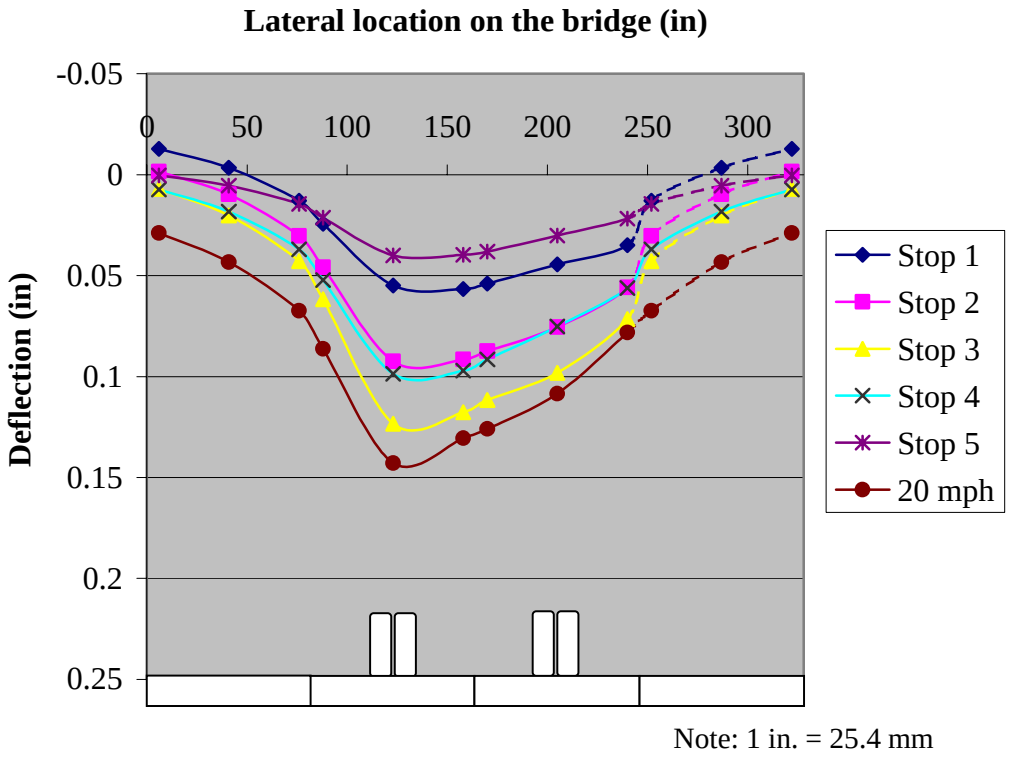

Figure 7.31 Deflected Shape – Pass 4 and 20 mph Pass – St. Francis Street

Figure 7.32 illustrates the load distribution as a percentage of the total load on the bridge for Passes 1 through 4. As was also exhibited in the plots of the deflected shape, it is observed that the vast majority of the load on the bridge is carried by the panels on which the load is directly places. There is minimal lateral distribution of load. Pass 2 is a perfect example; note that Panel 1 and Panel 2 each carry approximately 50 percent of the load on the bridge. This is synonymous with the fact that each panel was designed to carry one wheel-line of load (i.e., half of the weight of the truck).

To readily compare to the AASHTO wheel load distribution factors, the percentages in Figure 7.31 must be multiplied by two. The maximum distribution factor for the St. Francis Street Bridge would come from Panel 1 with a value of 1.241. When compared to the AASHTO distribution factor, 1.298, as would be computed for a multi-beam concrete deck, the value seems appropriate.

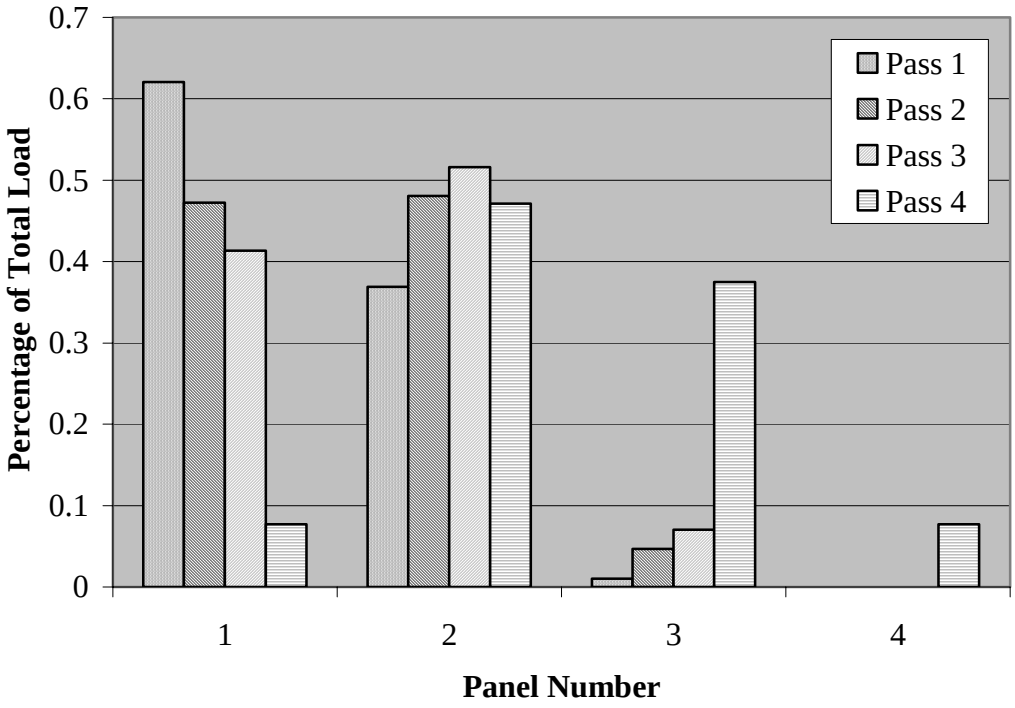

Figure 7.32 Percentage of Load Carried per Panel as a Percentage of Total Load on The Bridge – Passes 1 through 4 – St. Francis Street

Figure 7.33 illustrates the load distribution as a percent of the total load on the bridge for Pass 4 and the pass at 20 mph (32 kph). Although the total load experienced by the bridge is greater in the case of the 20-mph (32-kph) pass due to impact, the percentage of load carried by each respective panel is very similar.

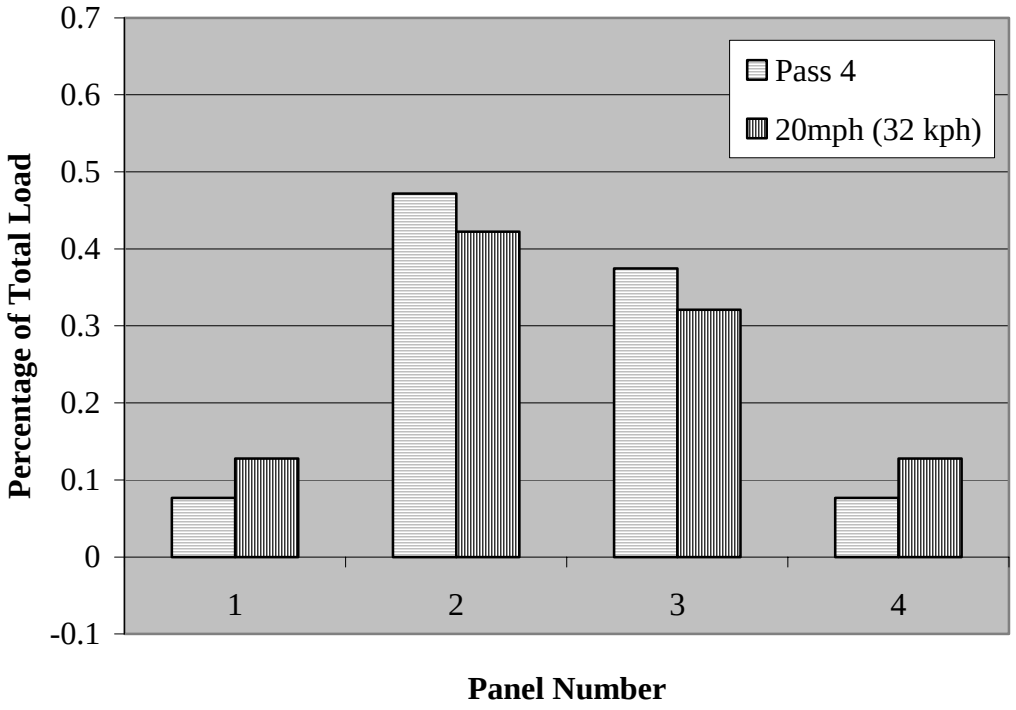

Figure 7.33 Percentage of Load Carried per Panel as a Percentage of Total Load on The Bridge – Pass 4 and 20 mph Pass – St. Francis Street

Due to the lateral distribution of load between panels, the theoretical deflection is difficult to determine, therefore a direct comparison will not be drawn. It is known however that the bridge panels themselves were designed to meet the AASHTO deflection requirement of span length divided by 800, which in this case, with a span length equal to 25.25 ft (7.70 m), corresponds to a deflection of 0.379 in (10.0 mm). The maximum observed deflection during the static load passes was 0.188 in (4.78 mm), yielding a span-to-deflection ratio of approximately 1610 or approximately 50 percent of the allowable deflections. Even considering the increased deflection experienced during the pass at 20 mph (32 kph), the span-to-deflection ratio is approximated at 2120 or approximately 35 percent of the allowable deflections. Moreover, Figure 7.34 illustrates the predicted deflection of the bridge for the design loading condition of one truck in

each of the two lanes. The principle of superposition was utilized assuming linear-elastic behavior of the bridge. The maximum deflection in this case is roughly 0.176 in (4.47 mm) for a span-to-deflection ratio of approximately 1720, or a deflection roughly 50 percent of the allowable deflection.

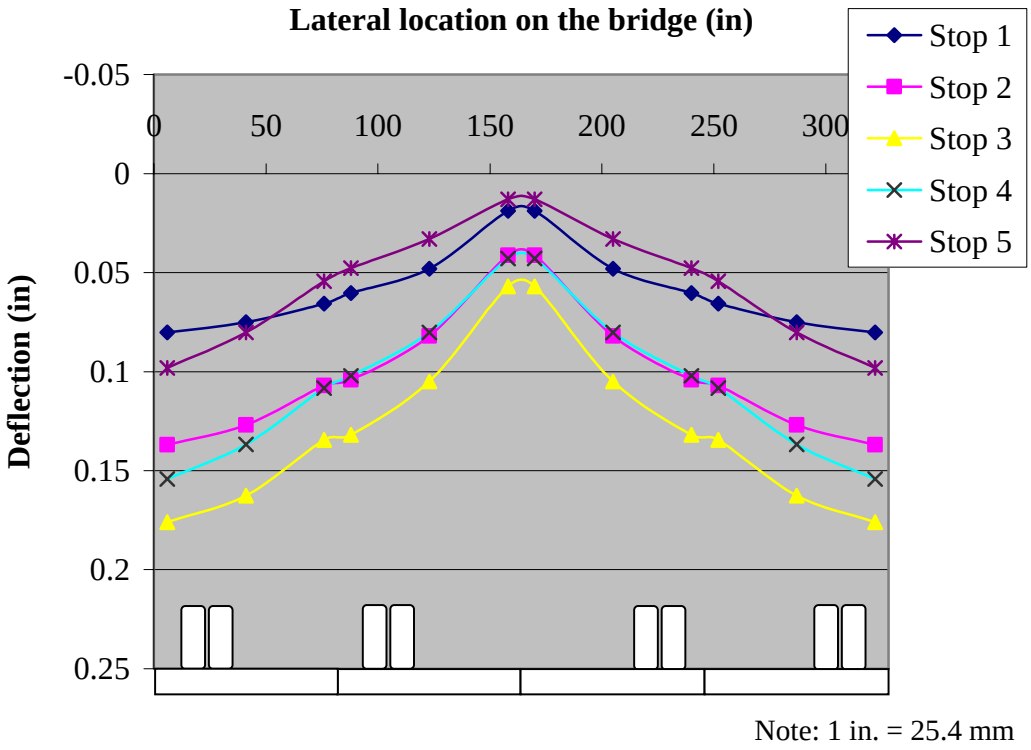

Figure 7.34 Deflected Shape – Superposition of Pass 1 – St. Francis Street

For the St. Francis Street Bridge only, an additional load test was performed in March of 2001. Although the complete results will not be presented herein, a comparison between the results of the two load tests will be made with the objective of determining the performance of the FRP materials over time while subjected to ambient outdoor conditions.

The axle spacing of the trucks utilized during the two load tests were identical, but the loads on the axles were slightly different; for comparison purposes, these differences were accounted for assuming linear-elastic behavior of the materials. Based on the maximum deflection measured for Passes 2, 3 and 4, which were conducted during both load tests, there was a general decrease in deflection. Decreases in deflection were on the order of zero to 12 percent, with an average value of approximately 4.5 percent, indicating an increase in stiffness. The increase in stiffness exhibited by the St. Francis Street Bridge in-situ is considerably smaller than the increases in stiffness exhibited by the conditioned FRP panels in the laboratory, which were on the order of 100 percent, and approximately equal to the increases in stiffness exhibited by the conditioned FRP laminates, which were on the order of zero to 4.6 percent. As mentioned previously, annual load tests will be conducted for two additional years; the results from those load tests will be utilized to draw further conclusions about the long-term performance of the materials.

7.4. WALTERS STREET BRIDGE

The main research objectives in testing this bridge were to determine the load distribution from panel to panel and the load-deflection behavior of the panels. Six DCVT transducers were located at mid-span and six were located near the supports. Again, in Figure 7.35, which illustrates the layout of the DCVT transducers, the DCVT transducers denoted in black were recorded continuously during the testing, however the DCVT transducers denoted in grey were only recorded periodically at pertinent times.

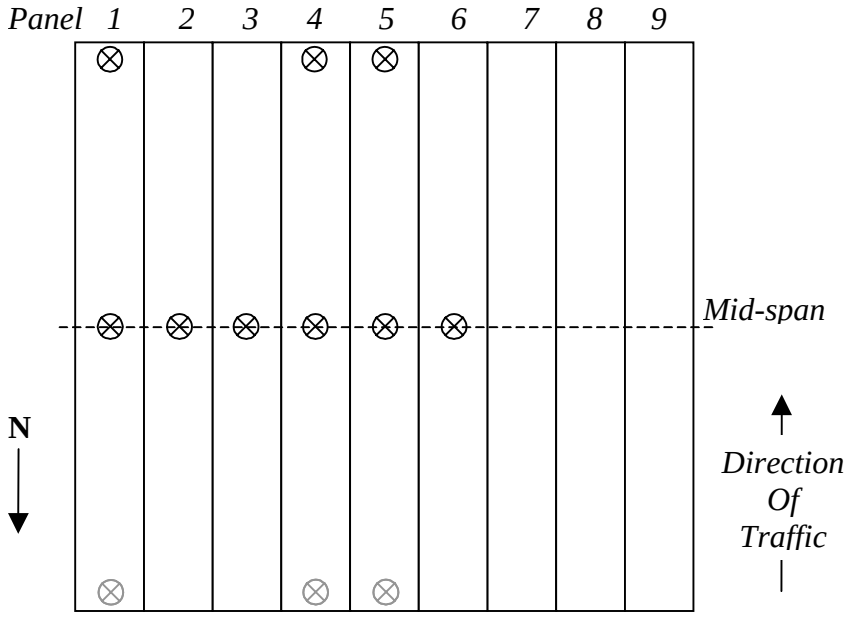

Figure 7.35 Layout of the DCVT Transducers – Walters Street

Figure 7.36 illustrates the lateral location of the first four truck passes. Additional passes were made at 20 mph (32 kph) at the same location as Pass 4 as were three passes that were symmetric to Passes 1 through 3. Assuming that the bridge behaved symmetrically, the measurements from the symmetric load passes were used to complete the deflected shapes for Passes 1 through 3. During each pass the truck was stopped at five longitudinal locations. Table 7.5 details the location of the truck stops. Due to the axle loads and axle spacing of the loading truck, truck location 3 corresponds to the worst-case loading condition. A picture of the bridge during the load test is shown in Figure 7.37.

The results of the load test for Passes 1 through 4 are presented in Figure 7.38 through Figure 7.41, respectively. It should be noted that the illustration at the bottom of

each figure depicts the layout of each of the nine panels and the lateral location of the tandem axles on the bridge for each pass. Furthermore, the dashed portion of the curve is taken from the abovementioned symmetric pass for each of the passes. For each of the figures, the progression of the deflected shape from the top curve to the bottom curve is consistent with the level of moment induced by each loading position. Stop 5 generates the least moment in the bridge; followed by Stop 1; Stops 2 and 4, which are nearly identical; and Stop 3, which produces the largest bending moment.

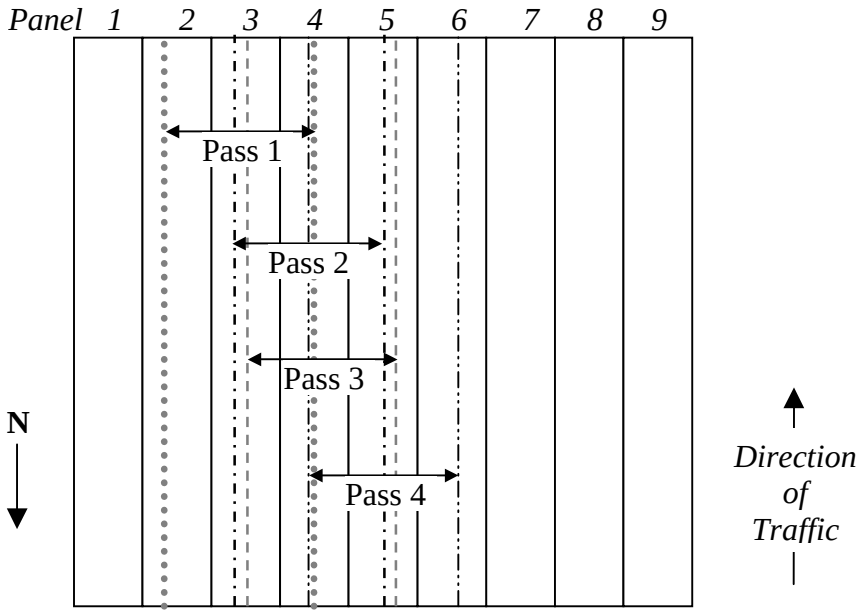

Figure 7.36 Lateral Location of Truck Passes 1 through 4

A preliminary examination of the data indicates that the readings are accurate. The consistency of the readings from stop to stop and from pass to pass lends credence to their validity. The curves also exhibit, in general, a smooth transition from point to point.

Table 7.5 Longitudinal Truck Locations – Walters Street

Stop	Truck Position
1	Middle and rear axles of the truck centered approximately 1 ft (0.30 m) onto the bridge from the north end
2	Middle and rear axles of the truck centered approximately 6 ft (1.83m) onto the bridge from the north end
3	Middle and rear axles of the truck centered approximately 11 ft (3.35 m) onto the bridge from the north end (i.e., at mid-span)
4	Middle and rear axles of the truck centered approximately 16 ft (4.88 m) onto the bridge from the north end
5	Middle and rear axles of the truck centered approximately 21 ft (6.40 m) onto the bridge from the north end

Figure 7.37 In-situ Bridge Load Test – Walters Street

A comparison of Figure 7.38 through Figure 7.41 illustrates that as the load progresses from Pass 1 through Pass 4 that the maximum deflection experienced by the bridge decreases due to the fact that a larger number of panels are engaged in sharing the load. A comparison of the maximum deflection during Pass 1 to the maximum deflection during Pass 4 confirms a decrease in deflection of approximately 20 percent.

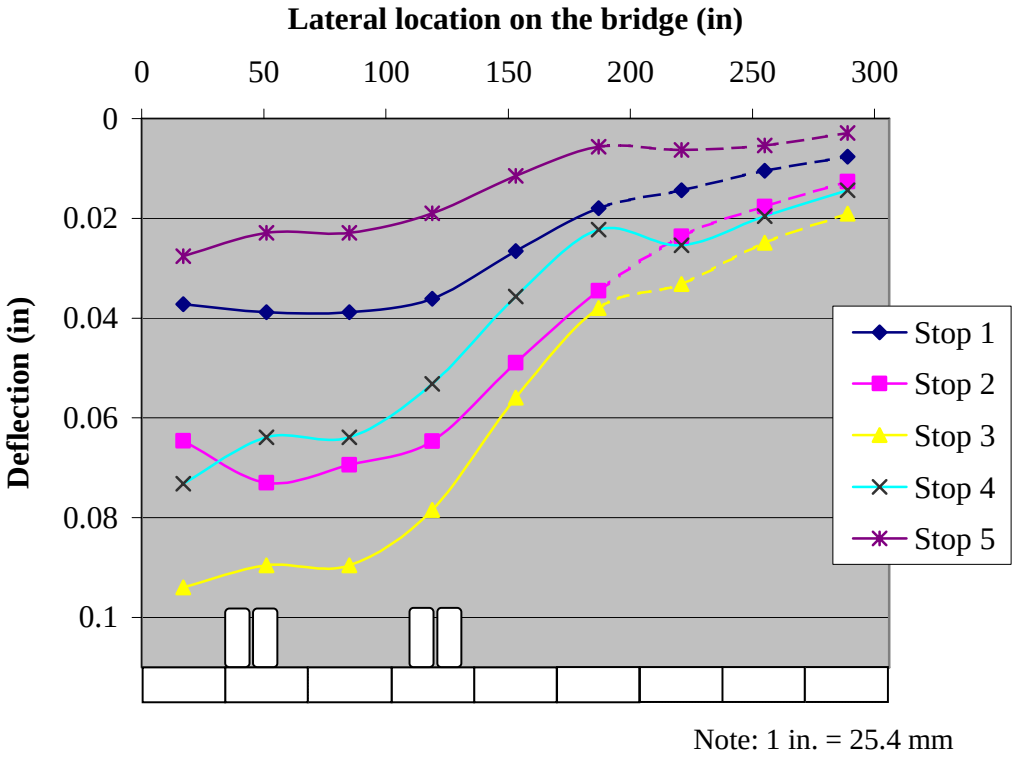

Figure 7.38 Deflected Shape – Pass 1 – Walters Street

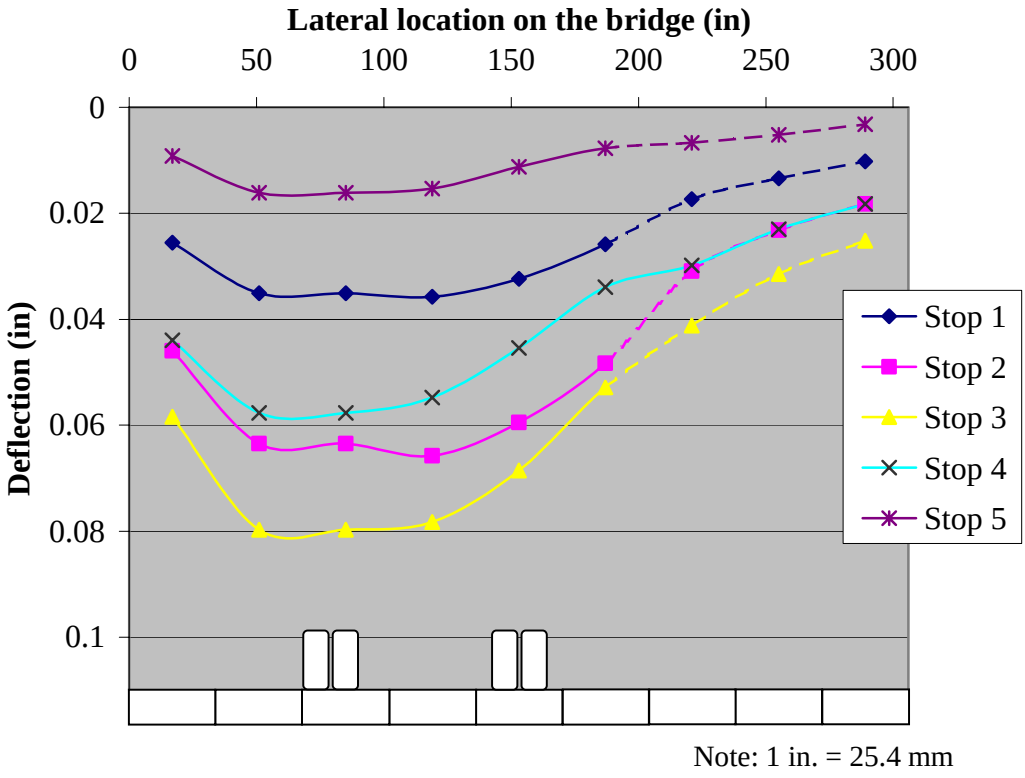

Figure 7.39 Deflected Shape – Pass 2 – Walters Street

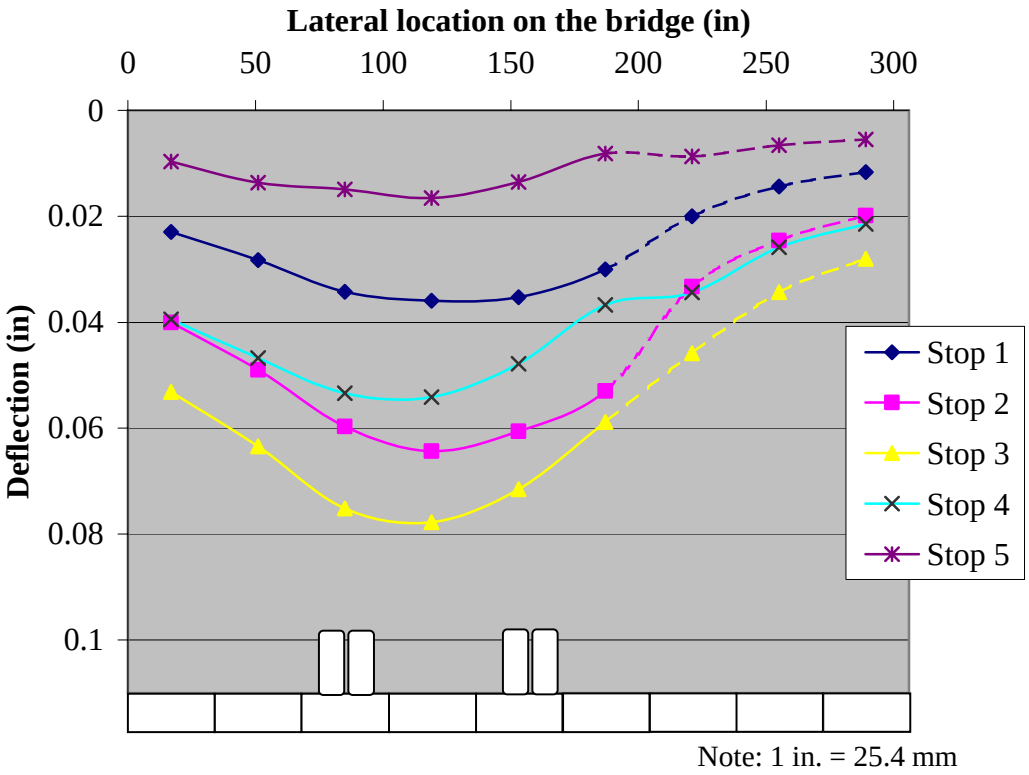

Figure 7.40 Deflected Shape – Pass 3 – Walters Street

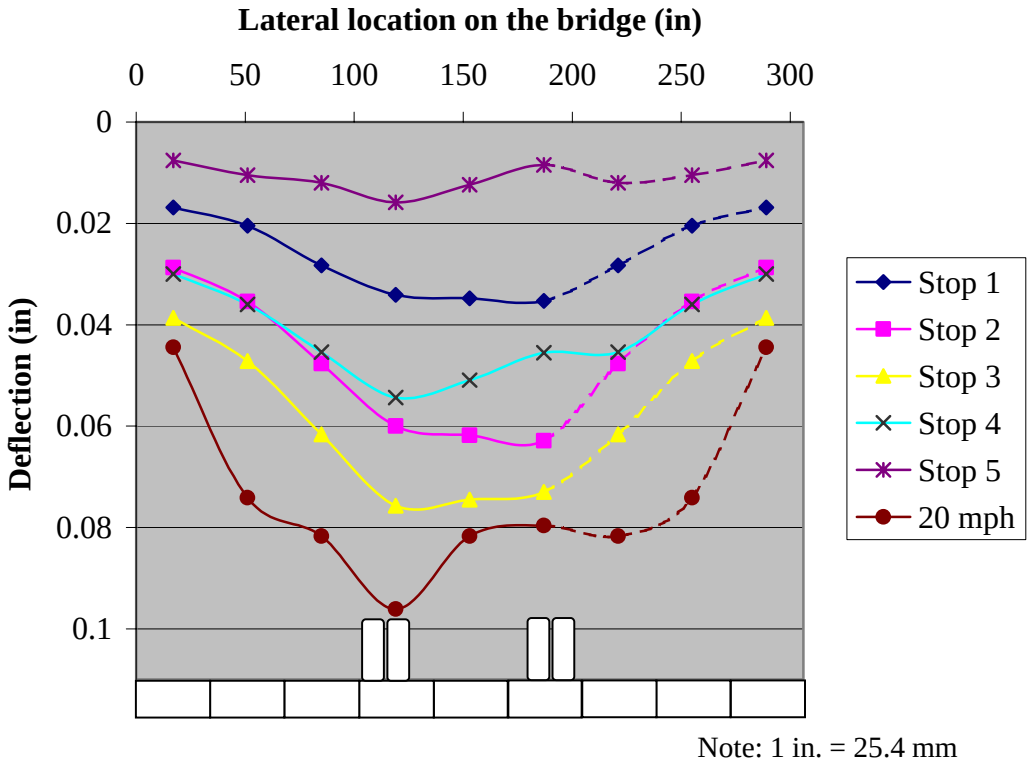

Figure 7.41 Deflected Shape – Pass 4 and 20 mph Pass – Walters Street

The live load impact factor was examined by conducting a pass in the same location as Pass 4 at a speed of approximately 20 mph (32 kph) (see Figure 7.41). The live load impact factor was computed as the ratio of the deflection obtained at 20 mph (32 kph) to the deflection obtained at Stop 3. The nine values, one for each panel, were averaged to obtain a live load impact factor of 0.28. Compared to the computed AASHTO live load impact factor for this bridge, which is 0.30, the AASHTO guidelines appear to be appropriate.

Distribution of load between panels was also examined by comparing the deflection of the bridge panels. If the cross-section of the panels is assumed to be uncracked the relationship between load and deflection is assumed to be linear and they are related by a single constant; this is a valid assumption because (a) the load induced during the load test in the panels, a maximum of approximately 2.7 kips (12.0 kN) is approximately 45 percent of the cracking load for the bridge panels and (b) it is unlikely that two fully-loaded trucks would be on the bridge at the same time given the surrounding community (i.e., the section should be uncracked). Under this assumption the ratio of the deflection of one panel to the sum of the deflections of the panels will be equal to the load on one panel divided by the total load on the bridge, as outlined in the previous sections. A comparison of these ratios quantifies the lateral distribution of load between the panels.

Figure 7.42 illustrates the load distribution as a percentage of the total load on the bridge for Passes 1 through 4. There is a clear progression of the peak load percentage from one side of the bridge toward the center as the load moves from Pass 1 to Pass 4. As was also exhibited in the plots of the deflected shape, it is observed that as the loading

truck goes from Pass 1 through Pass 4 the peak load percentage decreases as the number of panels sharing a larger portion of the load increases.

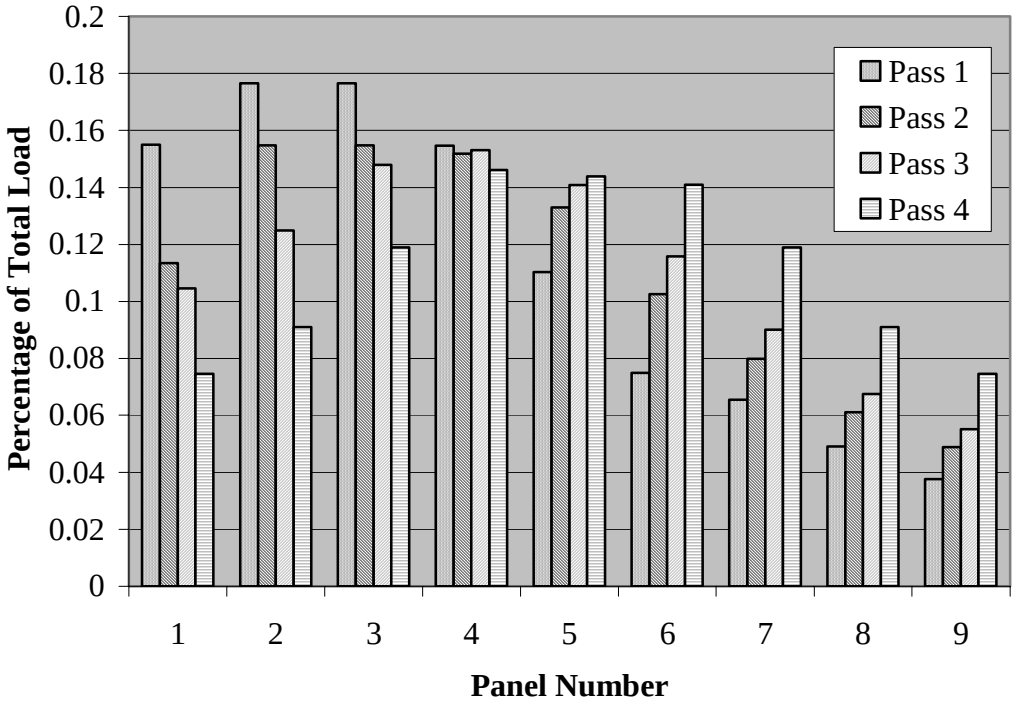

Figure 7.42 Percentage of Load Carried per Panel as a Percentage of Total Load on The Bridge – Passes 1 through 4 - Walters Street

It is desirable to determine the load carried by the girder as a fraction of one wheel line load so that the values can be readily compared to the AASHTO wheel load distribution factors. Equation 7.2 outlines the calculations with respect to the total load on the bridge. Since the load on one wheel load line is equal to half of the total load on the bridge, it follows that the percentages in Figure 7.42 must be multiplied by two. The maximum distribution factor for the Walters Street Bridge would come from Panel 2 with a value of 0.353. A comparison to the AASHTO distribution factor, 0.49, utilized in the

design (recall Section 3.4) seems to suggest the appropriateness of the AASHTO guidelines for use with FRP-RC panels.

Figure 7.43 illustrates the load distribution as a percent of the total load on the bridge for Pass 4 and the pass at 20 mph (32 kph). Although the total load experienced by the bridge is greater in the case of the 20-mph (32-kph) pass due to impact, the percentage of load carried by each respective panel is very similar. Furthermore, the peak load percentage carried by Panel 4 is identical for the two passes.

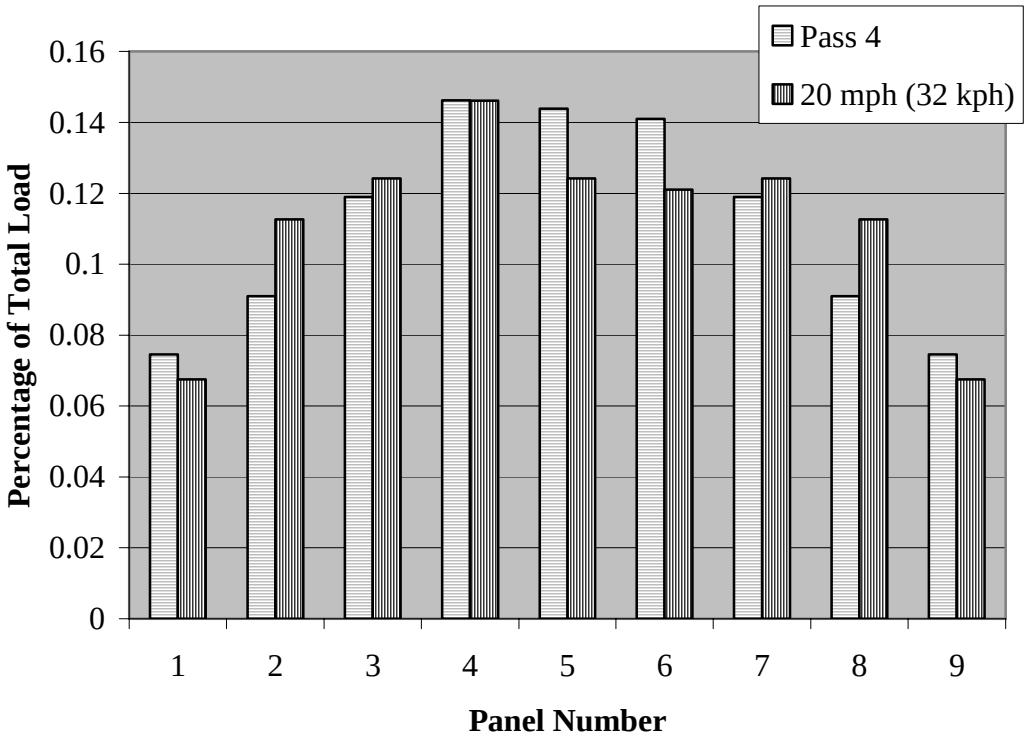

Figure 7.43 Percentage of Load Carried per Panel as a Percentage of Total Load on The Bridge – Pass 4 and 20 mph Pass – Walters Street

Due to the lateral distribution of load between panels, the theoretical deflection is difficult to determine, therefore a direct comparison will not be drawn. It is known however that the bridge panels themselves were designed to meet the AASHTO

deflection requirement of span length divided by 800, which in this case, with a span length equal to 23 ft (7.01 m), corresponds to a deflection of 0.345 in (8.76 mm). The maximum observed deflection during the static load passes was 0.094 in (2.4 mm), yielding a span-to-deflection ratio of approximately 2940 or approximately 25 percent of the allowable deflection. Even considering the increased deflection experienced during the pass at 20 mph (32 kph), the span-to-deflection ratio is approximated at 2870 or approximately 30 percent of the allowable deflection. Moreover, Figure 7.44 illustrates the predicted deflection of the bridge for the design loading condition of one truck in each of the two lanes. The principle of superposition was utilized assuming linear-elastic behavior of the bridge. The maximum deflection in this case is roughly 0.12 in (3.1 mm) for a span-to-deflection ratio of approximately 2300, or a deflection roughly 35 percent of the allowable deflection.

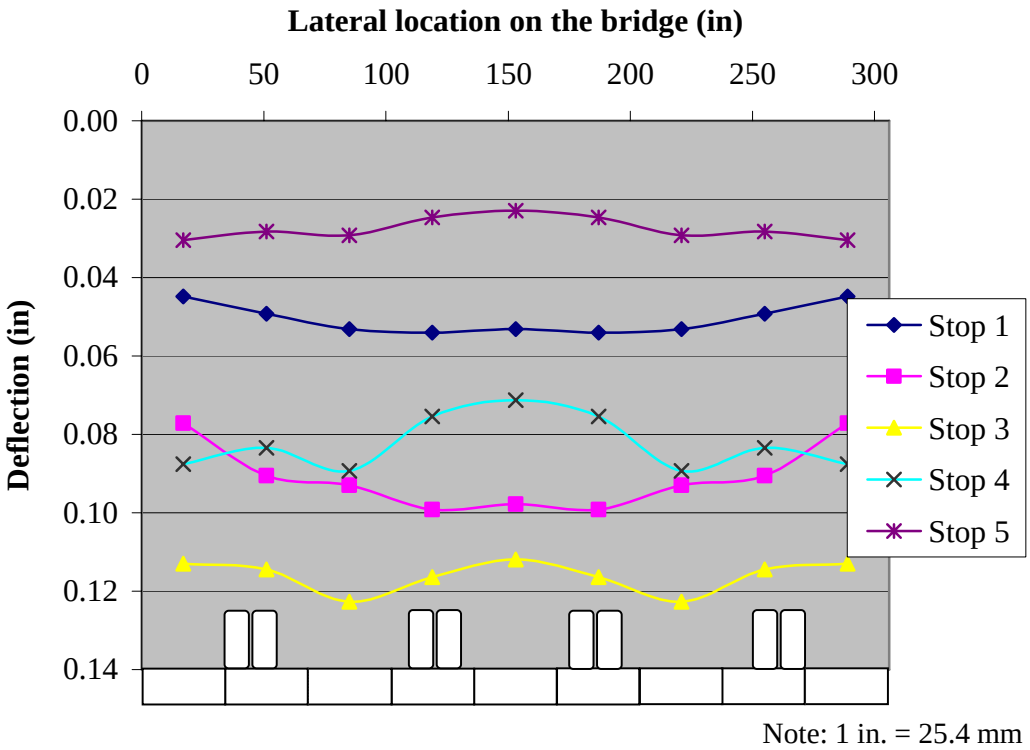

Figure 7.44 Deflected Shape – Superposition of Pass 1 – Walters Street

7.5. DISCUSSION OF RESULTS

The impact factors and wheel load distribution factors obtained from the bridge load testing are outlined for each of the bridges in Table 7.6. It should be noted that the values for the St. Johns Street and Jay Street Bridges are very similar. This is to be expected due to the vast similarities between the two bridges, which are both constructed using FRP panels supported by steel girders. Although the overall structure of the St. Francis Street and Walters Street Bridges is similar, due to the differences between the panels and the panel connections, the calculated factors are considerably different. There is a notable difference between the amount of lateral load transfer for the St. Francis Street and Walters Street Bridges.

Table 7.6 Summary of Impact Factors and Distribution Factors

Bridge	Impact Factor	Distribution Factor
St. Johns Street	-0.06	0.600
Jay Street	-0.04	0.613
St. Francis Street	0.64	1.241
Walters Street	0.28	0.353

The mechanism of load transfer between girders for the St. Johns Street and Jay Street Bridges is, as mentioned previously, the steel diaphragms that join the girders. For the St. Francis Street panels the load would be transferred by the FRP tubes installed in the joints between panels; due to their relatively weak connection to the panels and, assumedly, their material properties, there is an almost negligible amount of load

transferred between the panels. The connection of the precast panels in the Walters Street Bridge via welded shear keys is very effective in transferring the load, with a relatively small portion of the applied load actually carried by the loaded panel.

A comparison between the limiting design deflections and the measured deflections verifies the design calculations, in that all of the measured deflections are considerable less than the limiting design values. Table 7.7 details a summary of these deflections.

Table 7.7 Comparison of Deflections

Bridge	Design Deflection Limit (in)	Maximum Measured Static Deflection (in)
St. Johns Street	0.384	0.227
Jay Street	0.388	0.203
St. Francis Street	0.379	0.188
Walters Street	0.345	0.094

Note: 1 in. = 25.4 mm

8. CONCLUSIONS

Conclusions based on the installation of four bridge utilizing FRP materials can be summarized as follows. The four bridges utilized three FRP technologies, namely FRP panels supported by steel girders, FRP bridge panels, and FRP reinforcing bars for concrete.

- Utilizing FRP in the form of reinforcing bars allows for the use of many steel-RC concrete practices. The fabrication and installation details were nearly identical to the methods utilized by the concrete precaster for steel-reinforced panels.
- For all four of the bridges there is great appeal in the short timeline for installation. Due to the precast/prefabricated panels in installation of each bridge took approximately one week. This is in sharp contrast to the three to four weeks that traditional cast-in-place construction would have taken.
- The difference in panel alignment for FRP panel bridges necessitated different connections to the girders, however both could allow for installation of half of the bridge at a time. In an urban environment, this could be beneficial due to the possibility of closing only one at a time.
- FRP deck panels are light enough to move without heavy equipment. With a weight of approximately 15 to 16 psf (0.72 to 0.77 kN/m^2) they could be moved with equipment readily available to city and county municipalities. The fact that special equipment is not necessary for installation could be attractive in many instances.

- The application of FRP layers in the field (i.e., cured under ambient conditions) could pose durability issues in the future. Several FRP layers were applied over the panel joint of the St. Francis Street and Jay Street Bridges; these two bridges will be monitored closely in order to detect whether such issues will arise.
- The technique of attaching the guardrail posts to the FRP panels in the case of the St. Francis Street Bridge, which modeled the attachment of guardrail posts to timber decks, seems to be performing well. An unofficial test of the guardrail system conducted by KSCI, whereby a static horizontal load was applied to one of the guardrail posts, indicated deflection/rotation of the guardrail post without damage to the FRP panel.
- Installation of the bridges highlighted the fact that having an efficient system is more important than having adequate parts. Connections to each other and connections to the girders have shown the importance of design tolerances and detailed installation procedures.

Conclusions based on testing of the FRP panels and their constituent materials yield the following results:

- It is possible that the variability in the manufacturing process, manual hand lay-up, could have affected the results of the flexural testing. More meticulous quality assurance/quality control (QA/QC) techniques should be employed to decrease the variability in the panels.
- When exposed to accelerated aging or a saline solution at an elevated temperature the tensile strength of the GFRP laminates was not adversely

affected. In fact in most cases, the modulus and strength of the laminates increased due to the conditioning.

- The flexural behavior of GFRP sandwich panel beams exposed to accelerated aging in an environmental chamber or exposed to a saline solution at an elevated temperature is different from the behavior of the control specimen. The modulus of both conditioned specimens was higher than that of the control specimen.
- Comparison of failure stress values and span-to-deflection ratios at failure indicates that the structure of the FRP panel affects the performance.
- It appears that the failure stress, at 9825 psi (67.74 MPa), and span-to-deflection ratio, at 100, recommended by the manufacturer may not be conservative for all panel configurations. It is recommended that the manufacturer reconsider their recommendations and adopt a more conservative failure stress and span-to-deflection ratio.
- With further respect to the conservative nature of the design recommendations made by the manufacturer, it should be noted that the modulus value utilized in the design of the bridges was conservative for the vast majority of specimens tested.
- The typical failure occurs by lateral expansion of the core at one-quarter span and delamination of the core material from the top and/or bottom face of the panels.

Based on laboratory testing of FRP-RC and steel-RC specimens the following conclusions can be made regarding the behavior of FRP-RC:

- Laboratory testing exhibited good agreement between the experimental and theoretical stiffness values based on moment-curvature predictions.
- The flexural capacity of both the FRP-RC panel and the steel-RC panel were predicted very well by their respective design guidelines. The failure mode exhibited by the panels was also as expected based on design assumptions.
- The shear capacity predictions for both the steel-RC and FRP-RC panels were very conservative. This is due in part to the factor of two assumed for the contribution of the concrete to the shear capacity, the ratio used to reduce the concrete contribution to the shear capacity of the FRP-RC panel, and the limit of 0.002 on the strain in the FRP shear reinforcement.
- The experimental deflection of the FRP-RC panel in the laboratory was approximately 50 percent of the theoretical deflection as predicted by ACI 440 guidelines (2001), which use the modified Branson equation, indicating that the ACI 440 flexural design guidelines are conservative.
- The same level of conservatism is exhibited by the ACI 318 guidelines, which use the Branson equation, lending credibility to the adoption of the modified Branson equation by ACI 440.
- For material characterization of the FRP bars, the measured tensile strength exceeded the tensile strength recommended by the manufacturer. The CFRP bars exhibited a similar trend during testing demonstrating a higher tensile modulus of elasticity than the manufacturer's specifications. On the other hand, the GFRP bars exhibited a modulus of elasticity lower than that recommended by the manufacturer.

- The exposure to the environmental cycles appears to have no effect on the interlaminar shear strength of the GFRP bars.
- However, the results indicate that the alkaline conditioning conducted causes more degradation in the 1/2-in (12.7-mm) GFRP bars than the 3/8-in (9.5-mm) GFRP bars.
- Both tensile strength and tensile modulus of GFRP bars are affected by exposure to an alkaline solution at an elevated temperature. Degradation was generally within the recommended reduction factors offered by ACI (2001).

In-situ bridge load testing conducted on all four of the project bridges generated the following conclusions:

- The impact factors and wheel load distribution factors obtained for the St. Johns Street and Jay Street Bridges are very similar. This is to be expected due to the vast similarities between the two bridges, which are both constructed using FRP panels supported by steel girders.
- Although the overall structure of the St. Francis Street and Walters Street Bridges is similar, due to the differences between the panels and the panel connections the impact factors and wheel load distribution factors are considerably different. There is a notable difference between the amount of lateral load transfer for the St. Francis Street and Walters Street Bridges.
- The mechanism of load transfer between girders for the St. Johns Street and Jay Street Bridges is, as mentioned previously, the steel diaphragms that join the girders.

- For the St. Francis Street panels the load would be transferred by the FRP tubes installed in the joints between panels; due to their relatively weak connection to the panels and, assumedly, their material properties, there is an almost negligible amount of load transferred between the panels.
- The connection of the precast panels in the Walters Street Bridge via welded shear keys is very effective in transferring the load, with a relatively small portion of the applied load actually carried by the loaded panel.
- A comparison between the limiting design deflections and the measured deflections verifies the design calculations, in that all of the measured deflections are considerable less than the limiting design values.

9. RECOMMENDATIONS FOR STANDARD DEVELOPMENT

A set of standard test method specifications and supplier selection/procurement specifications is currently being written by the Market Development Alliance (MDA) for the FRP Composites Industry. The need for specifications in this case stems from the novelty of the materials involved. The civil engineering community is comfortable with the design of bridges. What they are not comfortable with are these new materials and the construction methods that accompany them. The private sector is, in general, responsible for developing any standards or specifications necessary to conduct their business and this is what MDA is attempting to do for the FRP bridge panel industry.

The comments provided herein are presented based on the experience gained from the installation of the four bridges utilizing FRP materials outlined by this report. Further comments of value to this discussion have been presented by Henderson (2000) based on the experience in the Salem Avenue Bridge project.

9.1. GENERAL STANDARD CRITERIA

Some general concepts about standards are as follows. A standard should:

- Be unbiased
- Serve a specific need in industry and be supported by industry
- Have a clear scope
- Be understandable to a layman or someone with very little knowledge of the subject, meaning that the terms used should be clearly defined
- Define a specific product/process/etc. as well as the necessity for that product/process/etc.

- Define all necessary requirements for acceptance/rejection
    - Testing method, QA/QC, measurement methods, sample preparation, analysis technique, limiting values, tolerances

Specifically, the types of standard discussed herein are for FRP bridge panels are (a) a specification for performance of the FRP panels themselves and (b) a contracting standard to define how construction responsibilities will change with the use of these new materials.

9.2. PANEL PERFORMANCE STANDARDS

The standard for the FRP panels, in the authors' opinion, should be a performance standard, due to the large number of FRP panel manufacturers and the variation of their panels. Others in support of a performance standard include Bank et al. (2002) who outlined "A Model Specification for Composites for Civil Engineering Structures," which details FRP classification systems as well as a number of performance standards including tensile strength, short beam shear strength, and long-term durability.

Instead of defining specific panel details, a performance standard would prescribe minimum properties for the FRP bridge panels. Furthermore, "performance standards, though usually more difficult to write and enforce, tend to be less restrictive than design standards, and more likely to encourage innovation" (Breitenberg, 1987). As this is a developing technology, innovation should be fostered as much as possible. One method for approval outlined by Breitenberg (1987) is the Canvass method, which required all representatives on the standards committee to approve the standard prior to adoption. If the representatives on the committee are chosen in such a manner that all portions of

industry interested in the standard (e.g., manufacturers, designers, etc.) would have representation, then all interests in the product/method are satisfied and acceptance of the standard in practice would be that much more likely.

To be an effective standard, the FRP panel performance standard should be:

- Unbiased toward one manufacturer or another. As each manufacturer has specific materials, manufacturing techniques, panel connection methods, etc., a specification should be applicable to all types of FRP panels and not favor any one type.
- Define the material properties that are necessary for the use of FRP panels in bridge construction (durability, flexural stiffness, shear stiffness, UV resistance, fire resistance, panel joint capacity, etc.).
    - define the test methods that will be used to evaluate these properties, this may require different test methods for different manufacturing methods
    - define test specimens on which the tests should be conducted
    - define the analysis technique to be utilized for the results
    - define satisfactory results – repeatability, QA/QC
- Enabling of acceptance of the product in the construction industry by:
    - assuring consumers of the panel properties
    - empowering manufacturers by giving them a means of “proving” their product
    - allowing for regulations by government agencies, if necessary
- Defined by industry professionals who have a vested interest in the product and a clear understanding of the standards purpose and scope.

- Should address all aspects of the design of the panels from the connections to the wearing surface, etc. The total FRP panel bridge system should be considered, as well as each of the components individually.

ASTM has put forth established sets of guidelines for material specifications and test methods. The outline of the ASTM Standard Specification and the ASTM Standard Test Method is available online (2001). It appears that all necessary aspects of a reasonable standard are outlined. The application of this outline to a specification for FRP panels would require definition of the necessary material properties. Test methods would need to be defined to determine the properties, which may already exist within the ASTM standard test methods or, due to the panel configurations and connection details, new test methods may need to be developed.

9.3. CONTRACTING STANDARDS

In terms of the contracting standard, there are an infinite number of examples that could be followed. Any agency that deals with construction contracts has a standard set of guidelines for bidding, contractor selection, and the contract itself. The difference with the process in this case is that the manufacturer of the FRP panels (at this stage of product acceptance) is the only one that has access to the proprietary information necessary to evaluate the capacity of the panels, the installation details of the panels, etc. This situation raises issues of design responsibility and product liability. Information provided during the supplier selection phase of the project will need to be more detailed and more technical in nature because the owner/contracting agency will not be, in general, familiar with the FRP panels. This is the reason that both performance/testing

standards and contacting standards are necessary in this case. A good contracting standard would recognize these issues and require additional involvement from the manufacturer than would be typical with an "accepted" construction material.

Another imperative factor to consider with the use of these new materials is the inspection of the bridge for acceptance immediately after installation and continued inspection policies to ensure performance of the bridge over time. Due to the varied nature of the FRP panels at this point, it seems that a manufacturer specific inspection manual would be the most appropriate. Again, the manufacturers are the only ones familiar with their system. It is essential that the manufacturer of the decks provide an inspection and maintenance manual for their product. It should outline both techniques and materials to be used. In this way, the owner will be able perform these activities independent of the manufacturer; although for major repairs, etc. it may be necessary for the manufacturer to become involved.

The contracting specifications should have elements of design standards within them. A possible range of values could be given whereby the designer could select design loads, acceptable deflections, and maximum strains depending on the application specifics. With respect to the amount of design details that should be defined prior to selection of the deck supplier, if there is a list of "pre-approved" supplier that had presented the results of the proposed tests and other pertinent design information then the general design details would already be known. The aforementioned performance standard could be the means by which this is accomplished. However, if there were no list of "pre-approved" suppliers this information should be outlined in the proposal and

could be up for discussion once the contract is awarded; it is important to ascertain whether the design specifics are reasonable or not.

It is important to be sure that the FRP panel system is sealed by a P.E. The liability issues may be confused or complicated if the manufacturer's engineer seals the FRP panel system and then the Owner's engineer seals the overall design. However, it seems logical that the manufacturer should take responsibility for all aspects of the design, including the connection details.

The involvement of the manufacturer in all aspects of design, installation, maintenance, etc. is crucial because they are the experts on their system. If changes or repairs need to be made or especially for the design of the connections, the manufacturer would be best suited to determine (based on knowledge from previous tests, applications, etc.) what the best course of action would be.

One suggestion is that a contractor for the owner would be responsible for installation of the bridge panels. However, installation of the panels could also be conducted by the manufacturer (or a contractor for the manufacturer) so that the manufacturer would have control over the process. This could both complicate and simplify the installation process. On the one hand, an additional contractor becomes involved in the installation, but on the other hand there should be less confusion between the instructions of the manufacturer and the instructions of the owner to the contractor.

9.4. PUBLISHED MATERIAL

Published material on the process of developing and documenting standards includes but is not limited to the following agencies.

1. American National Standards Institute website, http://www.ansi.org
2. American Society for Testing and Materials website, http://www.astm.org
3. Institute of Electrical and Electronic Engineers website, http://www.ieee.org
4. International Organization for Standardization website, http://www.iso.ch/iso/en/ISOOnline.frontpage
5. National Institute of Standards and Technology website, http://www.nist.gov

Two additional references are books by Harter (1979), which contains general information about the purpose and scope of standards as well as legal issues associated with standards that will be used in a regulatory fashion, and Abbett (1963), which contains an overview of contracts and engineering contract specifications and a considerable amount of general information.

Other code/standard organizations whose standards could be used as a model are as follows, however their websites do not contain information specifically about developing standards:

- American Society of Mechanical Engineers website, http://www.asme.org
- Society of Automotive Engineers website, http://www/sae.org
- International Conference of Building Officials website, http://www.icbo.org

To the best of the authors' knowledge, the only journal dedicated exclusively to the discussion of standards and standardization development is *ASTM Standardization News*.

10. RECOMMENDATIONS FOR FUTURE RESEARCH

Several recommendations for future research topics have been identified throughout the course of this project. They relate specifically to FRP panels, FRP-RC or the durability of FRP materials; the recommendations are grouped by these categories and briefly outlined as follows:

- Characterization of FRP panels via tests to failure considering a range of deck thickness values should be conducted in order to better identify the governing mode of failure, failure stress, modulus of elasticity, and shear modulus for the FRP sandwich panels manufactured by KSCI. This study could be expanded to include panels produced by other manufacturers and various span-to-depth ratios.
- Investigation of the FRP panel joint behavior. Their ability to transfer load could be enhanced through this study by employing both laboratory and field investigations.
- Determination of methods for repair and maintenance of FRP panels could become necessary as these structures remain in service. Investigations of patching methods for panels and joints could be of interest.
- Examination of the constructability issues for FRP panel bridges should be conducted through the development of further demonstration projects. The FRP panel system should be emphasized with at least equal weight to the individual components.
- Optimization of the FRP panels could be performed via further laboratory flexural testing, as could development of improved deflection prediction methods. The

relatively low modulus of the materials indicates that serviceability will control the design, resulting in panels that have ultimate capacities much higher than required. The optimization of the panels and improved methods of deflection prediction will ultimately save material and make the panels more economical.

- Establish protocols for QA/QC during the manufacturing process of the FRP panels in order to improve the consistency and quality of the product.
- Deflection prediction methods for FRP-RC need to be enhanced by further research. Confirmation of the conservatism employed by the design parameters is necessary.
- Study of the shear capacity of FRP-RC panels could help define relevant design parameters. The complexity of the issue is evidenced by the fact that this area is still not completely defined for steel-RC panels.
- Development and evaluation of a connection for precast concrete panels, such as those utilized for the Walters Street Bridge, utilizing FRP materials.
- Investigation of the bond characteristics and development length of bundled FRP reinforcing bars in concrete. Although the use of bundled bars has been shown in steel construction to decrease the bond between the reinforcing bars and the concrete (Lixin, 2001), to the best of the authors' knowledge, no research has been done with respect to FRP reinforcing bars.
- In-situ bridge load testing of a steel-RC bridge of the same configuration (i.e., panels precast by Oden Enterprises, Inc. with the same connections and panel dimensions) could be conducted to compare wheel load distribution factors for lateral load transfer. A comparison between the load transfer of steel-RC and

FRP-RC bridge panels could facilitate preliminary recommendations on the factors for FRP-RC for consideration by AASHTO.

- Exploration into the suitability of a profilometer to obtain deflection measurements during bridge load tests should be conducted. If viable, the profilometer could decrease testing times considerably due to the lack of instrumentation under the bridge that would be necessary.
- Investigation of the durability of FRP materials is necessary. The areas are many and are defined in Section 1.3. One issue highlighted by this research is the need for quantification of the post-curing issues, which could be facilitated by conducting longer term conditioning regimens.
- For future durability studies it is recommended that testing of specimens be conducted prior to conditioning as well as after conditioning in order to eliminate variability due to manufacturing. In this way the properties of specific panels will be compared against their virgin properties. It should be noted that it is still recommendable to have control specimens in order to compare failure modes.

APPENDIX A

FABRICATION OF FRP SANDWICH PANELS BY KSCI

Fabrication of the FRP honeycomb sandwich panels by Kansas Structural Composites is completed based on the following procedure. It should be noted that the pictures shown and the representative times for each step given are for the St. Francis Street panels. Fabrication of panels of different dimensions would vary accordingly.

1. The sections of core are produced utilizing manual lay-up. The completed sections have a width of approximately 12 in (304.8 mm) with a length varying according to the panel size. They are comprised of alternating layers of flat and fluted layers. The alternating layers form the corrugated shape of the core material, which has dimensions of approximately 2 by 4 in (50.8 by 101.6 mm).

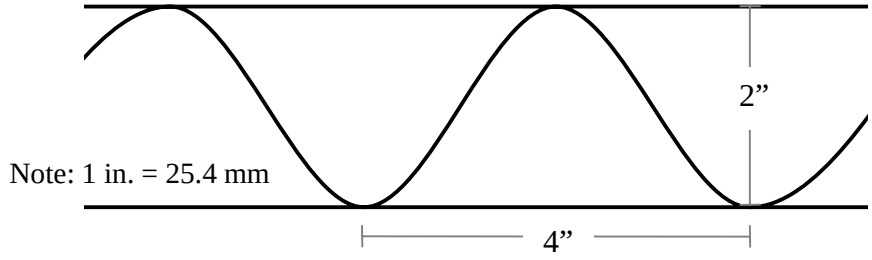

Figure A.1 Dimensions of the Corrugations in the FRP Sandwich Panels

2. The layers of the FRP material are laid-up on a frame to form the bottom face of the panel. This process took approximately 4 hours.

Figure A.2 Manual Lay-up of the Bottom Face

3. Pultruded FRP channels are utilized to close the sides of the panels. This process took approximately 1 hour.

Figure A.3 Installation of the Panel Edges

4. The sections of core are placed into position on the bottom face of the panel while it is still wet. This process took approximately 2 hours.

Figure A.4 Installation of the Core Sections

5. The core sections are weighted to press them into the bottom face for bonding purposes. The core and bottom face were allowed to cure with the weights on top over night (approximately 8 to 10 hours).

Figure A.5 Weighting of the Core Sections

6. The layers of FRP are laid-up on the top of the core sections in order to form the top face. This process took approximately 4 hours.

Figure A.6 Manual Lay-up of the Top Face

7. The final step in panel fabrication involves that application of the polymer concrete wearing surface to the top of the panels. This process is conducted at the manufacturing facility for increased quality control; the majority of the panel surface is covered with the exception of the regions near the joints where bonding of FRP materials will be conducted. This process is conducted after the top face resin has gelled, just prior to complete curing.

APPENDIX B

SECTIONS 1.F AND 1.G OF THE REQUEST FOR PROPSALS

SECTION 1.F.

PROGRAM REQUIREMENTS

A. BRIDGE DESIGN

1. The bridges shall demonstrate the potential of fiber reinforced polymer (FRP) materials for use in bridge construction. Therefore, innovation and a maximum demonstration of different features of this technology are desirable.

2. The bridges shall be designed using an FRP material. While emphasis should be placed on FRP materials, other materials are permitted.

3. The bridges shall be designed to carry a standard HS20 loading with a deflection that shall not exceed the AASHTO specification of L/800.

4. The bridges shall be designed such that the existing abutments will be used. A detail of the abutments is outlined on the project drawings, a copy of which is provided in these documents. Attention should be paid to the overall depth of the bridge structure, as those in excess of 20” are not desirable.

5. The bridges shall be designed with a cross slope (or superelevation) in accordance with AASHTO specifications, such that roadway drainage will be facilitated.

6. Each bridge shall include a wearing surface, which will be designed in accordance with AASHTO specifications for wearing surfaces found under the “Orthotropic Steel Deck” section of the manual.

7. Each bridge shall include guardrails, which will be designed in accordance with AASHTO design criteria. Use of FRP materials for the guardrails is desirable.

8. Rideability of the bridges shall be in accordance with AASHTO specifications. Pertinent sections of AASHTO would be those pertaining to requirements for rideability, joints, and seals.

9. Standard construction tolerances are allowed in the construction of the abutments. The proposer shall be aware of the fact that there are construction tolerances and design the bridges and their installation accordingly.

10. As-built measurements of the abutments shall be taken by the proposer prior to installation of the bridges. This activity shall be coordinated by the proposer with A&D Construction, St. James’ general contractor.

11. A licensed professional engineer shall oversee the design of the bridges. All computations, etc., which support the design shall be provided.

12. A ten- (10) year warranty shall be provided for materials and workmanship. The ten- (10) year period shall begin on the date of installation of the third bridge. The University shall have the unrestricted right to transfer this warranty to the City of St. James, MO.

B. BRIDGE MANUFACTURING

1. Manufacturing shall be performed by a method/process approved by a licensed professional engineer. Any one of the current manufacturing techniques for FRP materials, or any combination thereof, would be acceptable.

2. Manufacturing method/process shall have been used previously to manufacture FRP panels for use in another project(s). This other project(s) need not be highway bridge applications, but must demonstrate the effectiveness of the system.

3. The bridge that will be ready for installation on July 1, 2000 and all test articles will require the installation of sensors during manufacturing. The proposer shall be provided with these sensors and will be required to install them in the specimens.

C. BRIDGE INSTALLATION

1. The first two (2) bridges shall be ready for installation by May 15, 2000. Their installation shall occur no earlier than May 15, 2000, but may be postponed. The length of postponement will be dependent upon the readiness of A&D Construction, St. James' general contractor. However, a fifteen- (15) day notice shall be given as to the actual date of installation.

2. The third bridge shall be ready for installation no later than July 1, 2000, but may be ready any time between May 15, 2000 and July 1, 2000. The installation date of this bridge is also dependent upon the readiness of A&D Construction and the same fifteen- (15) day notice shall be given.

3. Bearing pads and other anchorage/installation requirements (e.g., drilling of holes into the concrete for bolts) shall be the responsibility of the proposer.

4. The City of St. James shall provide assistance to the proposer for the installation in the form of a crew of four (4) workers and a foreman, a tracked front-end loader, and a backhoe. This assistance shall be available only when the proposer's supervisor is on site for the installation and only for the time necessary for installation of the bridges. The number of days of assistance provided by the City of St. James shall not exceed nine (9) working days. If labor/equipment is required beyond those outlined above, they shall be the sole responsibility of the proposer.

D. TRANSPORTATION

1. Proposer will furnish, transport, and install all bridge items at the project site.

2. Transportation of the bridge panels to the bridge locations shall not cross the Walter's Street Bridge.

E. RESEARCH SPECIMENS

1. Test articles shall be of width and length representative of the panels used in the various construction/installation methods. Dimensions of the panels and a method of testing shall be outlined for each construction method. The testing method shall outline the test setup and a general description of the information that the test will provide.

2. Approval of the dimensions of the test articles shall be obtained from the University prior to manufacturing of the test articles.

3. Two (2) test articles representative of each significantly different bridge construction method shall be provided to the University by April 15, 2000.

4. Approval for manufacturing of the bridge panels shall be obtained from the University. The University shall provide its approval or disapproval within five (5) days of receipt of the test articles.

F. INSPECTION AND MAINTENANCE MANUAL

1. A manual that details the procedures for inspection and maintenance of the bridges shall be provided to the University upon installation of the first bridge. Said manual shall include a list of material suppliers that could be used if repairs were to be necessary and shall outline all relevant properties of materials that may be necessary.

2. Approval of the inspection and maintenance manual shall be obtained from the University. The University shall provide approval or disapproval within five (5) days of the receipt of the manual.

SECTION 1.G.

EVALUATION PROCEDURES

A. GENERAL INFORMATION/QUALITY POINTS

The purpose of the evaluation process is to establish, through the application of uniform criteria, the quality of the project contained in each proposal. Each proposal will be evaluated by an Evaluation Board appointed by the University. The University's Evaluation Board, at its discretion, may give consideration to proposed creative and innovative methods, which may not exactly match criteria listed in this section, yet fulfill the intent of the design objectives and meet the minimum standards of the Design/Build Guidelines. The University reserves the right to determine whether proposed creative and innovative methods fulfill the intent of the Design/Build Guidelines. Points will be assigned according to the maximums for each category in the following table:

1. Bridge Design	Sub-total Points -	125
2. Bridge Manufacturing	Sub-total Points -	75
3. Bridge Installation	Sub-total Points -	100
4. Research Specimens	Sub-total Points -	100
5. Inspection and Maintenance Manual	Sub-total Points -	50
6. Engineering and Specifications	Sub-total Points -	50
	TOTAL POINTS	500

These major areas are further defined in the Technical Evaluation Criteria included in this Section, and will be the basis upon which a total Quality Point Value will be assigned to each proposal. The Evaluation Board will assign points to each proposal within these major areas by evaluating each element in the Technical Evaluation Criteria.

B. EVALUATION PROCESS

Each proposal will undergo a two-phase evaluation procedure.

1. Evaluation Board

The Evaluation Board, selected by the University, will prepare a detailed review of each Technical Proposal and assign a Quality Point value to each item indicated in the Technical Evaluation Criteria. The Board may, in the course of their review, find that some clarification of a proposal is necessary and required for a fair and objective evaluation. In that event, such clarification will be requested in writing, by the University of Missouri Project Manager, and the bidder given an opportunity to respond in writing. Do not assume that you will be contacted or afforded an opportunity to clarify or discuss your proposal.

C. NON-RESPONSIVE PROPOSALS

During the evaluation process it may become apparent that one or more of the proposals do not qualify for consideration on the basis of technical evaluation deficiencies. If so determined by the Evaluation Board, these proposals will be returned to the bidder as non-responsive. Also, any proposal with less than 250 quality points will be considered non-responsive.

D. ESTABLISHMENT OF APPARENT LOW PROPOSER

After the review of proposals, the following equation will be used.

$$\frac{\text{Cost Proposal}}{\text{Quality Point Value}} = Cost \big/ Quality\ Value$$

The lowest cost per unit quality is thus determined and the apparent best bidder announced.

Example Proposals for Project:

Proposal 001 - 110,000/300 = 366.66
Proposal 002 - 135,000/400 = 337.50
Proposal 003 - 145,000/400 = 362.50
Proposal 004 - 150,000/425 = 352.94

Proposal 002 is determined to be the apparent best proposal. It must be noted that in this example, the low proposal does not represent the lowest cost submitted, but the lowest cost per unit quality. Bids that exceed budget may be rejected. Evaluation of the total proposal will be done utilizing the format indicated above. Award of the contract will be to the apparent best bidder of the total proposal, and subject to the Board of Curators approval.

Upon award of the contract, the Technical Proposal and other proposal documents, which have not been identified as confidential or proprietary, submitted by the apparent best bidder will be available for review by all interested participants. Detailed analysis and technical evaluation data for all other proposals will be retained by the University in confidence and will not be available for review.

E. TECHNICAL EVALUATION CRITERIA

1. Bridge Design (125)

This area of evaluation includes the general design requirements for the bridges, such as load and deflection requirements, as well as bridge accessories such as the wearing surface and guardrails.

a. General Requirements (65)
    1) Design load and deflections
    2) Depth of structure
    3) Wearing surface
    4) Guardrails/curb
    5) Cross slope/superelevation
    6) Anchorage method
    7) Panel connection detail
b. Innovation (40)
    1) How innovative is the design?
        a) Number of construction types
        b) Effective use of materials
        c) Ability to correct errors once on site
c. Aesthetics Issues (10)
d. Maintenance Issues (10)

2. Bridge Manufacturing (75)

This portion of the evaluation includes the general requirements for the bridge manufacturing. This includes, but is not limited to, the approval of the manufacturing method by a professional engineer and documentation of the effective use of said manufacturing technique for another project(s).

a. P.E. approval
b. Quality control program
c. Use of method on another project(s)

3. Bridge Installation (100)

This portion of the evaluation includes the general requirements for the bridge installation. Included herein are the installation details such as equipment, anchorage method, and panel connection method. Additionally, the speed and ease of installation will be considered in conjunction with the timeline for installation of the bridges.

a. Installation details
    1) Equipment necessary
    2) Anchorage method
    3) Panel connection

4) Installation timeline
    a) Speed
    b) Efficiency

4. Research Specimens (100)

This portion of the evaluation includes the general requirements for the research specimens. This includes, but is not limited to, an evaluation of whether the specimens are representative of the panels used in construction and an evaluation of the outline of the testing method proposed and the information obtained from said test.

a. Specimen dimensions
    1) Representative of bridge panels
b. Testing Methods
    1) Effectiveness
    2) Information obtained from tests

5. Inspection and Maintenance Manual (50)

This portion of the evaluation includes the general requirements for the outline of the inspection and maintenance manual. This includes, but is not limited to, the completeness and presentation of said manual and the overall maintenance requirements of the bridges.

6. Engineering and Specifications (50)

This portion of the evaluation includes the quality of the proposed construction materials and equipment, and the technical adequacy of the engineering features, operation and maintenance, and product specifications. Plans are preferred on AutoCAD.

APPENDIX C

AS-BUILT BRIDGE PLANS AND PROJECT VIDEOS ON CD-ROM

1. INTRODUCITON

Included with this report is a CD-ROM, which contains the bridge plans for all four of the project bridges and the two videos (mentioned in Section 1.5) that detail the installation of the bridges. Each of the bridge plan files are in Adobe Acrobat format and the videos can be viewed using QuickTime Player.

2. CONTENTS

StJohnsJayPlans.pdf

StFrancisPlans.pdf

WaltersPlans.pdf

FRP Panels.mov

FRP-RC.mov

APPENDIX D

INSTALLATION PICTURES

Figure D.1 Drilling of the Holes for the Anchor Bolts – St. Johns and Jay Street

Figure D.2 Installation of the Bearing Pads, Steel Plates and Anchor Bolts – St. Johns and Jay Street

Figure D.3 Installation of the Girders – St. Johns and Jay Street

Figure D.4 Welding of the Girders to the Anchored Plates – St. Johns and Jay Street

Figure D.5 Installed Steel Diaphragms – St. Johns and Jay Street

Figure D.6 Setting the Panels onto the Girders– St. Johns Street

Figure D.7 Setting the Panels onto the Girders– Jay Street

Figure D.8 Top View of Clamping Assembly – St. Johns Street

Figure D.9 Underside view of Clamping Assembly– St. Johns Street

Figure D.10 Clamping Assembly– Jay Street

Figure D.11 Underside View of Clamping Assembly– Jay Street

Figure D.12 Connection of the T-beam to the Girders– St. Johns and Jay Street

Figure D.13 Completed Abutment Assembly – St. Johns and Jay Street

Figure D.14 Filling of Joint Space with Polymer Concrete – St. Johns and Jay Street

Figure D.15 Lay-up of FRP Layers over the Joint Space – Jay Street

Figure D.16 Spacer Block Between the Girders and the Guardrail Posts – St. Johns and Jay Street

Figure D.17 Guardrails Installed – St. Johns and Jay Street

Figure D.18 Setting of the Panels onto the Abutments – St. Francis Street

Figure D.19 Steel Plate Utilized to Attach Guardrail Posts to the Panels – St. Francis Street

Figure D.20 Drilling Holes through the Deck to Attach the Guardrails to the Panels – St. Francis Street

Figure D.21 End Guardrail Post with Additional Connection to the Abutment – St. Francis Street

Figure D.22 Setting of the Bridge Panels – Walters Street

Figure D.23 Drilling Holes to Anchor the Panels to the Abutments – Walters Street

Figure D.24 Filling Panel Joints and Abutment Anchor Holes with Grout – Walters Street

Figure D.25 Installed Guardrail – Walters Street

LIST OF REFERENCES

Abbett, Robert W. Engineering contracts and specifications. 4th ed. New York: Wiley, 1963.

ACI Committee 440. *Recommended Test Methods for FRP Rods and Sheets*, unpublished draft specifications. Farmington Hills, MI: American Concrete Institute, 2001.

ACI Committee 440. *Guide for the Design and Construction of Concrete Reinforced with FRP Bars* (440.1R-01). Farmington Hills, MI: American Concrete Institute, 2001.

Alampalli, Sreenivas, Arthur Yannotti , Jerome O'Connor, Mark Norfolk, George Schongar, and Harry Greenberg. *In-service Monitoring of FRP Bridge in New York*. Structures Congress, CD-Rom Proceedings, Philadelphia, PA, May 2000.

Alampalli, Sreenivas, Jerome O'Connor, and Arthur Yannotti. *Fiber Reinforced Polymer Composites for Superstructure of a Short-span Rural Bridge*. Transportation Research Board Annual Meeting, CD-Rom Proceedings, Washington, D.C., January 2001.

Alkhrdaji, Tarek, Michelle Wideman, Abdeldjelil Belarbi, and Antonio Nanni. *Shear Strength of GFRP RC Beams and Slab*. Proceedings of the Composites in Construction International Conference, J. Figueiras, L. Juvandes, and R. Faria, Eds. October 10-12, 2001, Porto, Portugal, pp. 409-414.

Alkhrdaji, Tarek and Antonio Nanni. *Design, Construction, and Field-Testing of an RC Box Culvert Bridge Reinforced with GFRP Bars*. Non-Metallic Reinforcement for Concrete Structures (FRPRCS-5), July 16-18, 2001, Cambridge, pp. 1055-1064.

Allen, Howard G. Analysis and Design of Structural Sandwich Panels. New York: Pergamon Press, 1969.

American Association of State Highway and Transportation Officials. *Standard Specifications for Highway Bridges*. 16th ed. Washington D.C.: American Association of State Highway and Transportation Officials, 1996.

American Association of State Highway and Transportation Officials. *Manual for Condition Evaluation of Bridges*. 2nd ed. Washington D.C.: American Association of State Highway and Transportation Officials, 2000.

American Society of Testing and Materials. *ASTM Standards Development Tools – Specifications Standard Template*. West Conshohocken, PA: ASTM International, 2001.

American Society of Testing and Materials. *ASTM Standards Development Tools – Test Method Standard Template*. West Conshohocken, PA: ASTM International, 2001.

American Society of Testing and Materials. *Standard Test Method for Flexural Properties of Sandwich Constructions (C393-00)*, West Conshohocken, PA: ASTM International, 2000.

Bakht, Baidar and Leslie G. Jaeger. *Bridge Analysis Simplified*. New York: McGaw-Hill Book Company, 1985.

Bank, Lawrence C., T. Russell Gentry, Benjamin P. Thompson, and Jeffrey S. Russell. *A Model Specification for Composites for Civil Engineering Structures.* Transportation Research Board Annual Meeting, CD-Rom Edition of Proceedings, Washington, D.C., January 2002.

Bradberry, Timothy. *FRP-Bar-Reinforced Concrete Bridge Decks*. Transportation Research Board Annual Meeting, CD-Rom Proceedings, Washington, D.C., January 2001.

Breitenberg, Maureen A. *The ABC's Of Standards-Related Activities In The United States*, Report NBSIR 87-3576. Gaithersburg, MD: National Institute of Standards and Technology, May 1987.

Busel, John and James Lockwood, Eds. *Product Selection Guide: FRP Composite Products for Bridge Applications*. Harrison, NY: The Market Development Alliance of the FRP Composites Industry, 2000.

Chajes, Michael J. John W. Gillespie Jr., Dennis R. Mertz, Harry W. Shenton III, and Douglas A. Eckel II. *Delaware's First All-Composite Bridge*. Structures Congress, CD-Rom Proceedings, Philadelphia, PA, May 2000.

Chajes, Michael J., Harry W. Shenton III, and William W. Finch Jr. *Performance of a GFRP Deck on Steel Girder Bridge*. Transportation Research Board Annual Meeting, CD-Rom Proceedings, Washington, D.C., January 2001.

Civil Engineering Research Foundation. *Gap Analysis for Durability of Fiber Reinforced Polymer Composites in Civil Infrastructure.* USA: American Society of Civil Engineers, 2001.

Davalos, Julio F., Pizhong Qiao, Xi Xu, Justin Robinson, and Karl E. Barth. *Modeling and Characterization of Fiber-Reinforced Plastic Honeycomb Sandwich Panels*

for Highway Bridge Applications, Composite Structures, v 52 n 3-4 May/June 2001, pp. 441-452.

Faller, Ronald K., Barry T. Rosson, Michael A. Ritter, and Eric A Keller. *Development of Two TL-2 Bridge Railings and Transitions for Use on Transverse Glue-Laminated Deck Bridges*. Transportation Research Board Annual Meeting, CD-Rom Edition of Proceedings, Washington, D.C., January 2001.

Federal Highway Administration (FHWA), *National Bridge Inventory Data.* U.S. Department of Transportation, December 1998.

Gill, Stephen R. and Jerry D. Plunkett. *Testing, Evaluation, and Installation of Fiber-Reinforced Polymer Honeycomb Composite Panels in Bridge Deck Applications.* Transportation Research Board Annual Meeting, CD-Rom Proceedings, Washington, D.C., 2000.

Gill, Stephen R. and Jerry D. Plunkett. *Testing, Evaluation, and Installation of Fiber-Reinforced Polymer Honeycomb Composite Panels in Bridge Deck Applications*, Final Report, National Cooperative Highway Research Program, August 2000.

Harter, Phillip J. *Regulatory use of standards: the implications for standards writer*. Washington, D.C.: National Bureau of Standards, 1979.

Henderson, Mark, Ed. *Evaluation of Salem Avenue Bridge Deck Replacement: Issues Regarding the Composite Materials Systems Used, Final Report*. Ohio Department of Transportation, December 2000.

Lixin, Liu and Law Kwok-sang. *A Study on the Anchorage Properties of Bundled Bars in Reinforced Concrete Beams*, Proceedings of the Third International Conference on Concrete Under Severe Conditions: Environment and Loading, N. Banthia, K. Sakai, and O.E. Gjorv, Eds., Vancouver, BC, Canada, June 2001, pp. 949-956.

Lockwood, James and John Busel. *State of the Art FRP Composite Products for Bridge Applications*, Transportation Research Board Annual Meeting, CD-Rom Proceedings, Washington, D.C., January 2001.

Micelli, Francesco and Antonio Nanni. Mechanical Properties and Durability of FRP Rods. CIES report 00-22, March 2001.

Myers, John J., Sharath Murthy, and Francesco Micelli. *Effect of Combined Environmental Cycles on the Bond of FRP Sheets to Concrete.* Proceedings of the Composites in Construction International Conference, J. Figueiras, L. Juvandes, and R. Faria, Eds. October 10-12, 2001, Porto, Portugal, pp. 339-344.

Nagy, Geza and John Kunz. *Preliminary Design of a Composite Bridge Deck System and Test Panels for the First Salem Bridge in Dayton Ohio*. Prepared for the Ohio Department of Transportation, October 1998.

Nagy, Geza, Frieder Seible, and Gilbert Hegemier. *Experimental and Analytical Study of the Performance of Corrugated-Core Sandwich Deck Panels*, Report No. ACTT-96/01, University of California, San Diego, 1996.

Nanni, Antonio. *Relevant Field Applications of FRP Composites in Concrete Structures*. Proceedings of the Composites in Construction International Conference, J. Figueiras, L. Juvandes, and R. Faria, Eds. October 10-12, 2001, Porto, Portugal, pp. 661-670.

Reising, Reiner, Bahram Shahrooz, Victor Hunt, Mike Lenett, Sotir Christopher, Andy Neumann, Arthur Helmicki, Richard Miller, Shirisha Kondury, and Steve Morton. *Performance of a Five-Span Steel Bridge with Fiber Reinforced Polymer Composite Deck Panels*. Transportation Research Board Annual Meeting, CD-Rom Proceedings, Washington, D.C., January 2001.

Scott, Irene N. and K. Wheeler. *Plastic Bridges are the Future! An Australian Perspective on the USA Experience in the Use of Fibre Reinforced Polymer (FRP) Composites in Bridge Construction*. Australian Structural Engineers Conference, Gold Coast, Australia, 2001.

Shekar, Vimala, Samer Petro, and Hota GangaRao. *Construction of FRP Modular Decks for Highway Bridges*. Transportation Research Board Annual Meeting, CD-Rom Proceedings, Washington, D.C., January 2002.

Shipley, Tom. *FRP Reinforced Concrete: An Infrastructure Solution.* University of Missouri-Rolla Video Communications Center, 2001.

Shipley, Tom. *FRP Sandwich Panels: An Infrastructure Solution.* University of Missouri-Rolla Video Communications Center, 2001.

Springer, Georger S. Ed. *Environmental Effects on Composite Materials*. Westport, CT: Technomic Pub. Co., 1984.

Stone, D., A. Nanni and J. Myers. *Field and Laboratory Performance of FRP Bridge Panels.* Proceedings of the Composites in Construction International Conference, J. Figueiras, L. Juvandes, and R. Faria, Eds. October 10-12, 2001, Porto, Portugal, pp. 701-706.

Stone, Danielle, Andrea Prota and Antonio Nanni. *Performance Evaluation of an FRP-Reinforced Concrete Bridge*, 81st Annual Transportation Research Board Meeting, CD-Rom proceedings, January 13-17, 2002, Washington, D.C.

Stone, Danielle, Andrea Prota and Antonio Nanni. *Deflection Assessment of an FRP-Reinforced Concrete Bridge.* ACI Spring Convention, April 21-26, 2002, Detroit, MI.

Stone, Danielle, Daniel Koenigsfeld, John Myers and Antonio Nanni. *Durability of GRFP Rods, Laminates, and Sandwich Panels subjected to Various Environmental Conditions*. Second International Conference on Durability of Fiber Reinforced Polymer (FRP) Composites for Construction, May 29-31, 2002, Quebec, Canada, pp. 213-224.

Stone, Danielle, Steve Watkins, Halvard Nystrom and Antonio Nanni. *Investigation of FRP Materials for Bridge Construction*. Proceedings of the Fifth National Workshop on Bridge Research in Progress, C.K. Shield and A.E. Schultz, Eds. University of Minnesota, Twin Cities, October 8-10, 2001, Minneapolis, Minnesota, pp. 145-150.

Vijay, P.V., and Hota V.S. Ganga Rao. *Accelerated and Natural Weathering of Glass Fiber Reinforced Plastic Bars.* Non-Metallic Reinforcement for Concrete Structures (FRPRCS-5), November 1-4th, 1999, Baltimore, USA, pp. 605-614.

Vinson, J.R. & Sierakowski, R.L. *The Behavior of Structures Composed of Composite Materials.* Dordrecht: Martinus Nijhoff Publishers, 1986.

Wagh, Vikas P. *FRP Bridge Deck Design and Construction*, Structural Engineer, May 2001, pp. 46-50.

Zhou, Aixi, Jason T. Coleman, John J. Lesko, and Thomas E. Cousins. *Structural Analysis of FRP Bridge Deck Systems from Adhesively Bonded Pultrusions*, FRP Composites in Civil Engineering, Vol. II, Elsevier Science Ltd., New York, 2001, pp. 1413-1420.

Zoghi, Manoochehr, Daniel N. Fahrey, and Dean C. Foster. *Construction and Performance Evaluation of a Fiber-reinforced Polymer Composite Bridge*. Transportation Research Board Annual Meeting, CD-Rom Proceedings, Washington, D.C., January 2002.